Title
Transformations for variable-property turbulent boundary layers

Author
Trettel, Andrew James

Publication Date
2019

Peer reviewed|Thesis/dissertation

UNIVERSITY OF CALIFORNIA

Los Angeles

Transformations for variable-property turbulent boundary layers

A dissertation submitted in partial satisfaction of the requirements for the degree Doctor of Philosophy in Mechanical Engineering

by

Andrew James Trettel

2019

ABSTRACT OF THE DISSERTATION

Transformations for variable-property turbulent boundary layers

by

Andrew James Trettel

Doctor of Philosophy in Mechanical Engineering

University of California, Los Angeles, 2019

Professor J. John Kim, Co-Chair

Professor Xiaolin Zhong, Co-Chair

The Trettel-Larsson (TL) transformation is extended to two dimensions using mass conservation and an interpretation of Morkovin's hypothesis. This extension reveals the previously unknown limitations of the TL transformation. The TL transformation only works in channel flows, in the inner layer of high Reynolds number boundary layers, and in boundary layers where the viscosity varies with the square root of the density. The error in the TL velocity transformation correlates with the second derivative of the transformed coordinate (the semi-local scaling). The second derivative of the transformed coordinate measures the amount that the transformed outer layer coordinate does not equal the untransformed outer layer coordinate. The extended TL theory now includes a streamwise coordinate transformation and production rate scalings. The limitations of the TL theory state that the analogy between compressible turbulent boundary layers and incompressible turbulent boundary layers is limited in theory but nonetheless useful in practice when possible.

The dissertation of Andrew James Trettel is approved.

Marcelo Chamecki

Jeffery D. Eldredge

J. John Kim, Committee Co-Chair

Xiaolin Zhong, Committee Co-Chair

University of California, Los Angeles

2019

Contents

List of Figures

List of Tables

Acknowledgments

First, I would like to thank Professors John Kim, Xiaolin Zhong, and Jeff Eldredge for their support and comments throughout this work. I also would like to thank Professor Marcelo Chamecki for his detailed comments on the draft as well.

I would also like to thank Professor Johan Larsson of the University of Maryland, College Park for recommending this topic for my master's thesis. I did not expect to continue the work at UCLA but I am glad that I was able to.

I would also like to thank Professor Sergio Pirozzoli of the Sapienza Università di Roma for answering my questions about his direct numerical simulation data.

I would also like to thank Ben Trettel for reading a draft of the first two chapters.

Finally, I would like to thank Dr. Morad Alvarez for his useful discussions with me about the dilatation rates and compressibility effects in rough-wall compressible turbulent boundary layers.

Vita

2011	B.S. in Mechanical Engineering, University of Maryland, College Park.
2011–2013	Staff Engineer, Combustion Science & Engineering, Inc.
2015	M.S. in Mechanical Engineering, University of Maryland, College Park.

Chapter 1

Introduction

1.1 Problem statement

Compressible turbulent boundary layers are much more complex than incompressible turbulent boundary layers. Unlike incompressible turbulent boundary layers, compressible turbulent boundary layers require much more information to describe the flow. To describe the mean field alone, we need the mean density, mean viscosity, mean speed of sound, mean temperature, mean pressure, and mean Mach number profiles at the very least. To describe the turbulence structure, we need to take into account the turbulence statistics involving the velocity fluctuations but also many new quantities involving temperature, pressure, density, and viscosity fluctuations. While density-weighted averaging can provide a simpler way to account for most of these, we still need some additional variables to properly describe the flow. None of these complications emerge in incompressible flow, where the primary profiles that matter are the mean velocity profile and the turbulence statistics based on the velocity fluctuations alone.

Compressible turbulent boundary layers also introduce additional boundary conditions that greatly expand the parameter space researchers must consider. Primarily there are two additional boundary conditions: the freestream Mach number $\mathrm{Ma}_\mathrm{e} = u_\mathrm{e}/a_\mathrm{e}$, where a_e is the speed of sound at the boundary layer's edge; and the wall heat flux, q_w (or another equivalent variable). The wall heat flux also matters in incompressible turbulent boundary layers with heat transfer. These variables relate to the nature of the energy and heat transfer in the flow. They represent additional physical processes that we now must consider as fundamental to the physics of the boundary layers. For example, the Mach number controls for the amount of viscous heating in the boundary layer, and the wall heat flux controls for how much energy could enter or leave the domain. The nature of the heat transfer at the wall determines the kind of wall in the flow. An adiabatic wall is a wall that allows no heat to transfer through it, and an isothermal wall is a wall that has a constant temperature. The primary non-adiabatic wall condition is a "cold wall," which is a wall that is colder than the flow above it (such that heat flows out through the wall).

How should we approach the study of compressible turbulent boundary layers when we need so much more information to characterize them? The classical answer, pursued since the 1930s, has been to find a way to compare them to incompressible turbulent boundary layers. This comparison is most often achieved via analogy by developing a transformation that converts compressible turbulent boundary layer data into "equivalent" incompressible boundary layer data. The goal is to capture the net effect of all of this new information and reduce it to something familiar and better understood: the incompressible law-of-the-wall.

An analogy exists between two different phenomena when corresponding behavior exists between the two. In our problem, an analogy would specify the corresponding incompressible behavior of a compressible flow. For example, we can develop an analogy between the streamwise velocity in a compressible flow to the streamwise velocity in an incompressible flow. Such an analogy is usually referred to as a velocity transformation.

Researchers have identified many analogies in science and engineering. For example, a Reynolds analogy describes the relationship between momentum transfer and heat transfer in a system. In boundary layers, a specific form of the Reynolds analogy is a Crocco-Busemann relation (Busemann, 1931; Crocco, 1932a; Busemann, 1935), which relates the local velocity in a boundary layer to the local temperature. A common form of this analogy is (White, 2006, p. 509)

$$\frac{\mathrm{d}^2 T}{\mathrm{d}u^2} = -1\,. \tag{1.1}$$

In this equation, T is the local temperature and u is the local streamwise velocity in a boundary layer. This equation seems a bit odd at first, but when solved with the correct boundary conditions, it allows its user to find out the temperature profile given the velocity profile and vice versa. This example demonstrates why analogies are powerful: they can greatly simplify analysis and problem solving.

Nonetheless, most analogies have some limitations. For example, a Crocco-Busemann relation only works for unity Prandtl numbers ($\mathrm{Pr} = 1$). In all other circumstances the analogy breaks down due to our inability to match the thermal boundary layer thickness and the momentum boundary layer thickness. Still, the analogy remains useful, because gases like air have a Prandtl number of around 0.7. The analogy may no longer be exact, but it will suffice.

For our problem, we want to develop a transformation (analogy) that reduces compressible turbulent boundary layer data to incompressible form. In particular, we want to reduce

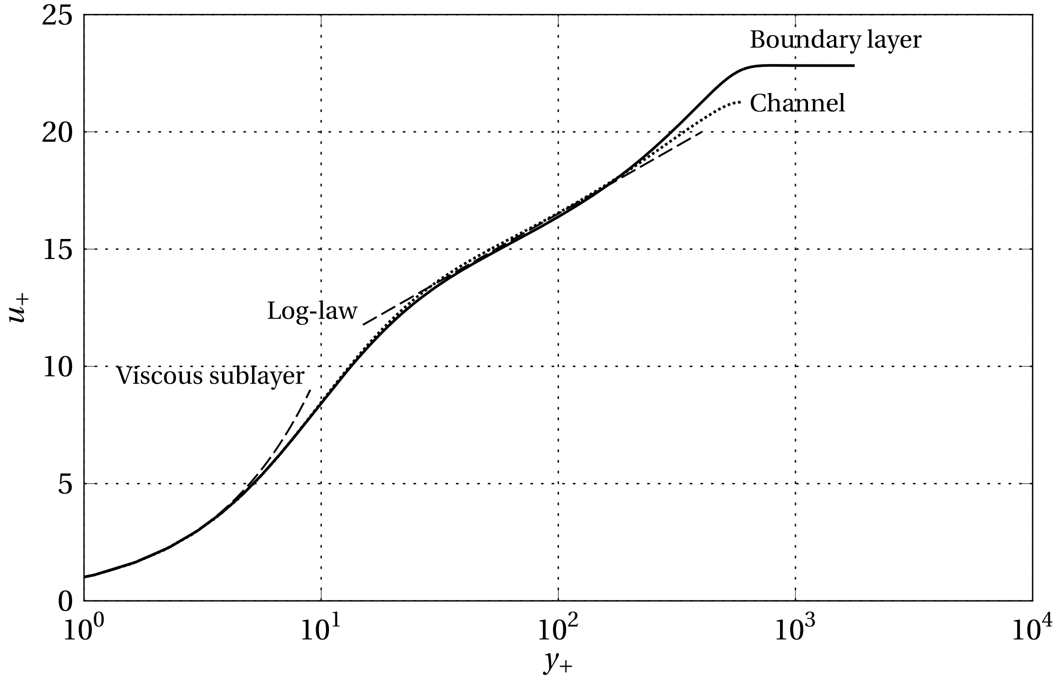

Figure 1.1: The incompressible law-of-the-wall for boundary layers (`2010-Jimenez-DNS-0201`) and for channels (`1999-Moser-DNS-0301`)

the compressible streamwise mean velocity to its familiar form as described by the law-of-the-wall. Such a transformation is often upheld as an example of the universal behavior of near-wall turbulence. Despite the changes in density and viscosity and other variables, the transformation demonstrates that the same law-of-the-wall is recovered, and therefore the same mechanisms driving the turbulence are expected to matter.

We can see the incompressible law-of-the-wall depicted in figure 1.1. The law-of-the-wall is the universal velocity scaling for the mean velocity profile (Prandtl, 1925; Kármán, 1930; Prandtl, 1932):

$$u_+ = \frac{\overline{u}}{u_\tau} = f\left(y_+ = \frac{y}{\ell_\nu}\right), \tag{1.2}$$

where u_τ is the friction velocity, defined as

$$u_\tau = \sqrt{\tau_{\mathrm{w}}/\varrho_r}\,, \tag{1.3}$$

and ℓ_ν is the viscous length scale, defined as

$$\ell_\nu = \frac{\mu_r}{\varrho_r u_\tau}\,. \tag{1.4}$$

Here, ϱ_r is the constant density of the incompressible flow, and μ_r is the constant viscosity of the incompressible flow. Together, the dimensionless variables u_+ and y_+ form "plus units" or "wall units," the standard notation for law-of-the-wall variables.

We can identify several regions of the flow in figure 1.1. The first region is the viscous sublayer, which covers up to $y_+ \approx 5$. In this region, viscosity dominates and damps out the turbulent fluctuations. The mean velocity profile in wall units is linear:

$$u_+ = y_+\,. \tag{1.5}$$

Above the viscous sublayer is the buffer layer, and above that is the logarithmic region. In this region, the velocity profile can be described using a logarithm:

$$u_+ = \tfrac{1}{\kappa}\ln y_+ + C\,. \tag{1.6}$$

Above the logarithmic region is the wake, and this is the only region where the difference between the channel velocity profile and the boundary layer velocity profile emerges. The boundary layer allows for spatial development, but a channel is a fully-developed flow between 2 parallel plates and undergoes no spatial development. Despite these physical differences, the velocity profiles are nearly identical when presented in wall units. This similarity demonstrates the power of the law-of-the-wall: we observe similar results even in quite difference circumstances.

But this is the incompressible law-of-the-wall. If some sort of analogy holds, we expect a similar structure to the law-of-the-wall plots for compressible flows — a viscous sublayer, a buffer layer, a log-law, and a wake — and we might even be able to transform data to recover the incompressible law-of-the-wall in some circumstances. That is the goal of this dissertation. Nonetheless, we may not find an exact analogy to incompressible flows even if we can identify similar regions of the flow or even similar physics. While unfamiliar or especially complex problems are often understood using analogies to more familiar and simpler problems, we cannot always assume that new problems are analogous to old problems. When analogies break down, we must realize that some problems are just different than others and we cannot expect them to always be analogous to familiar material. Compressible turbulent boundary layers might just be their own kind of boundary layers, and the comparison to incompressible turbulent boundary layers may in fact be limited. This is important to state, because many techniques rely on such an analogy existing, when in fact it never has conclusively been proved to exist for all circumstances. The fact that we cannot develop a perfect analogy between compressible and incompressible turbulent boundary layers does not mean that they are beyond our understanding. It merely means that we cannot describe them in the terms we have already used to describe previous problems. The problem still could be solvable, just not equivalent or analogous to what we have previously known. It may be an whole different beast. And that is where the new physics lie.

1.2 Notation

1.2.1 Conventional notation

We need to relate two different flow regimes, so we need two different but corresponding sets of notation: one for a variable-property regime and another for a constant-property regime. The variable-property regime includes not just compressible flow but also variable-property incompressible flow. The constant-property regime covers incompressible flow without heat transfer, usually assumed to be just incompressible flow in general.

We will start by defining the types of averaging we will use. For some quantities, we will use conventional unweighted averaging. The average of a quantity Q will be represented with an overbar like $\overline{Q}$. A fluctuation away from the conventional average is represented with a single prime, such that for any quantity

$$Q = \overline{Q} + Q' \tag{1.7}$$

Compressible turbulence often involves flows with large amounts of density variation, so we will also use a second averaging system to simplify the equations: density-weighted averaging (Favre averaging). The advantage of density-weighted averaging is that the momentum equation stays in the same form regardless of how much the density varies. No terms involving density fluctuations appear. Density weighted averages are defined via the following relationship:

$$\widetilde{Q} = \frac{\overline{\varrho Q}}{\overline{\varrho}}. \tag{1.8}$$

A density-weighted average is represented with a tilde over the variable and a density-weighted fluctuation is represented with double primes, such that for any quantity

$$Q = \widetilde{Q} + Q'' \tag{1.9}$$

More properties of density-weighted averaging are discussed in Cebeci and Smith (1974) and Mieghem (1973).

1.2.2 Regime-dependent notation

For much of this dissertation I will not directly use this more conventional notation for the various averaging systems, since I will instead adopt a different notation that makes clear the relationship between variables in the different flow regimes. For the most part, lowercase letters represent untransformed (variable-property) variables, and uppercase letters represent transformed (constant-property) variables. This notation is somewhat limiting but does unambiguously distinguish between the regimes. Table 1.1 describes the different systems of notation used in more detail.

In general, the notation in table 1.1 follows established conventions, but a few variables require different symbols. The notation simplifies the symbol for the density-weighted mean velocity covariance (Reynolds stress) to a single letter for brevity. The notation also uses the symbol b for the mean stream function. This choice follows the standard notation for the vector potential (Panton, 2005), which generalizes the stream function. Moreover, the stream function follows its compressible flow definition:

$$+\varrho u = \frac{\partial b}{\partial y}, \tag{1.10}$$

$$-\varrho v = \frac{\partial b}{\partial x}. \tag{1.11}$$

	"untransformed"	"transformed"		
Quantity	Variable-property	Constant-property	Conventional	Scale
Streamwise coordinate	x	X	x	ℓ_ν
Wall-normal coordinate	y	Y	y	ℓ_ν
Boundary layer thickness	δ	Δ	δ	ℓ_ν
Channel half-height	h	H	b	ℓ_ν
Similarity length	ℓ	L	ℓ	ℓ_ν
Similarity coordinate	η	η_*	$\eta = y/\ell$	1
Streamwise density-weighted mean velocity	u	U	$\widetilde{u}$	u_τ
Wall-normal density-weighted mean velocity	v	V	$\widetilde{v}$	u_τ
Mean stream function	b	B	$\overline{\psi}$	$\varrho_r u_\tau \ell_\nu$
Mean density	ϱ	ϱ_r	$\overline{\varrho}$	ϱ_r
Mean viscosity	μ	μ_r	$\overline{\mu}$	μ_r
Mean shear stress	t	T	$\overline{\tau} = \overline{\mu \frac{\partial u}{\partial y}} - \overline{\varrho}\, \widetilde{u''v''}$	τ_w
Mean pressure	p	P	$\overline{P}$	τ_w
Density-weighted mean velocity covariance	r	R	$\widetilde{u''v''}$	u_τ^2

Table 1.1: Systems of notation

Table 1.1 does have one slight though intentional inconsistency in notation. The primary difference between the variable-property regime and the constant-property regime is represented through the mean density and viscosity values. In the constant-property regime, these are taken at certain reference conditions and as such are constant values by definition. In general, the reference values are arbitrary, since the transformation should work for all constant-property flows. Hence, the subscript r is used. However, in practice, we must pick a single, constant reference value. The wall value is standard and simplifies many quantities when integrating from the wall, so I used it in all calculations.[1] Moreover, the wall shear stress τ_w is assumed to be the same in both regimes, so using the wall value as a standard extends that assumption.

Using these reference values, we now can define the scales for each of the variables in table 1.1. The friction velocity is

$$u_\tau = \sqrt{\tau_\mathrm{w}/\varrho_r}\,. \tag{1.3}$$

The wall shear stress depends on the streamwise coordinate x and again is assumed to be the same value in both regimes. The viscous length scale is

$$\ell_\nu = \frac{\mu_r}{\varrho_r u_\tau}\,. \tag{1.4}$$

[1] However, the choice of the wall value as the reference value creates a conflict between theory and practice. In theory the reference value is a constant, but in practice the wall value changes in the streamwise direction. The issue is that the reference value must be a constant so that it represents a transformed flow with constant properties. We can resolve this conflict by picking a single wall value rather than using the local wall value. This conflict does not emerge in channels or isothermal wall boundary layers or in any of the data selected in the database (see the next section), since each flow only had a single profile available (none showing the spatial development of the flow). In those cases, which wall value to use is unambiguous.

For each of the quantities in table 1.1, we can define a dimensionless wall units value (plus units) using the scale given in the final column. The same scale applies to both the variable-property and constant-property notations. For example, consider the streamwise coordinate:

$$x_+ = \frac{x}{\ell_v}, \tag{1.12}$$

$$X_+ = \frac{X}{\ell_v}. \tag{1.13}$$

Finally, we must define the friction Reynolds number for both regimes. Again, we use the same scales even though the regimes themselves are different:

$$\mathrm{Re}_\tau = \delta_+ = \frac{\delta}{\ell_v} = \frac{\varrho_r u_\tau \delta}{\mu_r}, \tag{1.14}$$

$$\mathrm{Re}_{\tau,\mathrm{eq}} = \Delta_+ = \frac{\Delta}{\ell_v} = \frac{\varrho_r u_\tau \Delta}{\mu_r}. \tag{1.15}$$

1.2.3 Additional notation

Additional variables are defined in table 1.2.

Quantity	Symbol and definition
Speed of sound	a
Temperature	T
Edge Mach number	$\mathrm{Ma}_\mathrm{e} = \frac{\widetilde{u}_\mathrm{e}}{\widetilde{a}_\mathrm{e}}$,
Dimensionless wall heat flux	$B_q = \frac{q_\mathrm{w}}{\varrho_r c_{p,r} T_r u_\tau}$
Momentum thickness	θ

Table 1.2: Additional notation

1.3 Database of direct numerical simulations

The ideas and questions raised here are broad and as such require a large amount of data to both verify and falsify. As a consequence, I have assembled a large database of direct numerical simulation cases to use. Tables 1.3 and 1.4 list all of the direct numerical simulations cited in this dissertation.

I selected a wide variety of incompressible flow cases to ensure that an incompressible reference profile exists at any suitable Reynolds number. However, several criteria limited what data I could include for the compressible flow cases. Near-wall resolution was the primary selection criteria for the compressible flow cases. As discussed in Trettel and Larsson (2016), transformations that endeavor to correctly transform the viscous sublayer require data in the viscous sublayer. As a consequence, the transformation derived in Trettel and Larsson (2016) requires data around $y_+ \approx 5$. This requirement disqualifies most experiments, unfortunately.[2]

There were several secondary selection criteria. All of these involved ensuring that there was enough data to transform the boundary layer in the first place. To that end, viscosity profiles were required, though temperature profiles could serve as a substitute provided that we approximate the mean viscosity via a Taylor series expansion:

$$\overline{\mu} \approx f(T = \overline{T}) + \frac{1}{2} \frac{\mathrm{d}^2 f}{\mathrm{d} T^2}\bigg|_{T=\overline{T}} \overline{(T')^2} \,. \tag{1.16}$$

Here, the instantaneous viscosity μ is defined through a viscosity law $f(T)$. This formula approximates the mean viscosity provided we are given the mean temperature and possibly

[2] Another secondary selection criteria was accurate wall shear stress measurements. However, the near-wall resolution requirements mandated that the database only include direct numerical simulations, so all wall shear stress data are accurate.

the RMS temperature fluctuations.

Table 1.3: List of direct numerical simulations of boundary layers cited and used

Identifier	Source	Ma_e	Re_τ	$\mathrm{Re}_{\tau,\mathrm{SL}}$	B_q	n_y
`2010-Jimenez-DNS-0101`	Jiménez et al. (2010)	0.0	445.5	445.5	+0.000	345
`2010-Jimenez-DNS-0201`	Jiménez et al. (2010)	0.0	577.8	577.8	+0.000	345
`2010-Jimenez-DNS-0301`	Jiménez et al. (2010)	0.0	690.4	690.4	+0.000	345
`2010-Jimenez-DNS-0401`	Sillero et al. (2013)	0.0	1306.9	1306.9	+0.000	535
`2010-Jimenez-DNS-0501`	Sillero et al. (2013)	0.0	1437.1	1437.1	+0.000	535
`2010-Jimenez-DNS-0601`	Sillero et al. (2013)	0.0	1571.2	1571.2	+0.000	535
`2010-Jimenez-DNS-0701`	Sillero et al. (2013)	0.0	1709.5	1709.5	+0.000	535
`2010-Jimenez-DNS-0801`	Sillero et al. (2013)	0.0	1847.7	1847.7	+0.000	535
`2010-Jimenez-DNS-0901`	Sillero et al. (2013)	0.0	1989.5	1989.5	+0.000	535
`2010-Schlatter-DNS-0101`	Schlatter et al. (2010)	0.0	252.3	252.3	+0.000	513
`2010-Schlatter-DNS-0201`	Schlatter et al. (2010)	0.0	359.4	359.4	+0.000	513
`2010-Schlatter-DNS-0301`	Schlatter et al. (2010)	0.0	492.2	492.2	+0.000	513
`2010-Schlatter-DNS-0401`	Schlatter et al. (2010)	0.0	671.1	671.1	+0.000	513
`2010-Schlatter-DNS-0501`	Schlatter et al. (2010)	0.0	830.0	830.0	+0.000	513
`2010-Schlatter-DNS-0601`	Schlatter et al. (2010)	0.0	974.2	974.2	+0.000	513
`2010-Schlatter-DNS-0701`	Schlatter et al. (2010)	0.0	1043.4	1043.4	+0.000	513
`2010-Schlatter-DNS-0801`	Schlatter et al. (2010)	0.0	1145.2	1145.2	+0.000	513
`2010-Schlatter-DNS-0901`	Schlatter et al. (2010)	0.0	1244.8	1244.8	+0.000	513

Continued on the next page.

Continued from the previous page.

Identifier	Source	$\mathrm{Ma_e}$	Re_τ	$\mathrm{Re}_{\tau,\mathrm{SL}}$	B_q	n_y
`2010-Schlatter-DNS-1001`	Schlatter et al. (2010)	0.0	1271.5	1271.5	+0.000	513
`2011-Pirozzoli-DNS-0101`	Pirozzoli et al. (2011)	2.0	204.8	421.3	+0.001	171
`2011-Pirozzoli-DNS-0201`	Pirozzoli et al. (2011)	2.0	251.9	518.3	+0.001	171
`2011-Pirozzoli-DNS-0301`	Pirozzoli et al. (2011)	2.0	447.8	920.5	+0.001	221
`2011-Pirozzoli-DNS-0401`	Pirozzoli et al. (2011)	2.0	583.1	1198.9	+0.001	221
`2011-Pirozzoli-DNS-0501`	Pirozzoli et al. (2011)	2.0	842.6	1732.3	+0.001	331
`2011-Pirozzoli-DNS-0601`	Pirozzoli et al. (2011)	2.0	898.5	1847.3	+0.001	331
`2011-Pirozzoli-DNS-0701`	Pirozzoli et al. (2011)	2.0	998.1	2052.0	+0.001	331
`2011-Pirozzoli-DNS-0801`	Pirozzoli et al. (2011)	2.0	1113.4	2289.4	+0.001	331
`2011-Pirozzoli-DNS-0901`	Pirozzoli et al. (2011)	3.0	402.5	1556.7	+0.003	221
`2011-Pirozzoli-DNS-1001`	Pirozzoli et al. (2011)	3.0	502.0	1941.0	+0.003	221
`2011-Pirozzoli-DNS-1101`	Pirozzoli et al. (2011)	4.0	398.2	2175.8	+0.003	221
`2011-Pirozzoli-DNS-1201`	Pirozzoli et al. (2011)	4.0	504.6	2755.0	+0.003	221
`2018-Zhang-DNS-0101`	Zhang et al. (2018)	2.5	510.0	1263.9	+0.001	260
`2018-Zhang-DNS-0201`	Zhang et al. (2018)	5.9	450.0	1126.5	-0.138	330
`2018-Zhang-DNS-0301`	Zhang et al. (2018)	5.9	453.0	5305.8	-0.018	310
`2018-Zhang-DNS-0401`	Zhang et al. (2018)	7.9	480.0	5635.9	-0.058	310
`2018-Zhang-DNS-0501`	Zhang et al. (2018)	13.7	646.0	10052.3	-0.192	430

End of table.

Table 1.4: List of direct numerical simulations of channels cited and used

Identifier	Source	Ma_c	Re_τ	$\mathrm{Re}_{\tau,\mathrm{SL}}$	B_q	n_y
`1999-Moser-DNS-0101`	Moser et al. (1999)	0.0	178.1	178.1	+0.000	65
`1999-Moser-DNS-0201`	Moser et al. (1999)	0.0	392.2	392.2	+0.000	129
`1999-Moser-DNS-0301`	Moser et al. (1999)	0.0	587.2	587.2	+0.000	129
`2016-Trettel-DNS-0101`	Trettel and Larsson (2016)	0.8	437.4	396.4	-0.011	90
`2016-Trettel-DNS-0201`	Trettel and Larsson (2016)	0.8	652.1	591.1	-0.010	130
`2016-Trettel-DNS-0301`	Trettel and Larsson (2016)	1.6	321.6	196.6	-0.057	66
`2016-Trettel-DNS-0401`	Trettel and Larsson (2016)	1.6	663.1	406.3	-0.053	125
`2016-Trettel-DNS-0501`	Trettel and Larsson (2016)	1.6	971.7	595.8	-0.050	194
`2016-Trettel-DNS-0601`	Trettel and Larsson (2016)	2.2	649.9	208.3	-0.131	130
`2016-Trettel-DNS-0701`	Trettel and Larsson (2016)	2.2	1232.5	395.5	-0.123	242
`2016-Trettel-DNS-0801`	Trettel and Larsson (2016)	2.2	1876.1	600.7	-0.116	210
`2016-Trettel-DNS-0901`	Trettel and Larsson (2016)	2.4	1017.5	202.8	-0.189	194

End of table.

The database lacks data in several areas. All boundary layer cases are zero-pressure-gradient, for example. Only limited data is available for adverse or favorable pressure gradient compressible turbulent boundary layers, so I excluded these cases from the database. Most boundary layer cases are adiabatic wall cases. The database contains only a few cold wall boundary layer cases (cases where heat flows from the fluid out through the wall). Again, most cases in the literature are adiabatic wall cases (cases where no heat flows through the wall). As such, the database has excellent coverage of adiabatic wall boundary layer behavior but poor coverage of cold wall behavior.

To improve the coverage of cold wall behavior, I also included channel flows in the database. There are several differences between boundary layers and channels. Some differences emerge from channels having no spatial development. All derivatives in the streamwise direction are zero. As a consequence, the mean dilation rate is always zero, so the effects of compressibility fundamentally differ from boundary layers. Channels always have a pressure gradient and always have cold walls (and the wall heat transfer rate depends on the Mach number). Channels also have a known linear shear stress distribution (not true in boundary layers). Despite these differences, the channel flow data greatly expand the database to cover a wide range of Mach numbers, Reynolds numbers, and wall heat transfer rates.

1.4 Previous work

This section details two previous "classical" approaches to solving this problem. The next chapter details a more modern method published more recently (Trettel and Larsson, 2016).

1.4.1 The Van Driest transformation

The classical solution to convert compressible turbulent boundary layer data into equivalent incompressible turbulent boundary layer data is the Van Driest transformation (Van Driest, 1951; Danberg, 1964). The transformation is based off the log-law velocity profile. The coordinate and velocity transformations are

$$Y_{\mathrm{VD},+} = y_+ = \frac{\varrho_r u_\tau y}{\mu_r}, \tag{1.17}$$

$$U_{\mathrm{VD},+} = \underbrace{\int_0^{u_+} \left(\frac{\varrho}{\varrho_r}\right)^{+1/2} \mathrm{d}u_+}_{\text{The most common form}} = \int_0^{u} \frac{\mathrm{d}u}{\sqrt{\tau_\mathrm{w}/\varrho}}. \tag{1.18}$$

The coordinate itself is simply the wall-normal coordinate in wall units without any adjustment. The velocity transformation does all of the work. We can think of the velocity transformation as an analogy between differential changes in the transformed and untransformed velocities:

$$\mathrm{d}U_{\mathrm{VD},+} = \frac{\mathrm{d}u}{\sqrt{\tau_\mathrm{w}/\varrho}}. \tag{1.19}$$

Here, the left-hand side represents a differential change in the dimensionless equivalent incompressible velocity, and the right-hand side represents a differential change in the velocity divided by a local friction velocity. The equation adjusts the velocity profile for local changes in the friction velocity, in other words. To calculate the transformed velocity at any one point, you must integrate the velocities from the wall to the point in question. It may seem odd to integrate with respect to the streamwise velocity rather than the wall-normal coordinate, but this formula is how it has been done in practice. The practice's validity relies on the streamwise velocity being monotonic, which is true for all non-separating boundary layers. An equivalent formula that uses the wall-normal coordinate is

$$U_{\mathrm{VD},+} = \int_0^{y_+} \left(\frac{\varrho}{\varrho_r}\right)^{+1/2} \frac{\mathrm{d}u_+}{\mathrm{d}y_+} \mathrm{d}y_+. \tag{1.20}$$

We can simplify this formula to the common form using the chain rule.

Figure 1.2 depicts the Van Driest transformation applied to an adiabatic wall boundary layer. You may look at this figure and marvel at the near perfect fit. Why do we need to continue

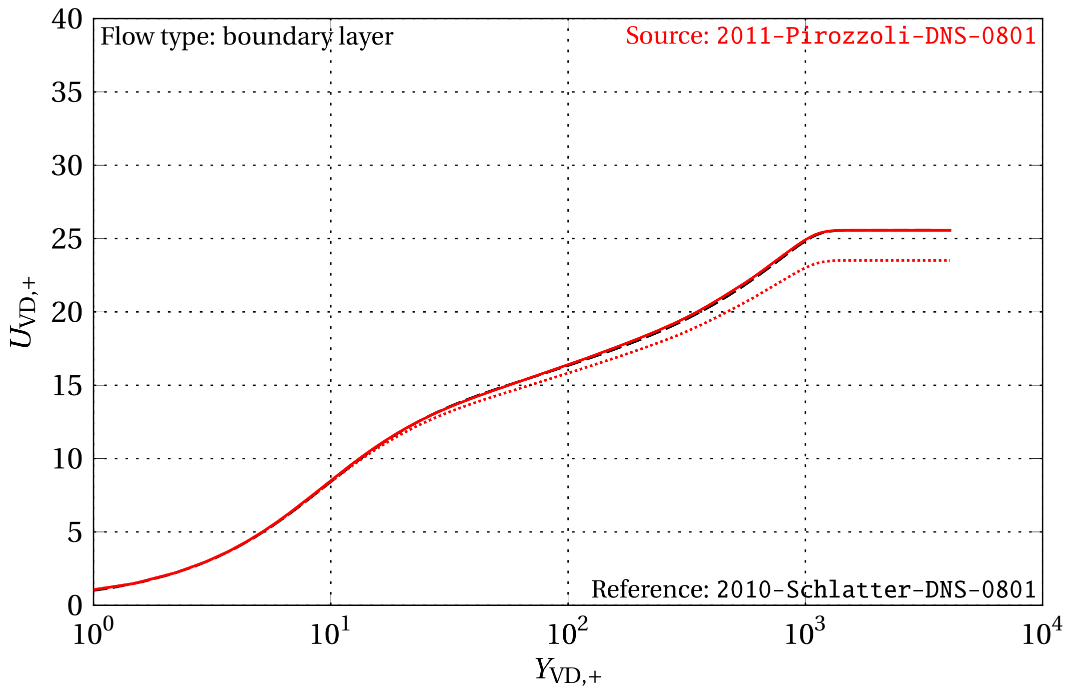

Figure 1.2: VD-transformed law-of-the-wall for `2011-Pirozzoli-DNS-0801` at $Re_{\tau,eq} = 1113.4$, compared to the incompressible reference of `2010-Schlatter-DNS-0801` at $Re_\tau = 1145.2$. Solid red line, transformed profile; dotted red line, untransformed profile; dashed black line, incompressible reference.

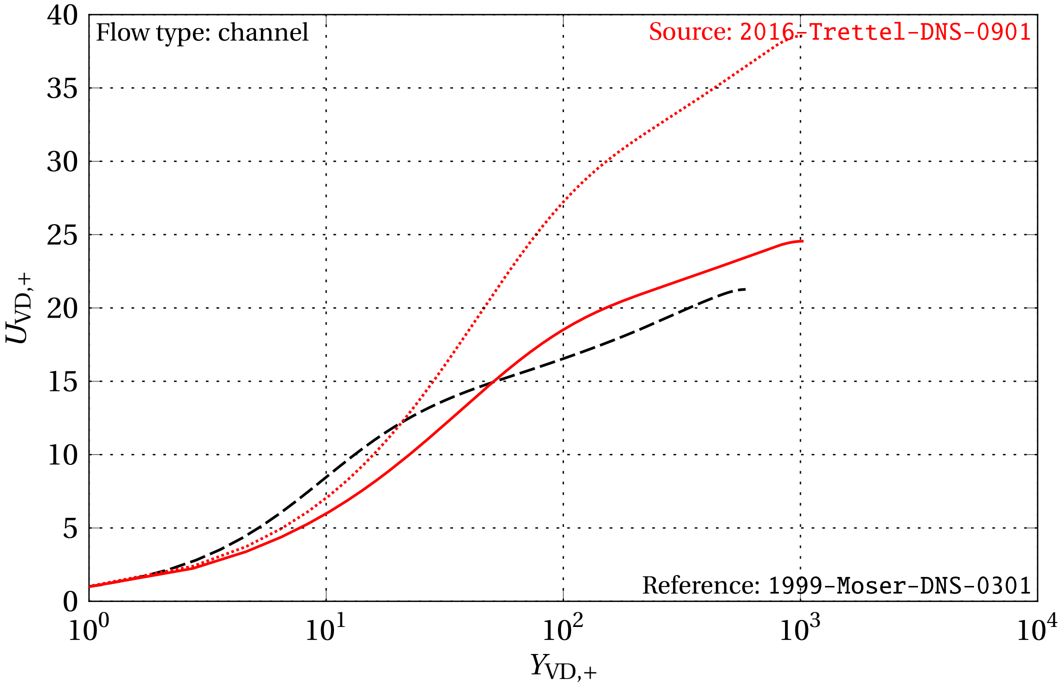

Figure 1.3: VD-transformed law-of-the-wall for `2016-Trettel-DNS-0901` at $\mathrm{Re}_{\tau,\mathrm{eq}} = 1017.5$, compared to the incompressible reference of `1999-Moser-DNS-0301` at $\mathrm{Re}_\tau = 587.2$. Solid red line, transformed profile; dotted red line, untransformed profile; dashed black line, incompressible reference.

when the answer appears to be at hand? The problem is that the Van Driest transformation only works for adiabatic wall boundary layers like the one depicted. Looking at the untransformed velocity profile makes apparent why: the untransformed profile hardly disagrees with the incompressible reference profile. In fact, it only begins to deviate at $y_+ \approx 20$, well past the viscous sublayer and into the buffer layer.

Figures 1.3 and 1.4 depict the Van Driest transformation applied to a channel flow and a cold wall boundary layer. Neither flow has an adiabatic wall, and in neither case does the Van Driest transformed profile match the incompressible reference at the same Reynolds number. Danberg (1964) first noticed this mismatch experimentally but Coleman et al. (1995) and

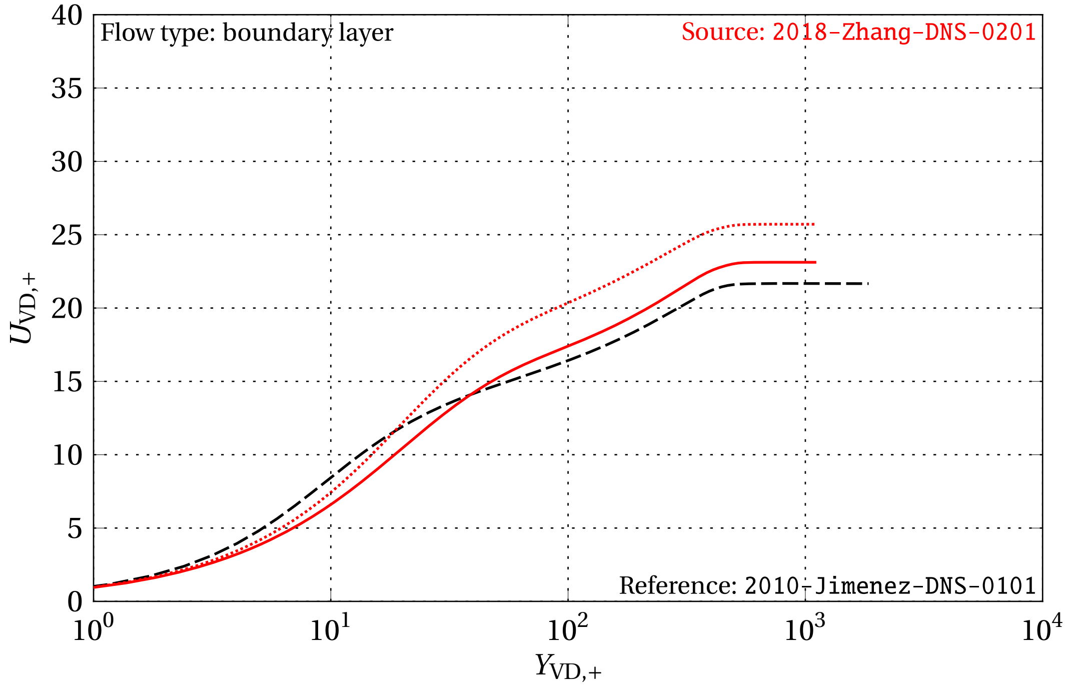

Figure 1.4: VD-transformed law-of-the-wall for `2018-Zhang-DNS-0201` at $\mathrm{Re}_{\tau,\mathrm{eq}} = 450.0$, compared to the incompressible reference of `2010-Jimenez-DNS-0101` at $\mathrm{Re}_\tau = 445.5$. Solid red line, transformed profile; dotted red line, untransformed profile; dashed black line, incompressible reference.

Huang et al. (1995) re-discovered it later when running channel simulations. Later boundary layer studies confirmed it (Maeder, 2000; Duan et al., 2010).

Note that despite the transformation failing to match the incompressible profiles, both of the transformed profiles nonetheless have roughly analogous regions of the flow. The profiles are stretched, but there still is a viscous sublayer, a buffer layer, a log-law region, and a wake. The untransformed profile for the channel, however, does not appear to have the correct von Kármán constant for the log-law, but the transformation does in fact correct for that. In the end, despite the Van Driest transformation's failure, it still results in an answer that is roughly analogous to the incompressible answer.

We can measure how much the Van Driest-transformed (VD-transformed) profile disagrees with the incompressible reference profile using 2 quantities:

1. the error in the transformed viscous sublayer slope S, and
2. the error in the transformed log-law intercept C.

From the viscous sublayer velocity profile (equation 1.5), we can see that the viscous sublayer slope should roughly equal 1 (in practice the value is slightly less than 1). The log-law intercept varies slightly based on the flow type and the Reynolds number but should be around 5 (roughly).

Figure 1.5 plots the negative of the heat flux through the wall against the error in the measured viscous sublayer slope (measured up to $y_+ = 4$). The data forms a single curve that increases as the wall becomes colder. Figure 1.6 plots the negative of the heat flux through the wall against the error in the measured log-law intercept. This plot is much more scattered, but the error still increases as the wall becomes colder. Note that all adiabatic wall cases have little

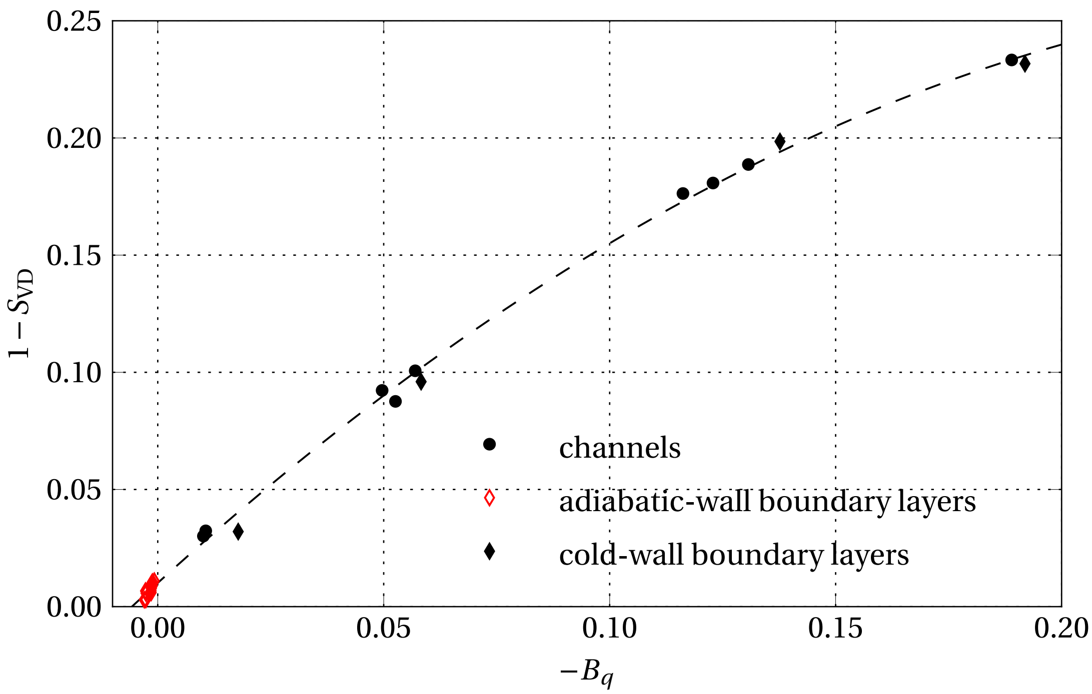

Figure 1.5: Error in the viscous sublayer slope for the VD-transformation as a function of the wall heat flux

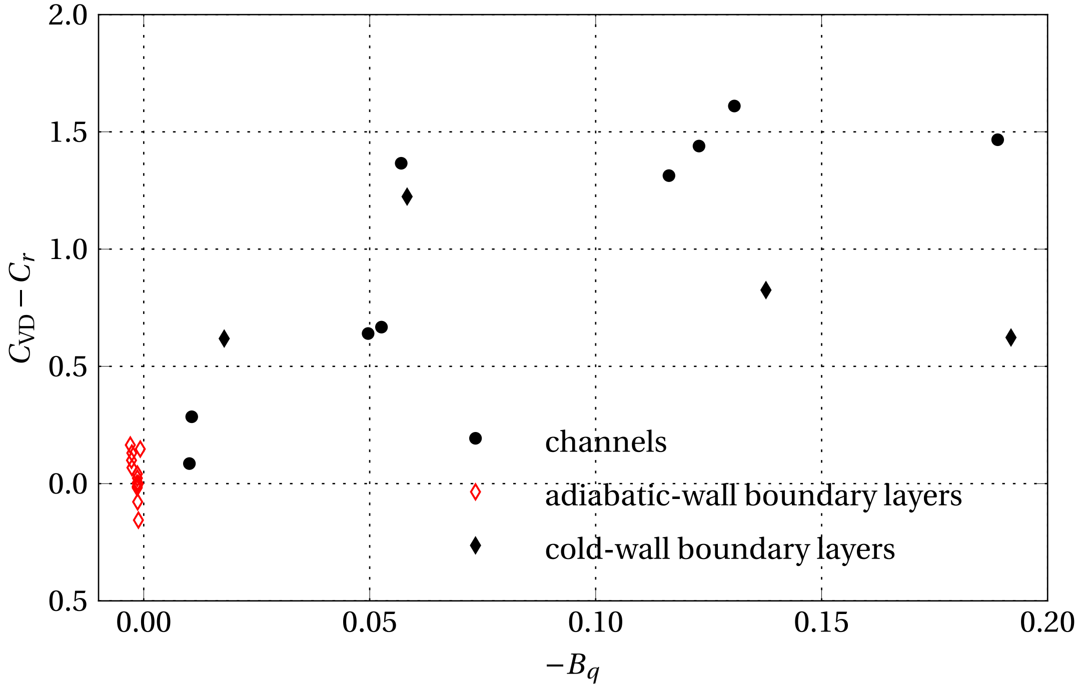

Figure 1.6: Error in the log-law intercept for the VD-transformation as a function of the wall heat flux

error, in general, though there is some scatter nonetheless.

However, I must note that while the wall heat flux appears to control the error, we still have not established the precise mechanism through the wall heat flux causes the transformed profile to change from the incompressible reference profile. The wall heat flux controls for the error but we still have not established why the error occurs in the first place. I discuss this mechanism in chapter 2.

1.4.2 The viscous sublayer transformation

The error in the viscous sublayer slope can be corrected using a different transformation than the Van Driest transformation. The viscous sublayer transformation (Carvin et al., 1988; Smits et al., 2006) derives from the same arguments used to derive the viscous sublayer velocity profile for incompressible flow. In fact, we can consider it the compressible version of the viscous sublayer velocity profile. The viscous sublayer transformation is[3]

$$Y_{\mathrm{VS},+} = y_+ = \frac{\varrho_r u_\tau y}{\mu_r}, \tag{1.21}$$

$$U_{\mathrm{VS},+} = \int_0^{u_+} \left(\frac{\mu}{\mu_r}\right) \mathrm{d}u_+ . \tag{1.22}$$

Because this transformation is explicitly based upon a stress balance taken at the wall, its validity falls apart outside of the viscous sublayer. Nonetheless, it does in fact collapse all profiles in the viscous sublayer. Figures 1.7, 1.8, and 1.9 depict the viscous sublayer transformed (VS-transformed) profiles for the same 3 cases depicted before. In all 3 cases, the match in the viscous sublayer is nearly perfect, but the transformed profiles outside of the viscous sublayer bear no resemblance to the incompressible law-of-the-wall at all in some cases. Consider the channel case. The profile “takes off” and no log-law even appears. We should expect this kind of behavior, because the analogy here is expressly limited by the physics used to derive the transformation, and those physics apply only to the viscous sublayer.

1.4.3 Some thoughts before continuing

Here I have reviewed the 2 classical transformations used before the last 10 years or so. In both cases, the physics used to derive the transformation ultimately limit the transformation

[3] We can also implement a viscous sublayer transformation as a coordinate transformation (Cope et al., 1948):

$$Y_{\mathrm{CH},+} = \int_0^{y_+} \left(\frac{\mu_r}{\mu}\right) \mathrm{d}y_+ ,$$

$$U_{\mathrm{CH},+} = u_+ .$$

Brun et al. (2008) used this coordinate in their transformation, for example, as an attempt to match the profile in the viscous sublayer.

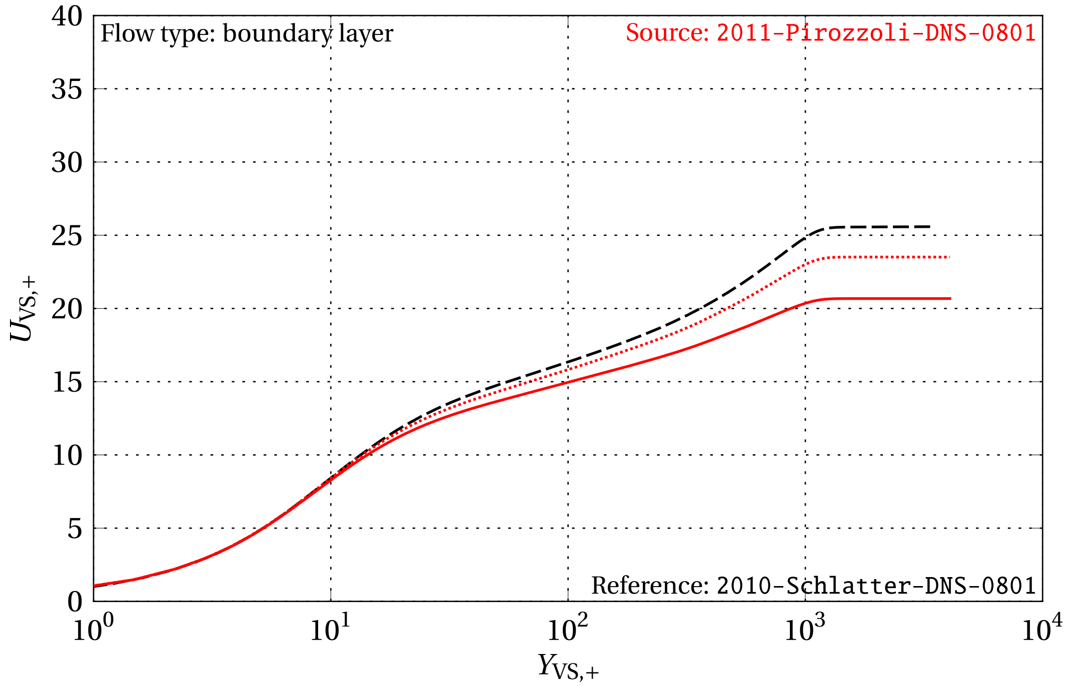

Figure 1.7: VS-transformed law-of-the-wall for `2011-Pirozzoli-DNS-0801` at $Re_{\tau,eq} = 1113.4$, compared to the incompressible reference of `2010-Schlatter-DNS-0801` at $Re_\tau = 1145.2$. Solid red line, transformed profile; dotted red line, untransformed profile; dashed black line, incompressible reference.

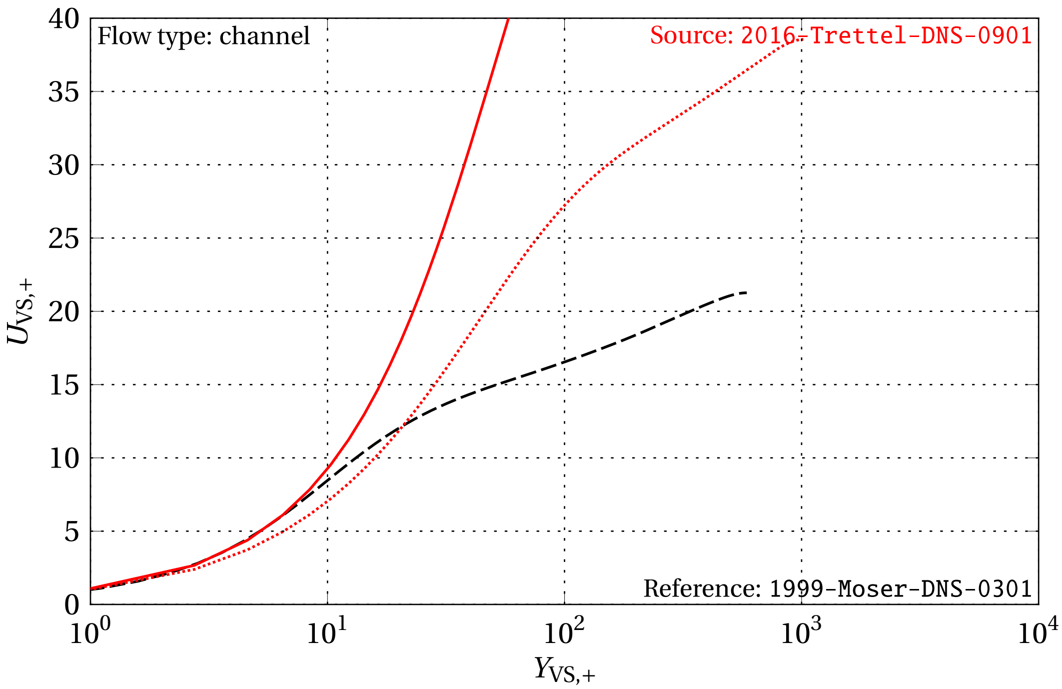

Figure 1.8: VS-transformed law-of-the-wall for `2016-Trettel-DNS-0901` at $\mathrm{Re}_{\tau,\mathrm{eq}} = 1017.5$, compared to the incompressible reference of `1999-Moser-DNS-0301` at $\mathrm{Re}_{\tau} = 587.2$. Solid red line, transformed profile; dotted red line, untransformed profile; dashed black line, incompressible reference.

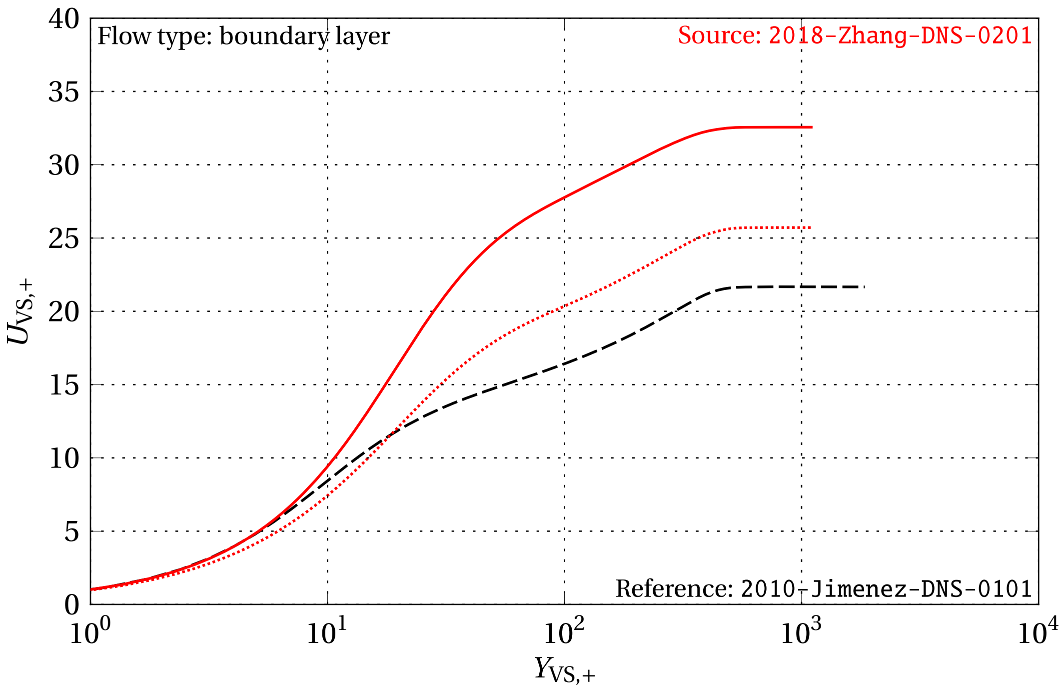

Figure 1.9: VS-transformed law-of-the-wall for `2018-Zhang-DNS-0201` at $Re_{\tau,eq} = 450.0$, compared to the incompressible reference of `2010-Jimenez-DNS-0101` at $Re_\tau = 445.5$. Solid red line, transformed profile; dotted red line, untransformed profile; dashed black line, incompressible reference.

and where it remains valid. The Van Driest transformation derives only from the log-law, so the untransformed profile must match the incompressible profile below $y_+ \approx 30$ for the Van Driest transformation to work. Therefore, the Van Driest transformation can only work for adiabatic wall boundary layers (which by definition do not have any heat transfer near the wall, so they behave like incompressible boundary layers for some distance). The viscous sublayer layer transformation derives only from the physics of the viscous sublayer, so its validity is limited to the viscous sublayer only.

Individually, these transformations are faithful to the physics they consider, and if those were the only physics that matter, they would work in general. But each transformation neglects the physics that the other transformation considers, and fails for that reason. The next approach, considered in chapter 2 and developed independently by several research groups over the last few years, seeks to develop a transformation that obeys both sets of physics that the Van Driest transformation and viscous sublayer transformation obey. The goal is to develop a more general analogy that it not limited to any particular region of the flow.

Chapter 2

The Trettel-Larsson transformation

2.1 Motivation

Why does the Van Driest transformation fail for cold walls? This question recently drove several researchers[1] to develop an alternative transformation to the Van Driest transformation. As shown in the previous section, the error in the Van Driest transformation increases as the wall heat flux increases. We can measure the error in two locations — the error in the viscous

[1] I use the term "Trettel-Larsson transformation" because that term is already popular. However, I should also recognize the work of others. This transformation is a textbook case of multiple discovery, when multiple researchers working independently arrive at the same result at the same time. I first derived the TL transformation theory in 2014 while working on my master's thesis under the direction of Prof. Johan Larsson at the University of Maryland, College Park (Trettel, 2015). Prof. Larsson and I published a paper on the subject in early 2016 (Trettel and Larsson, 2016), but around the same time two other research groups also published papers on the same theory (Modesti et al., 2016; Patel et al., 2016), though they arrived at the result using somewhat different methods. I was pleasantly surprised when I found out. As the old saying goes, nobody believes the theory except the theorist, but at least here I had good company.

sublayer, and the error in the log-law intercept — but only the error in the viscous sublayer had a near perfect correlation with the wall heat flux. Moreover, a second transformation (the viscous sublayer transformation) clearly shows how to remove the error in the viscous sublayer, but this transformation's validity is limited to the viscous sublayer alone.

Nonetheless, the viscous sublayer transformation contains an idea that the Van Driest transformation lacks: momentum conservation. Granted, the viscous sublayer transformation uses a momentum conservation condition that only works in the viscous sublayer, but the idea has merit. We can now understand the physical mechanism that explains why the Van Driest transformation fails. The viscosity profile changes, and without adjusting for the changes in viscosity, the transformed momentum cannot be conserved. If we do adjust for the effects of viscosity and correct for the momentum imbalance, then the profile should at the least match through the viscous sublayer and possibly through the buffer layer, at which point the log-law aspects of the transformation (the basis of the Van Driest transformation) take over. The goal for the transformation described in this chapter is to satisfy the same conditions that lead to the Van Driest transformation while also satisfying momentum conservation in a simplified manner (the stress balance condition). The result is the so-called "Trettel-Larsson transformation" (Trettel, 2015; Trettel and Larsson, 2016; Modesti et al., 2016; Patel et al., 2016) or TL transformation for short.

2.2 The chain rule for one-dimensional shear flows

The Van Driest and Trettel-Larsson transformations assume that the flow is a simple one-dimensional shear flow. They neglect the spatial development in the flow. This assumption greatly simplifies the mathematics involved, though it cannot be justified physically, seeing as boundary layers do in fact have spatial development. Nevertheless, the approach has some advantages that we will see shortly.

Consider a simple shear flow. If we wanted to transform the coordinate and velocity in this flow, we would have consider the velocity gradients. We can relate the velocity gradients using the chain rule:

$$\frac{\mathrm{d}u}{\mathrm{d}y} = \frac{\mathrm{d}u}{\mathrm{d}U}\frac{\mathrm{d}Y}{\mathrm{d}y}\frac{\mathrm{d}U}{\mathrm{d}Y}, \tag{2.1}$$

$$\frac{\mathrm{d}U}{\mathrm{d}Y} = \frac{\mathrm{d}U}{\mathrm{d}u}\frac{\mathrm{d}y}{\mathrm{d}Y}\frac{\mathrm{d}u}{\mathrm{d}y}. \tag{2.2}$$

The first equation writes the untransformed velocity gradient $\frac{\mathrm{d}u}{\mathrm{d}y}$ in terms of the transformed velocity gradient $\frac{\mathrm{d}U}{\mathrm{d}Y}$, and the second equation writes the transformed velocity gradient $\frac{\mathrm{d}U}{\mathrm{d}Y}$ in terms of the untransformed velocity gradient $\frac{\mathrm{d}u}{\mathrm{d}y}$. The term $\frac{\mathrm{d}U}{\mathrm{d}u}$ is the velocity transformation and the term $\frac{\mathrm{d}Y}{\mathrm{d}y}$ is the coordinate transformation. These two variables are the variables we will later solve for. Using these variables, we can calculate the transformed coordinate and transformed velocity by integrating:

$$Y = \int_0^y \frac{\mathrm{d}Y}{\mathrm{d}y}\mathrm{d}y, \tag{2.3}$$

$$U = \int_0^u \frac{\mathrm{d}U}{\mathrm{d}u}\mathrm{d}u. \tag{2.4}$$

As noted in chapter 1, we can integrate in terms of the streamwise velocity since it increases monotonically for non-separating flows. Therefore it always acts as a surrogate for the coordinate. Of course, in both cases we assume that the transformation itself is monotonic, since these equations only make physical sense if it is. Any non-monotonicity would suggest a breakdown in whatever theory we are developing.

Since the flow is one-dimensional, all derivatives are exact. This property allows us to exploit the simple inverse relationships between the derivatives:

$$\left(\frac{\mathrm{d}Y}{\mathrm{d}y}\right) = \left(\frac{\mathrm{d}y}{\mathrm{d}Y}\right)^{-1} , \tag{2.5}$$

$$\left(\frac{\mathrm{d}U}{\mathrm{d}u}\right) = \left(\frac{\mathrm{d}u}{\mathrm{d}U}\right)^{-1} . \tag{2.6}$$

This property is only true for one-dimensional flows. For higher-dimensional flows, the inverse relationships are much more complicated (see chapter 5).

Before moving on, I should describe the transformation procedure that I will use. The procedure requires that we already have a version of the chain rule relating variables in both regimes. This step is trivial here but quite involved in chapter 5.

The procedure takes three steps:

1. First, I will write the constant-property and variable-property equations to be in terms of the same constant.

2. Next, I will apply the chain rule to the variable-property form of the equation, writing it in terms of constant-property variables.

3. Finally, I will set each component of the variable-property equation equal to its corresponding component in the constant-property equation.

Here, a component is a term in an equation or even a group of terms acting as a single unit. I will give a more concrete example of this in the next section.

The first and final steps require some interpretation. In the first step there is ambiguity in deciding how to represent the equation — what constant the equation should equal — and this ambiguity comes up again in chapter 3 in the context of the stress balance. In the final step there is ambiguity in deciding what constitutes a component, and this ambiguity comes up in chapter 5 in particular in the context of the production rate terms. For the moment, we will ignore these issues and concentrate on how previous studies have approached the transformation problem and how the coordinate and velocity transformations turn each component of the variable-property equation into a corresponding component of the constant-property equation.

2.3 Stress balance condition

Momentum conservation in boundary layers is represented through the following equation:

$$\varrho u \frac{\partial u}{\partial x} + \varrho v \frac{\partial u}{\partial y} = -\frac{\mathrm{d}p}{\mathrm{d}x} + \frac{\partial t}{\partial y}, \tag{2.7}$$

where the total shear stress is[2]

$$t = \mu \frac{\partial u}{\partial y} - \varrho r_{xy}. \tag{2.8}$$

For the inner layer of a boundary layer, where $y/\delta \to 0$, we can simplify momentum conservation to a simple "stress balance" condition:

$$\tau_\mathrm{w} \approx \mu \frac{\partial u}{\partial y} - \varrho r_{xy}. \tag{2.9}$$

Momentum conservation is simpler in channels than in boundary layers, so channels follow a similar "stress balance" condition for the entire range of wall-normal coordinates, rather than just close to the wall:

$$\tau_\mathrm{w} \left(1 - \frac{y}{h}\right) = \mu \frac{\partial u}{\partial y} - \varrho r_{xy}. \tag{2.10}$$

[2] Note that this assumes that the viscosity fluctuations are small. This point is discussed slightly more in chapter 3.

We want to develop a transformation that works for both boundary layers and channels, so we need to find a way to generalize this equation. A simple way to generalize this equation is to also consider transforming the total shear stress t itself in some way. We can then use the definition of the total shear stress as our momentum equation:

$$t = \mu \frac{\partial u}{\partial y} - \varrho r_{xy} \,. \tag{2.8}$$

Note that we can also write this equation in terms of wall units:

$$t_+ = \left(\frac{\mu}{\mu_r} \right) \frac{\partial u_+}{\partial y_+} - \left(\frac{\varrho}{\varrho_r} \right) r_{xy,+} \,. \tag{2.11}$$

This is where we can start to derive the TL transformation. First, we should set the equation equal to a constant. This step sets up a fair comparison between the variable-property and constant-property equations, since both are now scaled similarly. Here we will assume that the constant is zero; in chapter 3 we will assume it is a different constant. We will also assume that all quantities are functions of the wall-normal coordinate only.

$$0 = \mu \frac{\mathrm{d}u}{\mathrm{d}y} - \varrho r_{xy} - t \,. \tag{2.12}$$

The constant-property counterpart to this equation is

$$0 = \mu_r \frac{\mathrm{d}U}{\mathrm{d}Y} - \varrho_r R_{XY} - T \,. \tag{2.13}$$

The next step is to apply the chain rule to the variable-property equation to write it in terms of constant-property variables:

$$0 = \mu \frac{\mathrm{d}u}{\mathrm{d}U} \frac{\mathrm{d}Y}{\mathrm{d}y} \frac{\mathrm{d}U}{\mathrm{d}Y} - \varrho r_{xy} - t \,. \tag{2.14}$$

Finally, we set each corresponding component of this equation equal to its constant-property counterpart. In this equation, the components are the viscous stress term, the Reynolds shear stress term, and the shear stress term. This step states that individually each of these components should be the same in both regimes. If we set each corresponding component equal, we get the following three equations:

$$\frac{\mathrm{d}U}{\mathrm{d}Y}: \qquad \mu \frac{\mathrm{d}u}{\mathrm{d}U}\frac{\mathrm{d}Y}{\mathrm{d}y} = \mu_r\,, \tag{2.15}$$

$$-R_{XY}: \qquad \varrho r_{xy} = \varrho_r R_{XY}\,, \tag{2.16}$$

$$-t: \qquad t = T\,. \tag{2.17}$$

This decomposition results in three equations:

$$\frac{\mathrm{d}U}{\mathrm{d}u} = \left(\frac{\mu}{\mu_r}\right)\frac{\mathrm{d}Y}{\mathrm{d}y}\,, \tag{2.18}$$

$$\varrho r_{xy} = \varrho_r R_{XY}\,, \tag{2.19}$$

$$t = T\,. \tag{2.20}$$

These equations form the basis for the rest of the TL transformation.

The first equation was derived first in Trettel (2015) and Trettel and Larsson (2016). It relates how the velocity transformation $\frac{\mathrm{d}U}{\mathrm{d}u}$ relates to the coordinate transformation $\frac{\mathrm{d}Y}{\mathrm{d}y}$. It is easy to see that this equation extends the ideas behind the viscous sublayer transformation. For example, setting $Y = y$ recovers the viscous sublayer transformation. But unlike the viscous sublayer transformation, this equation has an additional degree of freedom.

The second equation is Morkovin's scaling for the Reynolds stresses. It forms a major part of Morkovin's hypothesis, which is an analogy between the turbulence structure and turbulence production mechanisms in compressible and incompressible turbulent boundary layers. Morkovin's scaling can take many useful forms:

$$R_{XY,+} = \left(\frac{\varrho}{\varrho_r}\right) r_{xy,+} = \frac{r_{xy}}{\tau_\mathrm{w}/\varrho} = \frac{\varrho r_{xy}}{\tau_\mathrm{w}}\,. \tag{2.21}$$

This scaling was first considered by Rotta (1959) in the context of similarity laws, but Morkovin (1962) was the first to observe that it correctly collapses the Reynolds stress profiles from experiments at many different Mach numbers onto the same curve. Strictly speaking, the derivation of Morkovin's scaling given here only applies to the shear stress term $\widetilde{u''v''}$, but in practice it is observed to work for the normal Reynolds stress terms as well, though $\widetilde{u''u''}$ appears to have some dependence on Mach number in channel flows at least (Modesti et al., 2016).

There are several ways to think about what this scaling means physically. The first form considers it as a density-weighted adjustment to the dimensionless Reynolds stress profile, the second form considers it as a ratio between the velocity covariance and the square of the local friction velocity $\sqrt{\tau_{\mathrm{w}}/\varrho}$, and the third considers it as a ratio of shear stresses. In the end, all three of these forms are based on the idea that the turbulence has a similar structure to incompressible turbulence provided that we remove the effects of density variation (that is, remove the effects of any changes in inertia).

The third equation states that the transformed shear stress equals the untransformed shear stress. This basically states that the shear stress profile is invariant in both regimes. Chapter 3 will show that the second and third equations are in fact equivalent to some degree. That is, assuming Morkovin's scaling is true is the same as assuming that the shear stresses are the same. In the present context this result is difficult to see, though.

2.4 Log-law condition

The log-law equation (equation 1.6) forms the basis of the Van Driest transformation. We can use the log-law to derive an equation similar to equation 2.18, the velocity transformation derived from the stress balance. A form of this equation was first used by Haberkorn (2004) and Brun et al. (2008) using the Cope-Hartree transformation (Cope et al., 1948) as the coordinate transformation.[3]

Here, since we will use the chain rule, we will write the log-law in terms of a velocity gradient. The original work on a compressible log-law assumed some form of mixing length model (Frankl et al., 1937; Wilson, 1950; Van Driest, 1951), but dimensional analysis can arrive at the log-law even in compressible flow situations (Bradshaw, 1994) without resorting to modeling assumptions. The method used to arrive at the log-law does not matter. What matters here is that we interpret the density to be the local mean density ϱ instead of a constant value of density ϱ_r.

We start with the "diagnostic function" form of the log-law:

$$\frac{1}{\kappa} = y \left(\frac{\varrho}{\tau_\mathrm{w}} \right)^{+1/2} \frac{\mathrm{d}u}{\mathrm{d}y}. \tag{2.22}$$

The "diagnostic function" form expresses this equation in terms of a constant, the first step in our transformation procedure. The corresponding constant-property equation is

$$\frac{1}{\kappa} = Y \left(\frac{\varrho_r}{\tau_\mathrm{w}} \right)^{+1/2} \frac{\mathrm{d}U}{\mathrm{d}Y}. \tag{2.23}$$

[3] Patel et al. (2016) derives the TL transformation without using a log-law condition. Instead, Patel et al. (2016) assumes that the semi-local scaling is the correct coordinate, based on their observational and theoretical reasoning given in Patel, Peeters, et al. (2015), and then applied the semi-local scaling to a similar stress balance condition as given in the previous section. The choice to assume that semi-local scaling's validity is the primary difference between how the TL transformation is derived in Trettel and Larsson (2016) and Patel et al. (2016). Instead, Trettel and Larsson (2016) presented the problem in a way where the coordinate itself was an unknown to be solved for rather than something already known. I follow that principle again here.

Here I assume that the value of the von Kármán constant κ is the same in both the constant-property and variable-property regimes. Physically this is the same as interpreting that the turbulent production mechanisms are the same in both regimes (a statement of Morkovin's hypothesis).[4]

The next step is to apply the chain rule to the velocity gradient to the variable-property equation:

$$\frac{1}{\kappa} = y\left(\frac{\varrho}{\tau_\mathrm{w}}\right)^{+1/2} \frac{\mathrm{d}u}{\mathrm{d}U}\frac{\mathrm{d}Y}{\mathrm{d}y}\frac{\mathrm{d}U}{\mathrm{d}Y}. \tag{2.24}$$

Finally, we set this equation equal to the constant-property version and set corresponding terms equal:

$$\frac{\mathrm{d}U}{\mathrm{d}Y}: \qquad y\left(\frac{\varrho}{\tau_\mathrm{w}}\right)^{+1/2} \frac{\mathrm{d}u}{\mathrm{d}U}\frac{\mathrm{d}Y}{\mathrm{d}y} = Y\left(\frac{\varrho_r}{\tau_\mathrm{w}}\right)^{+1/2}. \tag{2.25}$$

We yield a single equation relating the velocity transformation $\frac{\mathrm{d}U}{\mathrm{d}u}$ to the coordinate transformation $\frac{\mathrm{d}Y}{\mathrm{d}y}$:

$$\frac{\mathrm{d}U}{\mathrm{d}u} = \left(\frac{y}{Y}\right)\left(\frac{\varrho}{\varrho_r}\right)^{+1/2} \frac{\mathrm{d}Y}{\mathrm{d}y}. \tag{2.26}$$

It is easy to see how this equation extends the ideas behind the Van Driest transformation. For example, setting $Y = y$ recovers the Van Driest transformation. Again, the difference here is that we have an extra degree of freedom.

[4] For stably-stratified boundary layers, it is possible to derive an extension to the Monin-Obukhov similarity theory using the log-law condition described here, a Van-Driest transformed Monin-Obukhov similarity theory. See Williams et al. (2017). However, the derivation as given here is only appropriate for neutral atmospheric conditions.

2.5 The semi-local scaling

2.5.1 The transformed wall-normal coordinate

At this point, we have two equations (the velocity transformations as functions of the coordinate transformations) and two unknowns (the transformed velocity and coordinate), so we have a determined system. We can solve directly for the transformed coordinate by setting equation 2.18 and equation 2.26 equal:

$$\frac{\mathrm{d}U}{\mathrm{d}u} = \left(\frac{\mu}{\mu_r}\right)\frac{\mathrm{d}Y}{\mathrm{d}y} = \left(\frac{y}{Y}\right)\left(\frac{\varrho}{\varrho_r}\right)^{+1/2}\frac{\mathrm{d}Y}{\mathrm{d}y}\,. \tag{2.27}$$

From this equation, we can see that

$$\left(\frac{\mu}{\mu_r}\right) = \left(\frac{y}{Y}\right)\left(\frac{\varrho}{\varrho_r}\right)^{+1/2}\,. \tag{2.28}$$

Only one coordinate satisfies both conditions:

$$Y = Y_{\mathrm{SL}} = \left(\frac{\varrho}{\varrho_r}\right)^{+1/2}\left(\frac{\mu}{\mu_r}\right)^{-1} y\,. \tag{2.29}$$

This coordinate is known as the semi-local scaling Y_{SL} (more commonly referred to as "y-star" or y^* in conventional notation). It is more often given in terms of wall units as

$$Y_+ = Y_{\mathrm{SL},+} = \frac{\varrho\left(\tau_{\mathrm{w}}/\varrho\right)^{1/2} y}{\mu} = \frac{\left(\tau_{\mathrm{w}}\varrho\right)^{1/2} y}{\mu}\,. \tag{2.30}$$

This derivation involved many quantities — the velocities, Reynolds stresses, and shear stresses — so we should expect this coordinate to be the universal coordinate for all quantities that we have considered so far. This wall-normal coordinate is the same as the standard incompressible y-plus, but the density and viscosity are replaced with the local mean values. The shear stress, however, is based on the wall value. As a consequence, the variables considered as neither fully local nor fully based on the wall values — they are semi-local.

The semi-local scale has a storied history. In the early days of research into compressible turbulent boundary layers, the question of what wall-normal coordinate to use was up to debate. Using wall properties or local properties in y-plus were the most obvious choices, but wall properties quickly won out due to the success of skin friction formulations that use the Van Driest transformation, which uses wall properties (see equation 1.17). For example, a technical report (Lobb et al., 1955b) by the Naval Ordnance Laboratory on experimental measurements of hypersonic turbulent boundary layers considered both a standard coordinate and a semi-local coordinate, but only the plots using the standard coordinate were published in a more open journal article (Lobb et al., 1955a).

However, the semi-local scaling did have some theoretical support at the time over the standard wall-based scaling. For example, the similarity laws derived by Rotta (1959) explicitly used the semi-local scaling, though the plots only plotted curves as a function of the wall-based coordinate scaling. Rotta (1959, p. 267) argued that using local properties better represents the turbulence production mechanism. Consider this quote from the paper's English translation (Rotta, 1988, p. 10) given in modern, conventional notation:

> "[The mean velocity gradient equation] is based on the assumption that the mechanism of turbulence can be controlled by the local conditions; that is, that the quantity $-\overline{\varrho}\,\widetilde{u''v''}/\tau_\mathrm{w}$ is only a function of $\eta = \frac{y\sqrt{\tau_\mathrm{w}\overline{\varrho}}}{\overline{\mu}}$ and does not depend explicitly on Ma_τ and B_q." (Rotta, 1988, p. 10)

However, at the time, experimental evidence supported using a wall-based coordinate. Evidence against this idea did not emerge until later, when Huang et al. (1995) observed that using the semi-local scaling collapses the Reynolds stresses all onto the same curve when using Morkovin's scaling for the Reynolds stresses. Like Rotta (1959), Huang et al. (1995) argued through a heuristic and empirical method that the semi-local scaling matters:

> "Although there is no unique definition of y^+ that will collapse all compressible channel flow data, we find that y^* (which is based on τ_w and local properties) is perhaps the best among three possible definitions for the wall coordinate" (Huang et al., 1995, p. 187)

The understatement here obscures the fact that the collapse for the Reynolds stresses, published in Coleman et al. (1995), was almost perfect. Indeed, the observations by Huang et al. (1995) were key to re-discovering the semi-local scaling as a viable concept. However, the arguments in Rotta (1959) and Huang et al. (1995) about the importance of using local properties were incomplete, since they do not state a physical reason to support why local properties matter. Trettel and Larsson (2016) provides the reason why. The semi-local scaling is the only coordinate possible for a momentum-conserving log-law. If local properties are not used, then the coordinate does not conserve momentum in the log-law, and the transformed velocity and Reynolds stress profiles cannot match their constant-property counterparts.

2.5.2 The transformed friction Reynolds number

Now that we know the transformed coordinate, we can also determine the transformed friction Reynolds number. In compressible boundary layers, no single Reynolds number can fully characterize the flow (Kutateladze et al., 1964; Smits et al., 2006). As with incompressible flow, defining what length scale characterizes the flow is a problem — should we use the momentum thickness or the displacement thickness? — but the bigger issue now is that the density and viscosity values change, often by an order of magnitude, and that complicates what scales we think truly characterize the flow. Traditionally, researchers have used a Reynolds number based on the momentum thickness and edge values of density and viscosity (Kutateladze et al., 1964, pp. 10–11):

$$\mathrm{Re}_{\theta} = \frac{\varrho_{\mathrm{e}} u_{\mathrm{e}} \theta}{\mu_{\mathrm{e}}}. \tag{2.31}$$

Alternatively, the work of Walz (1969, p. 117) preferred to use the wall viscosity to better account for the friction at the wall:

$$\mathrm{Re}_{\delta_2} = \frac{\varrho_{\mathrm{e}} u_{\mathrm{e}} \theta}{\mu_{\mathrm{w}}}. \tag{2.32}$$

Researchers use both of these Reynolds numbers, and we can make solid arguments in favor of both, but in the context of our transformation theory, it is easier to think in terms of transformed friction Reynolds numbers. Just as with incompressible boundary layers, we evaluate the transformed dimensionless coordinate at the channel half-height or boundary layer thickness. This Reynolds number is known as the semi-local friction Reynolds number (more commonly called "R E tau star" or Re_{τ}^{*} in conventional notation).

For channels, the semi-local friction Reynolds number is

$$\mathrm{Re}_{\tau,\mathrm{eq}} = H_{+} = \frac{H}{\ell_{\nu}} = \frac{\varrho_{\mathrm{c}} \left(\tau_{\mathrm{w}}/\varrho_{\mathrm{c}}\right)^{1/2} h}{\mu_{\mathrm{c}}}. \tag{2.33}$$

For boundary layers, the semi-local friction Reynolds number is

$$\mathrm{Re}_{\tau,\mathrm{eq}} = \Delta_{+} = \frac{\Delta}{\ell_{\nu}} = \frac{\varrho_{\mathrm{e}} \left(\tau_{\mathrm{w}}/\varrho_{\mathrm{e}}\right)^{1/2} \delta}{\mu_{\mathrm{e}}}. \tag{2.34}$$

Note that the semi-local friction Reynolds number bears some similarities to the arguments by Walz (1969) that the friction at the wall matters in how we characterize the flow. This point is discussed more in Trettel and Larsson (2016).

Patel, Peeters, et al. (2015) and Patel et al. (2016) argue that instead of considering any single transformed friction Reynolds number, we must instead consider the range of local transformed friction Reynolds numbers, based on the local mean density and viscosity.[5] They created a variable to represent a point-wise transformed Reynolds number based on the idea of the semi-local scaling. Patel, Peeters, et al. (2015) and Patel et al. (2016) applied this idea exclusively to channels. They argue that since any compressible flow cannot be characterized by a single Reynolds number, the only way to truly match a transformed compressible flow to an equivalent incompressible flow is for its profile of local friction Reynolds numbers to match or at least behave similarly to the incompressible flow. A flow with a more constant profile of point-wise semi-local friction Reynolds numbers would behave more similarly to an incompressible flow. They defined the point-wise semi-local friction Reynolds number as

$$\mathrm{Re}_{\tau,\mathrm{local}} = \left(\frac{\varrho}{\varrho_r}\right)^{+1/2} \left(\frac{\mu}{\mu_r}\right)^{-1} \mathrm{Re}_\tau = \underbrace{\frac{\varrho \left(\tau_\mathrm{w}/\varrho\right)^{1/2} h}{\mu}}_{\text{for channels}} = \underbrace{\frac{\varrho \left(\tau_\mathrm{w}/\varrho\right)^{1/2} \delta}{\mu}}_{\text{for boundary layers}} \; . \tag{2.35}$$

They considered this concept important enough that they framed their version of the TL transformation in terms of this point-wise semi-local friction Reynolds number rather than in terms of the transformed coordinate (the semi-local scaling) or in terms of mean density and

[5] This concept was also considered earlier by Morinishi et al. (2004).

There is a theoretical issue with the idea of characterizing the flow with a range of Reynolds numbers rather than a single Reynolds number. The point of the transformation is to reduce the amount of information that we have to consider. An incompressible flow has a single friction Reynolds number, and ideally our compressible flow should have a single transformed friction Reynolds number. Considering a range of Reynolds numbers defeats the purpose of the transformation in the first place. The question is which Reynolds number characterizes the compressible flow as an equivalent incompressible flow. Only one can matter. So in practice we can identify a range of Reynolds numbers, but in theory only a single Reynolds number should suffice to characterize the flow.

viscosity.

The idea that the flow occupies a range of Reynolds numbers has merit, but evidence presented in section 2.8 suggests that using the single value of the semi-local friction Reynolds number (the transformed friction Reynolds number) suffices to identify the corresponding incompressible data for channels. Matching the entire profile of local transformed friction Reynolds number may be ideal but does not appear to be necessary.

The idea of a point-wise semi-local friction Reynolds number is limited to channels. These limitations are discussed in chapters 4 and 5.

2.6 Velocity transformation

We now have the transformed coordinate, so we can solve for the transformed velocity. We can start by taking the gradient of the transformed wall-normal coordinate:

$$\frac{\mathrm{d}Y}{\mathrm{d}y} = \left(\frac{\varrho}{\varrho_r}\right)^{+1/2} \left(\frac{\mu}{\mu_r}\right)^{-1} \left[1 + \frac{1}{2}\frac{1}{\varrho}\frac{\mathrm{d}\varrho}{\mathrm{d}y}y - \frac{1}{\mu}\frac{\mathrm{d}\mu}{\mathrm{d}y}y\right]. \tag{2.36}$$

We can now plug this into either equation 2.18 or 2.26 to get the velocity transformation:

$$\frac{\mathrm{d}U}{\mathrm{d}u} = \left(\frac{\varrho}{\varrho_r}\right)^{+1/2} \left[1 + \frac{1}{2}\frac{1}{\varrho}\frac{\mathrm{d}\varrho}{\mathrm{d}y}y - \frac{1}{\mu}\frac{\mathrm{d}\mu}{\mathrm{d}y}y\right]. \tag{2.37}$$

Just as before, we solve for the transformed velocity by integrating this equation with respect to the untransformed velocity:

$$U_+ = \int_0^{u_+} \left(\frac{\varrho}{\varrho_r}\right)^{+1/2} \left[1 + \frac{1}{2}\frac{1}{\varrho}\frac{\mathrm{d}\varrho}{\mathrm{d}y}y - \frac{1}{\mu}\frac{\mathrm{d}\mu}{\mathrm{d}y}y\right] \mathrm{d}u_+ = \int_0^{u} \left[1 + \frac{1}{2}\frac{1}{\varrho}\frac{\mathrm{d}\varrho}{\mathrm{d}y}y - \frac{1}{\mu}\frac{\mathrm{d}\mu}{\mathrm{d}y}y\right] \frac{\mathrm{d}u}{\sqrt{\tau_\mathrm{w}/\varrho}}. \tag{2.38}$$

At this point, we have all of the components of a complete transformation system. We can begin to test the transformation.

2.7 Alternative forms of the velocity transformation

The previous section presents only one way to represent the velocity transformation. Indeed, several different forms prove useful in different contexts.

2.7.1 Robust forms of the velocity transformation

Trettel and Larsson (2016) numerically tested out two forms of the TL transformation:

1. the previously given equation 2.38 (dubbed the "long form" of the transformation), and

2. equation 2.39 (dubbed the "short form" of the transformation).

The short form is

$$U_{\mathrm{TL},+} = \int_{0}^{u_+} = \left(\frac{\mu}{\mu_r}\right) \frac{\mathrm{d}Y_{\mathrm{SL},+}}{\mathrm{d}y_+} \mathrm{d}u_+ \,. \tag{2.39}$$

The short form has several advantages. This form only requires the user to calculate a single gradient rather than two gradients. More importantly, this form behaves much more robustly on sparse data sets — that is, data sets that do not have good near-wall resolution. The "long form" requires resolution below $y_+ \approx 5$, while the "short form" only requires resolution below $y_+ \approx 10$. This extra spacing may not seem like much, but it could make the transformation more useful on experimental data or on data from turbulence models.

All plots use the "short" form of the transformation in this dissertation.

2.7.2 Reduced forms of the velocity transformation

Patel et al. (2016) wrote the TL velocity transformation in terms of the point-wise semi-local Reynolds number as a way to consolidate the effects of property variation into a single variable.

This choice reduces the bracketed term in the transformation from a function of density and viscosity to only a single variable:

$$U_{\mathrm{TL},+} = \int_0^u \left[1 + \frac{y}{\mathrm{Re}_{\tau,\mathrm{local}}} \frac{\mathrm{dRe}_{\tau,\mathrm{local}}}{\mathrm{d}y}\right] \frac{\mathrm{d}u}{\sqrt{\tau_{\mathrm{w}}/\varrho}}. \tag{2.40}$$

The stated advantage to this form is that it reduces the transformation to a function of just a single variable, the point-wise local friction Reynolds number. According to this form, the difference between the TL transformation and the Van Driest transformation is due to changes in this point-wise semi-local friction Reynolds. Profiles with constant point-wise semi-local Reynolds numbers would then transform to the Van Driest transformation.

However, this form is not the simplest form possible, nor does it explain how the transformation relates to the changes in the flow geometry.

We can re-consider the "short form" of the transformation. We created the numerically robust form by using the stress-balance velocity transformation, but the log-law velocity transformation clarifies how the flow geometry affects the velocities:

$$\frac{\mathrm{d}U_{\mathrm{TL}}}{\mathrm{d}u} = \left(\frac{y}{Y_{\mathrm{SL}}}\right)\left(\frac{\varrho}{\varrho_r}\right)^{+1/2} \frac{\mathrm{d}Y_{\mathrm{SL}}}{\mathrm{d}y}. \tag{2.26}$$

We can re-arrange some terms to write it as

$$U_{\mathrm{TL},+} = \int_0^u \left(\frac{y}{Y_{\mathrm{SL}}}\right) \frac{\mathrm{d}Y_{\mathrm{SL}}}{\mathrm{d}y} \frac{\mathrm{d}u}{\sqrt{\tau_{\mathrm{w}}/\varrho}}. \tag{2.41}$$

This form of the transformation is simpler than the form given in Patel et al. (2016). It shows that we can explain the role of the bracketed term without resorting to creating new variables like the point-wise semi-local friction Reynolds number. Instead, the existing variables in the problem suffice. The bracketed term represents how much the transformation alters the flow's geometry — literally the local rate of change $\frac{\mathrm{d}Y_{\mathrm{SL}}}{\mathrm{d}y}$ divided by the overall rate of change $\frac{Y_{\mathrm{SL}}-0}{y-0}$.

When the semi-local scale equals the untransformed coordinate, then the flow geometry remains the same, and the TL transformation turns into the Van Driest transformation. Chapter 4 discusses other consequences of the semi-local scaling equaling the untransformed coordinate (in particular, how it relates to the outer layer coordinates).

2.8 Channel results

The TL transformation collapses compressible channel data onto the incompressible law-of-the-wall (Trettel and Larsson, 2016; Modesti et al., 2016; Patel et al., 2016). This phrasing is understated, but the TL transformation greatly improves upon the complete failure of the Van Driest transformation in channel flows.

Figure 2.1 depicts the TL-transformed velocity profile of a channel flow. The behavior depicted in this figure is consistent with the behavior of the transformation overall, but in this case the difference between the untransformed velocity profile and the transformed one is quite stark. In this figure, the transformed data is compared to an incompressible profile at the closest semi-local friction Reynolds number in the database. The two profiles match nearly perfectly, though if you look closely you will notice that the transformed profile slightly overshoots the incompressible reference profile around $Y_{\mathrm{SL},+} \approx 50$. Nonetheless, compared to the Van Driest transformation, the fit is what we should expect from a transformation.

We can observe the TL transformation's performance further by examining its momentum transfer properties. The stress balance for an constant-property flow is

$$T_{+} = \frac{\partial U_{+}}{\partial Y_{+}} - R_{XY,+} \,. \tag{2.42}$$

This equation proves useful as we examine figure 2.2, which depicts the shear stress terms

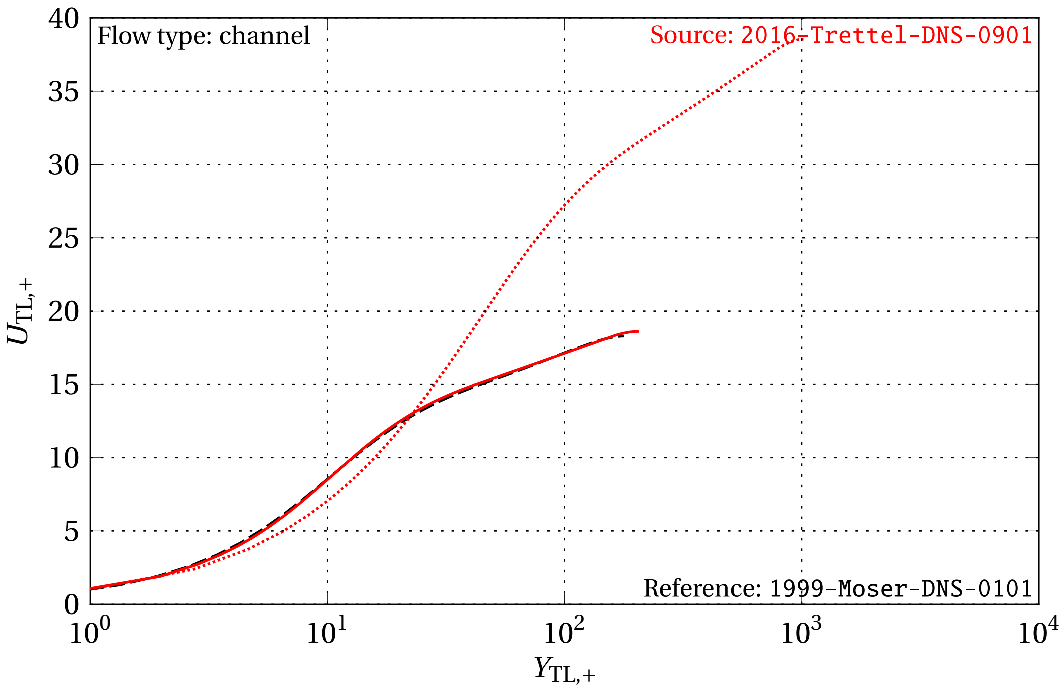

Figure 2.1: TL-transformed law-of-the-wall for `2016-Trettel-DNS-0901` at $Re_{\tau,eq} = 202.8$, compared to the incompressible reference of `1999-Moser-DNS-0101` at $Re_\tau = 178.1$. Solid red line, transformed profile; dotted red line, untransformed profile; dashed black line, incompressible reference.

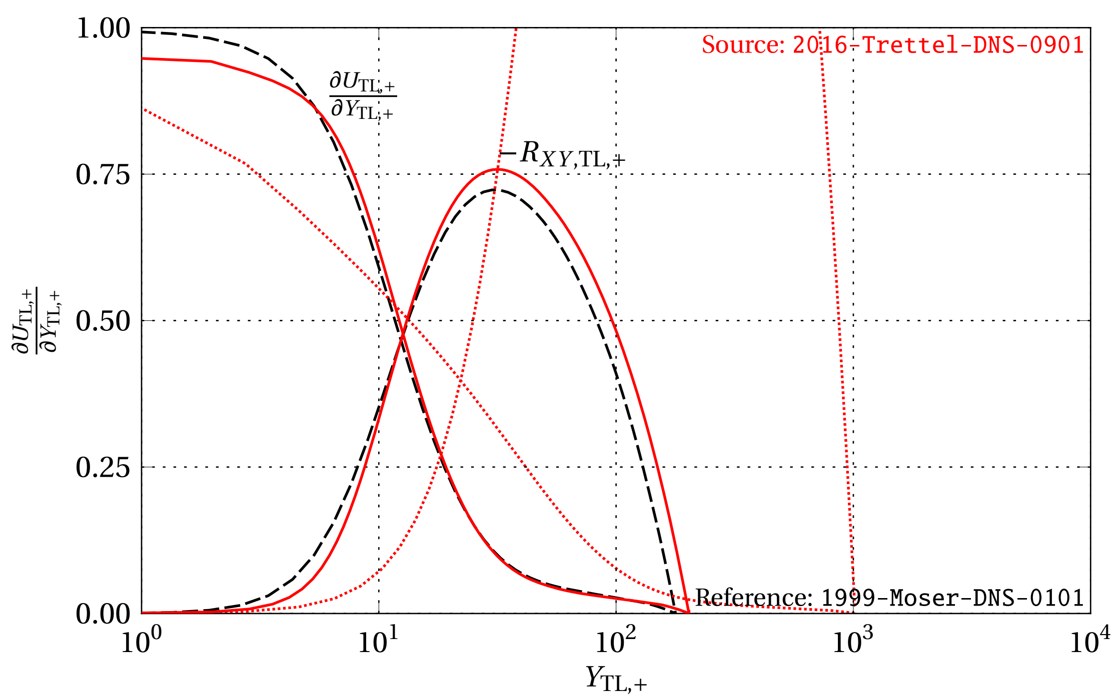

Figure 2.2: TL-transformed shear stress terms for `2016-Trettel-DNS-0901` at $\mathrm{Re}_{\tau,\mathrm{eq}} = 202.8$, compared to the incompressible reference of `1999-Moser-DNS-0101` at $\mathrm{Re}_\tau = 178.1$. Solid red line, transformed profile; dotted red line, untransformed profile; dashed black line, incompressible reference.

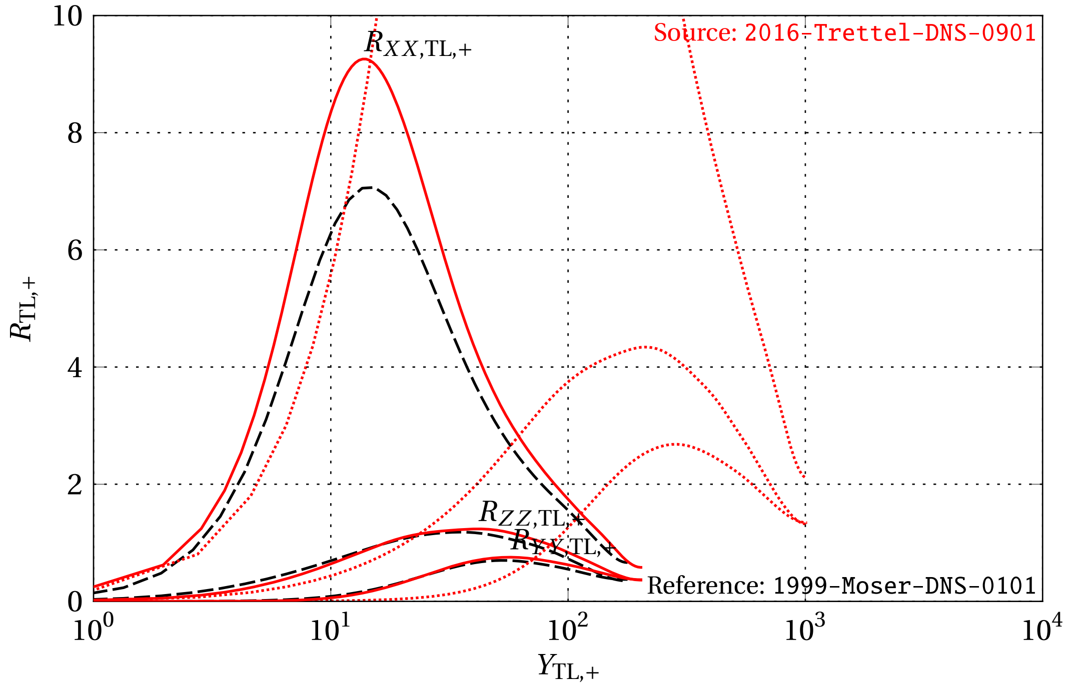

Figure 2.3: TL-transformed Reynolds normal stresses for `2016-Trettel-DNS-0901` at $\mathrm{Re}_{\tau,\mathrm{eq}} = 202.8$, compared to the incompressible reference of `1999-Moser-DNS-0101` at $\mathrm{Re}_\tau = 178.1$. Solid red line, transformed profile; dotted red line, untransformed profile; dashed black line, incompressible reference.

in this equation.[6] Unlike the law-of-the-wall plot, the disagreement here is more apparent. The transformed data and the incompressible reference match well, but the match here is by no means perfect as the law-of-the-wall plot implies.

The transformed velocity gradient generally matches well, with some minor undershoot in the viscous sublayer and some slight overshoot in the buffer layer. The untransformed velocity gradient is nowhere near as sharp as necessary; the transformation recovers that sharpness.

The transformed Reynolds shear stress matches the incompressible reference profile well. The combination of Morkovin's scaling for the Reynolds stresses and the semi-local scaling for the wall-normal coordinate works well here, as first observed by Huang et al. (1995). Some disagreement exists in the viscous sublayer — the transformed profile undershoots the incompressible reference — but in general any such errors are small.

Finally, figure 2.3 compares the Reynolds normal stresses to their incompressible counterparts, again using Morkovin's scaling and the semi-local scaling as determined by the TL theory. The match for the streamwise Reynolds normal stress ($\widetilde{u''u''}$) is poor. It is the only quantity that disagrees. Here the maximum value is much higher than expected based on the incompressible reference. This discrepancy has been observed elsewhere (Modesti et al., 2016) and appears to be a Mach-number effect (with some possible dependence on the wall heat transfer rate), though no mechanism has been established for the error. The other two transformed Reynolds normal stresses behave as expected, however.

[6] The slight difference in the viscous sublayer between the velocity gradient plots given here and the plots given in Trettel and Larsson (2016) is due to different numerical methods being used to calculate the gradients. The implementation had to change to allow for a more general procedure that works for a broader range of data sources. Nonetheless, the differences were small and did not affect the law-of-the-wall plots.

The results depicted here are only for a single case, but multiple studies for a broad range of Reynolds number and Mach numbers have confirmed these results for channels (Trettel and Larsson, 2016; Modesti et al., 2016; Patel et al., 2016). Boundary layers are where the real problems emerge instead.

2.9 Boundary layer results

While the TL transformation works well in channels, the results for boundary layer data range from decent performance to rather poor performance, especially farther from the wall, usually starting in the buffer layer, and at higher Mach numbers.

Figure 2.4 depicts the transformation as applied to a Mach 2 adiabatic wall boundary layer. Here, the transformation works decently, though not perfectly. The velocity profile does not match precisely — the log-law intercept is slightly too high — but in general the curves mirror each other. Some issues do appear in the outer layer of the flow. These are most apparent in the Reynolds shear stress and the streamwise Reynolds normal stresses, which are lower than the expected incompressible profile. However, from a practical point-of-view, the transformation works here.

Figure 2.5 depicts the transformation as applied to a Mach 4 adiabatic wall boundary layer. In this case, the error in the log-law intercept increases. This transformed velocity profile does not follow the incompressible law of the wall and diverges from it starting in the buffer layer. Again, both the Reynolds shear stress and streamwise Reynolds normal stresses are too low in the outer layer.

Figure 2.6 depicts the transformation as applied to a Mach 6 cold wall boundary layer. Just

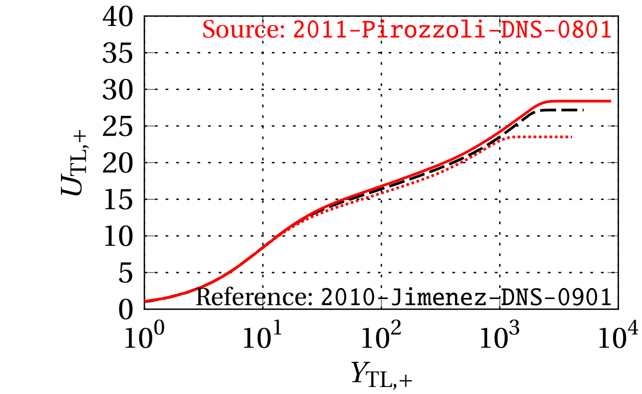

(a) Law-of-the-wall

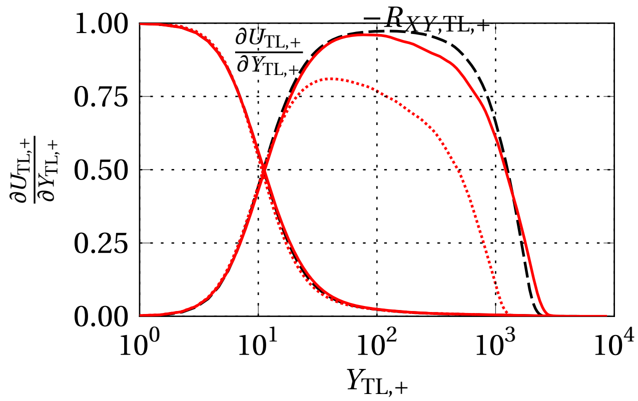

(b) Stress balance terms

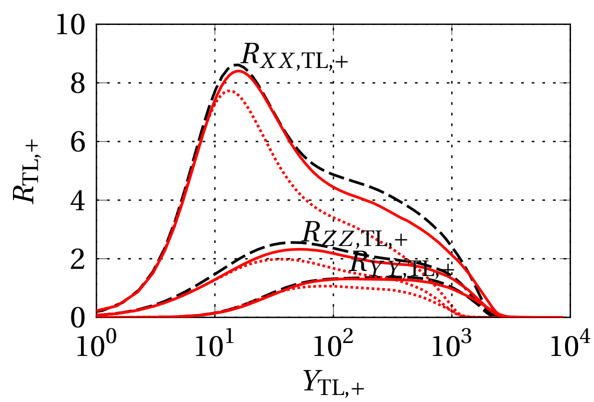

(c) Reynolds normal stresses

Figure 2.4: TL transformation for `2011-Pirozzoli-DNS-0801` at $\mathrm{Re}_{\tau,\mathrm{eq}} = 2289.4$, compared to the incompressible reference of `2010-Jimenez-DNS-0901` at $\mathrm{Re}_\tau = 1989.5$. Solid red line, transformed profile; dotted red line, untransformed profile; dashed black line, incompressible reference.

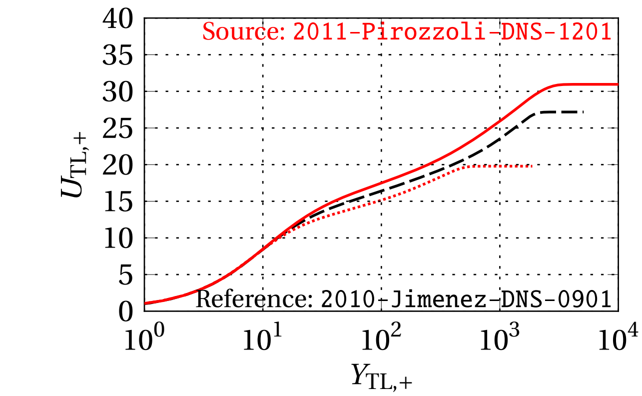

(a) Law-of-the-wall

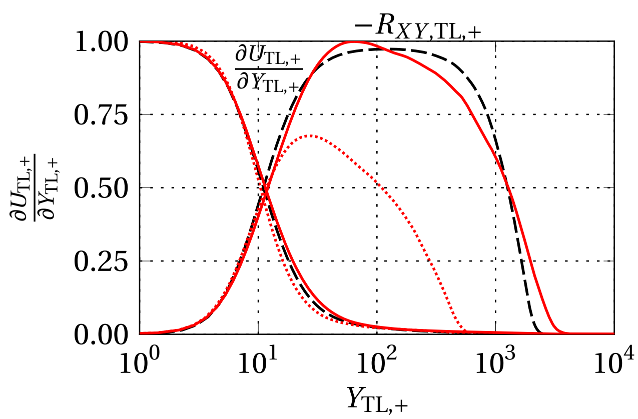

(b) Stress balance terms

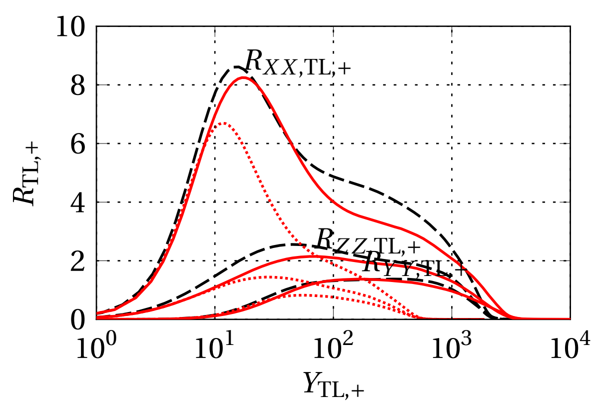

(c) Reynolds normal stresses

Figure 2.5: TL transformation for `2011-Pirozzoli-DNS-1201` at $\mathrm{Re}_{\tau,\mathrm{eq}} = 2755.0$, compared to the incompressible reference of `2010-Jimenez-DNS-0901` at $\mathrm{Re}_{\tau} = 1989.5$. Solid red line, transformed profile; dotted red line, untransformed profile; dashed black line, incompressible reference.

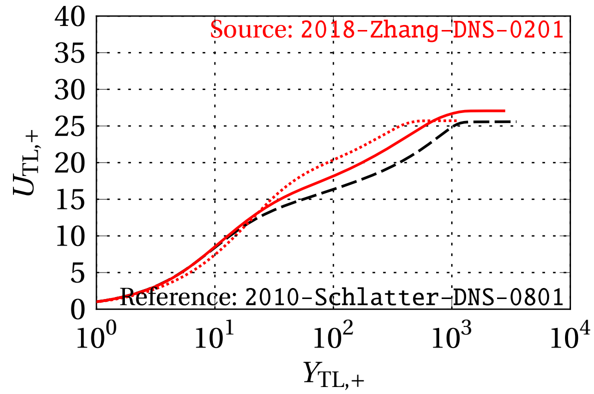

(a) Law-of-the-wall

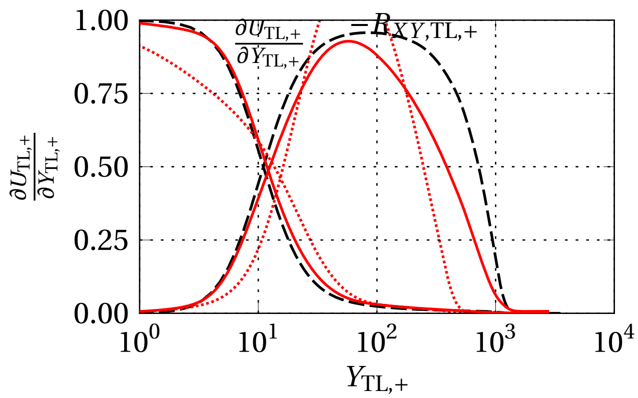

(b) Stress balance terms

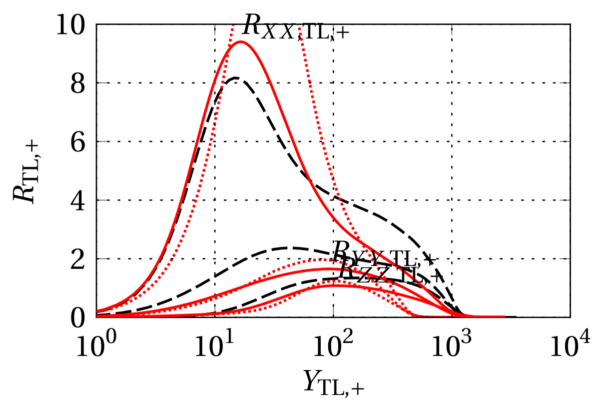

(c) Reynolds normal stresses

Figure 2.6: TL transformation for `2018-Zhang-DNS-0201` at $\mathrm{Re}_{\tau,\mathrm{eq}} = 1126.5$, compared to the incompressible reference of `2010-Schlatter-DNS-0801` at $\mathrm{Re}_{\tau} = 1145.2$. Solid red line, transformed profile; dotted red line, untransformed profile; dashed black line, incompressible reference.

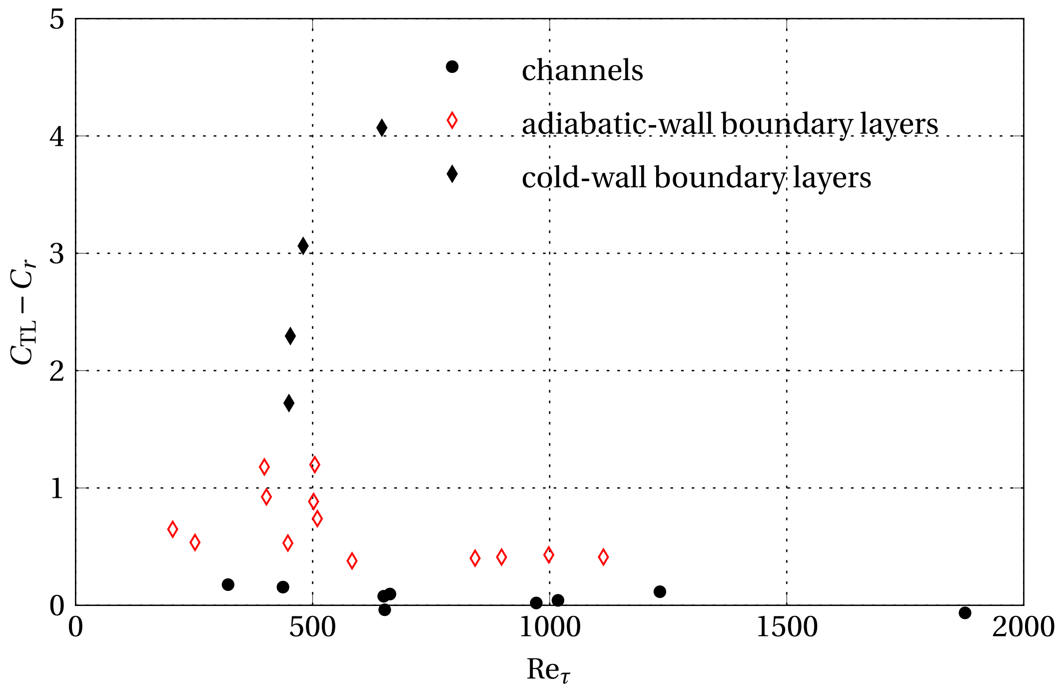

Figure 2.7: Change in the log-law intercept for the TL transformation as a function of the friction Reynolds number

as in the Mach 4 adiabatic wall case, the log-law intercept of the transformed velocity profile is too high, and the Reynolds stresses in the outer layer are too low. Here, however, we also notice that the streamwise Reynolds normal stress is too high at its peak, just like in the channel cases.

Despite these failures, I should note what works with the TL transformation. The velocity profile matches through the viscous sublayer and into the buffer layer, and the slope of the log-law reduces to the inverse of the von Kármán constant. These successes prove that the TL transformation does in fact perform just as well as the viscous sublayer and Van Driest transformations for the criteria that those transformations should individually match. The advantage here is that both criteria are satisfied in a single transformation.

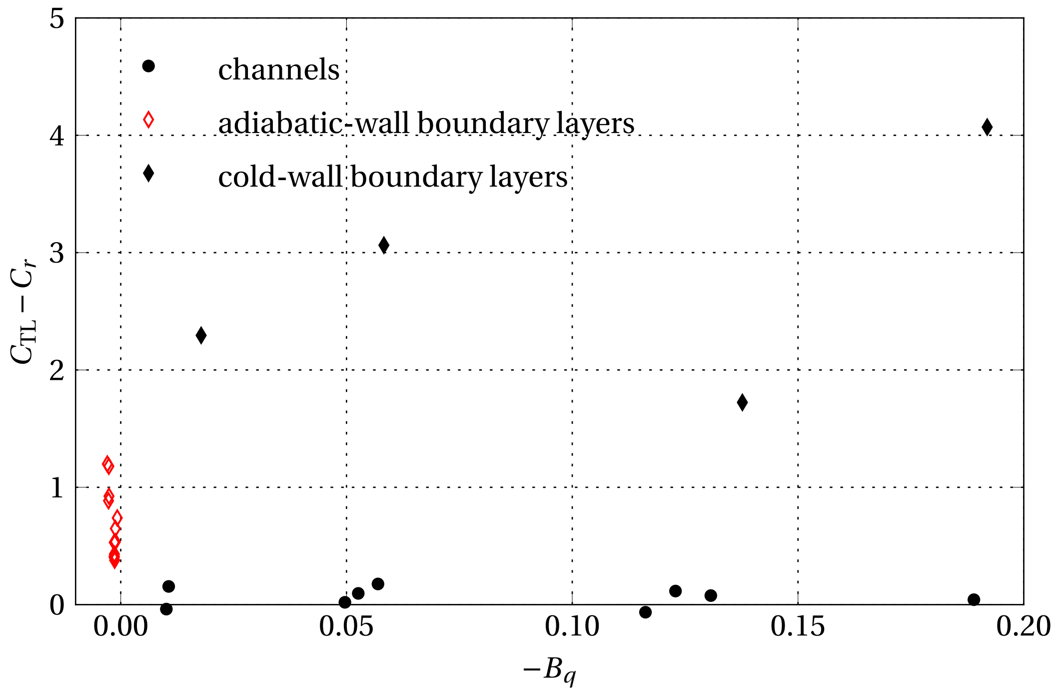

Figure 2.8: Change in the log-law intercept for the TL transformation as a function of dimensionless wall heat flux

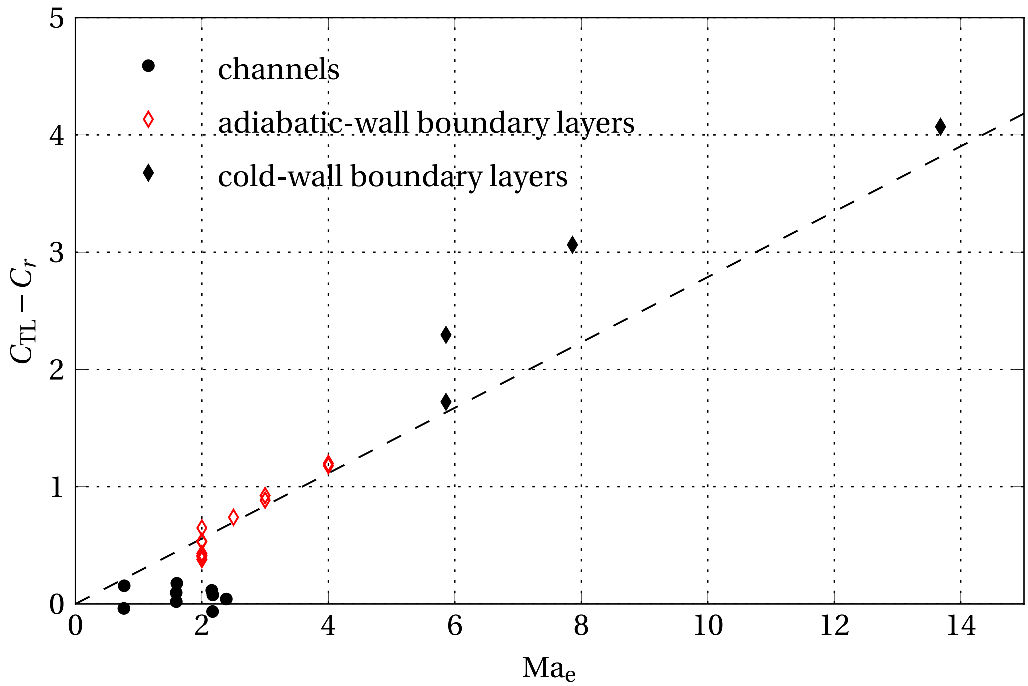

Figure 2.9: Change in the log-law intercept for the TL transformation as a function of the edge Mach number

While looking at multiple profiles can help, to explain the source of the error in this transformation requires us to look at the error over all available cases as a function of several variables. Figures 2.7 and 2.8 depict the error in the transformed log-law intercept plotted as a function of the friction Reynolds number and the dimensionless wall heat flux, respectively. In both cases, the error does not appear to be a function of these variables. Instead, these plots only appear to show distribution of the test cases rather than anything in particular. Note, however, that for all 9 channel cases considered, all from Trettel and Larsson (2016), the error is nearly zero. This shows that the error is in fact a function of the flow type more than anything else, according to these plots at least.

Figure 2.9 plots the error in the log-law intercept as a function of the edge Mach number. Here, however, we see a clear though scattered trend: the error increases with Mach number for boundary layers, but is generally small in channels. The variation around the trend line is due to Reynolds number effects. Take the string of symbols at Mach 2, for example. The error here decreases as the Reynolds number increases, though by no more than 0.5. This figure suggests that the source of the error is Mach-number dependent, but that is puzzling, since nothing derived here explicitly depends on the Mach number.

2.10 Missing pieces

The TL transformation offers a more modern take on the problem of developing an analogy between variable-property and constant-property wall turbulence, but the theory is incomplete in many ways. The theory does not work in large part for boundary layers, and we can potentially attribute this error to the theory's one-dimensionality. It treats the shear flow as being a function only of the wall-normal coordinate. For boundary layers, this assumption is unrealistic. It ignores mass conservation, the spatial development of the flow, and assumes largely that the streamwise coordinate itself plays no role in the analysis.[7] Indeed, the theory here did not specify anything about the nature of the spatial development or the streamwise coordinate, and mass conservation has not even been discussed until now. Moreover, the theory also only specifies the Reynolds stress scaling for the Reynolds shear stress, but it is clear that using this same scaling on the streamwise Reynolds normal stress does not match the peaks correctly. In many respects, the TL theory is missing several vital pieces, and we should seek those pieces as we develop new theories.

[7] Some authors (Morinishi et al., 2004; Modesti et al., 2019) have assumed a semi-local streamwise coordinate. This idea may be useful but it enjoys no theoretical support, at least from the analysis in this chapter.

Chapter 3

Morkovin's hypothesis and the production rates

3.1 The definition of Morkovin's hypothesis

Note: this section uses conventional notation rather than the regime-dependent notation.

3.1.1 Compressibility effects in turbulent boundary layers

What is a "compressibility effect?" Typically the term "compressibility effect" refers to phenomena that depend on the mean dilatation rate $\frac{\partial \tilde{u}_i}{\partial x_i}$ or on the Mach number $\mathrm{Ma_e}$. In many situations, the mean dilatation rate and Mach number go hand in hand — a nonzero Mach number means a nonzero mean dilatation rate — but in boundary layers, the mean dilatation rate can be small even when the Mach number is supersonic. This observation leads to Morkovin's hypothesis (Morkovin, 1962), which is a statement about the turbulence production mechanisms in compressible turbulent boundary layers.[1] The simplest definition of Morkovin's hypothesis is the hypothesis that "the turbulence structure is unaffected by compressibility" (Bradshaw and Ferriss, 1971, p. 83), but this short definition does not capture all of the nuance in such a terse statement.

For compressible turbulent boundary layers, there are two main compressibility effects: the effects of compressibility on the mean flow, and the effects of compressibility on the turbulence. Typically the Mach number controls the effects of compressibility on the mean flow. Consider the Walz equation, which approximately relates the temperature and velocity fields for flows of perfect gases (Walz, 1969, p. 69):

$$\frac{\widetilde{T}}{T_\mathrm{e}} \approx \frac{T_\mathrm{w}}{T_\mathrm{e}} + \left(\frac{T_\mathrm{r} - T_\mathrm{w}}{T_\mathrm{e}}\right)\left(\frac{\widetilde{u}}{u_\mathrm{e}}\right) - \frac{1}{2} r \left(\gamma - 1\right) \mathrm{Ma}_\mathrm{e}^2 \left(\frac{\widetilde{u}}{u_\mathrm{e}}\right)^2. \tag{3.1}$$

Here the Mach number directly controls for the amount of temperature variation (and hence the amount of density variation). As a result, the greater the Mach number, the more that the mean density varies throughout the flow.

Note that mean density variation is a mean flow compressibility effect. Morkovin's hypothesis does not deal with the effect of compressibility on the mean flow, but the effect of compressibility on the turbulence structure. In short, Morkovin (1962) argued that for non-hypersonic boundary layers compressibility does not a play a role in the turbulence production. All of the data at the time was "consistent with the idea of the M-independence of the basic mechanisms" (Morkovin, 1962, p. 379). To see how compressibility affects the turbulence itself, consider the Reynolds stress transport equation for compressible flows (Cebeci

[1] Note that Morkovin himself argued that it should be the "Morkovin-Bradshaw hypothesis" (Morkovin, 1992, p. 279) to recognize Peter Bradshaw's work on the idea, but that term has not gained popularity.

and Smith, 1974, pp. 58–59):

$$
\begin{aligned}
\frac{\partial}{\partial t}\left(\overline{\varrho u_i'' u_j''}\right) + \widetilde{u}_k \frac{\partial}{\partial x_k}\left(\overline{\varrho u_i'' u_j''}\right) &= -\overline{u_j'' \frac{\partial P}{\partial x_i}} - \overline{u_i'' \frac{\partial P}{\partial x_j}} + \overline{u_j'' \frac{\partial \tau'_{ik}}{\partial x_k}} + \overline{u_i'' \frac{\partial \tau'_{jk}}{\partial x_k}} \\
&\quad - \overline{\varrho u_i'' u_k''}\frac{\partial \widetilde{u}_j}{\partial x_k} - \overline{\varrho u_j'' u_k''}\frac{\partial \widetilde{u}_i}{\partial x_k} - \underbrace{\overline{\varrho u_i'' u_j''}\frac{\partial \widetilde{u}_k}{\partial x_k}}_{\text{Compressibility effects}} - \frac{\partial}{\partial x_k}\left(\overline{\varrho u_i'' u_j'' u_k''}\right).
\end{aligned}
\tag{3.2}
$$

This equation is rather long, but only one single term, marked as "Compressibility effects" involves the mean dilatation rate. In isolation, this term demonstrates that expansion $\frac{\partial \widetilde{u}_i}{\partial x_i} > 0$ decreases the turbulent kinetic energy and that compression $\frac{\partial \widetilde{u}_i}{\partial x_i} < 0$ increases the turbulent kinetic energy (Bradshaw, 1974, p. 462). This interpretation agrees with data on the shock-turbulence interaction, where isotropic turbulence is advected through a normal shock. The normal shock compresses the flow and the turbulent kinetic energy increases accordingly (Larsson et al., 2013).

What controls the mean dilatation rate in channels and boundary layers? The mean dilatation rate in channel flows is always identically zero. This is due to the lack of spatial development and the no-flow-through boundary condition on the walls.

The mean dilatation rate in boundary layers is not identically zero but in many cases is small. Zero-pressure-gradient boundary layers do not have distinct regions of expansion or compression (as in the case of a shock wave), so their mean dilatation rate is small for non-hypersonic Mach numbers. Boundary layers with pressure gradient may have regions of mean expansion or compression. Bradshaw (1974, p. 457) argues (using an approximation) that the mean dilatation rate divided by the velocity gradient scales with the pressure gradient times the edge Mach number squared. As a consequence, provided that the Mach number is small enough, the mean dilatation rate is small compared to the rate of shear (velocity gradient), regardless of the pressure gradient (though the pressure gradient does play a role). Numerical results for zero-pressure-gradient boundary layers support the idea that the mean dilatation is small compared to the rate of shear. Lagha et al. (2011) measured the dilatation rate probability-density function (PDF) using direct numerical simulations of adiabatic wall boundary layers up to $\mathrm{Ma_e} = 20$. The PDF widens as the Mach number increases, and the width of the PDF scales with mean density. The PDF is largely symmetric about zero dilatation rate for non-hypersonic Mach numbers, but it skews negative slightly for $\mathrm{Ma_e} = 20$. Alvarez (2017) ran direct numerical simulations of rough-wall adiabatic wall boundary layers, and generally encountered mean dilatation rate values an order-of-magnitude smaller than the mean rate of shear (edge velocity divided by the boundary layer thickness) for simulations up to $\mathrm{Ma_e} = 5$. All of these observations agree with the notion that the mean dilatation rate is small for non-hypersonic boundary layers.

The compressibility effects in the Reynolds stress transport equation involve the mean dilatation rate rather than the Mach number itself, so it is possible for the Mach number to be supersonic but the dilatation rate term to be negligible. As a result, for boundary layers we can assume that each production mechanism is roughly analogous to its incompressible production mechanism, just with mean density variation. We can assume this equivalence since no direct compressibility effect remains in the equations; the only indirect one left is through mean density variation. In general, there is no intrinsic compressibility effect in the turbulence production, provided that the Mach number is non-hypersonic.

In review, we can now see that the Mach number effects appear to affect the mean flow first, but since the mean dilatation rate is small even at supersonic Mach number, the effects of compressibility on the turbulence itself may be negligible in compressible turbulent boundary layers until the flow becomes hypersonic. As a result, the turbulence production mechanisms become variable density extensions of their incompressible counterparts.

3.1.2 The role of thermodynamic fluctuations

So far we have considered only how compressibility affects the mechanical aspects of turbulence. Since we are speaking of compressible flow, we also need to consider how compressibility affects the thermodynamic and transport aspects of the turbulence as well, specially how it affects the temperature, density, and viscosity fluctuations. In incompressible turbulent boundary layers without heat transfer these fluctuations are by definition identically zero, but in compressible turbulent boundary layers they are small and negligible when compared to their mean values, provided we are discussing non-hypersonic boundary layers.

The usual way to see the negligibility of thermodynamic fluctuations is through Morkovin's strong Reynolds analogy (Morkovin, 1962). If we assume that the total temperature ($T_{\mathrm{tot}} = T + \frac{1}{2}V^2/c_p$) fluctuations are negligible, we can develop a rough approximation connecting the level of velocity fluctuations to the level of temperature fluctuations (Morkovin, 1962; Cebeci and Bradshaw, 1984):

$$\frac{T'}{\overline{T}} \approx -\left(\gamma - 1\right)\overline{\mathrm{Ma}}^2 \frac{u'}{\overline{u}}. \tag{3.3}$$

This equation is quite crude, but its trends for non-hypersonic flow do bear out.[2] Provided

[2] This equation implies that the temperature fluctuations grow without bound as the Mach number increases. This growth could technically result in negative absolute temperatures, so Morkovin's strong Reynolds analogy falls apart at higher Mach numbers. The temperature fluctuations cannot grow without limit as the Mach number increases.

Rotta (1963) developed an empirical equation based on the experiments by Kistler (1959) that avoids this issue:

$$\overline{(T')^2}_{\mathrm{peak}}/\overline{T} \approx 10\mathrm{Ma}_\tau^2.$$

that the local mean Mach number is small, the temperature fluctuations would be small too, even if the velocity fluctuations are large. Note that for a boundary layer, the local mean Mach number is always small near the wall, since the velocity approaches zero at the wall.

This equation is useful because we can connect the temperature fluctuations to density fluctuations or viscosity fluctuations using the linearized small fluctuations formula from the ideal gas law ($\varrho'/\overline{\varrho} \approx -T'/\overline{T}$) or, as it was done for mean viscosity in equation 1.16, using a Taylor series expansion.[3]

Regardless of how we calculate the fluctuation levels, we see that the for non-hypersonic Mach numbers, the level of thermodynamic and transport fluctuations is small when compared to their mean values. This observation has already been used in the derivation of the stress balance equation used previously in the TL transformation, which assumes that the viscosity fluctuations are much smaller than the mean viscosity value.

In the past, this observation has been used to physically justify that the turbulence production mechanisms do not depend on compressibility for non-hypersonic Mach numbers (Bradshaw, 1967; Bradshaw and Ferriss, 1971). The idea here is that if the density fluctuations are small enough, then the turbulent momentum transfer occurs largely through the same means as in incompressible flow, the only difference being mean density variation. This view is no longer necessary due to the popularization of density-weighted averaging in the 1970s, after Morkovin's work in the early 1960s. If density-weighted averaging is used, it is no longer

The friction Mach number $\mathrm{Ma}_\tau = u_\tau / a_\mathrm{w}$ never exceeds 0.3, so this equation cannot suffer from negative absolute temperatures. In the end, we should treat Morkovin's strong Reynolds analogy as a decent approximation for non-hypersonic Mach numbers but be wary of some of its implications.

[3] See Ievlev (1975, pp. 93–94) for an example of calculating the density fluctuations through a Taylor series expansion.

necessary to invoke that the density fluctuations are small, since we can always extract the mean density from any term involving it. As a consequence, all equations look similar to their incompressible counterparts, just with variable mean density. There is no longer a need to require that the density fluctuations are small, though it still is necessary to invoke that for other quantities like viscosity fluctuations.

3.1.3 A working definition of Morkovin's hypothesis

This section serves to explain the nature of compressibility effects in compressible turbulent boundary layers, but the primary purpose of this section is to drill down what Morkovin's hypothesis means to such a degree that we can develop a mathematical analogy out of it — to turn it into a series of equations. To that end, here is my working definition of Morkovin's hypothesis:

> The turbulence production mechanisms are the same in incompressible and compressible turbulent boundary layers. There is no intrinsic turbulence production mechanism driven by compressibility (the dilatation rate or Mach number) in boundary layers, provided that the Mach number is non-hypersonic.

There are many definitions of Morkovin's hypothesis. This definition may not encompass everything about Morkovin's hypothesis for all people, but it is useful because I can take it literally and re-write it directly in terms of mathematics. This definition also interprets Morkovin's hypothesis as an analogy between the turbulence production mechanisms in incompressible turbulent boundary layers and compressible turbulent boundary layers. This interpretation works well here, since we are developing analogies between incompressible and compressible wall turbulence, but strictly speaking it is only one interpretation of Morkovin's hypothesis.

As we will see in the rest of this chapter, Morkovin's hypothesis as stated here is about the analogy between the production mechanisms in incompressible and compressible flow but not an equivalence of the production rates (equal opportunity but not equal outcomes). The production rates are not equivalent. Instead, we see that the production rates are scaled by the mean viscosity variation, and that near the wall the shear stress must be untransformed or else the production rates do not match (and Morkovin's scaling would not work).

3.2 The scaling of production rates

Now that we have a working definition of Morkovin's hypothesis, we can consider how it affects the production rates. Like in the TL transformation, we will treat the boundary layer as a one-dimensional shear flow. In a one-dimensional shear flow there is only a single production term, p_{xy}. In boundary layers, there are four production terms. We will transform this single production rate term while assuming momentum conservation through a modified stress balance equation (modified to allow for shear stress transformations).

3.2.1 Stress balance conditions that allow for shear stress transformations

We can start by re-considering the total shear stress equation, equation 2.8. This time around, instead of setting the equation to zero and creating three terms to match, we will set it equal to 1 and create two terms to match. The resulting equation for the variable-property regime is

$$1 = \left(\frac{\mu}{t}\right)\frac{\mathrm{d}u}{\mathrm{d}y} - \frac{\varrho r_{xy}}{t}\,. \tag{3.4}$$

The point of this re-scaling is to try to match the ratio of the viscous term over the total shear stress and the ratio of the Reynolds stress term over the total shear stress, rather than trying to match each component individually. This adjustment provides an additional degree of freedom and lets us examine how good the assumption that $T = t$ really is.

The constant-property counterpart to this equation is

$$1 = \left(\frac{\mu_r}{T}\right)\frac{\mathrm{d}U}{\mathrm{d}Y} - \frac{\varrho_r R_{XY}}{T}\,. \tag{3.5}$$

The next step is to apply the chain rule to the variable-property equation to write it in terms of constant-property variables:

$$1 = \left(\frac{\mu}{t}\right)\frac{\mathrm{d}u}{\mathrm{d}U}\frac{\mathrm{d}Y}{\mathrm{d}y}\frac{\mathrm{d}U}{\mathrm{d}Y} - \frac{\varrho r_{xy}}{t}\,. \tag{3.6}$$

Finally, we set each corresponding component of this equation equal to its constant-property counterpart:

$$\frac{\mathrm{d}U}{\mathrm{d}Y}: \qquad \left(\frac{\mu}{t}\right)\frac{\mathrm{d}u}{\mathrm{d}U}\frac{\mathrm{d}Y}{\mathrm{d}y} = \left(\frac{\mu_r}{T}\right), \tag{3.7}$$

$$R_{XY}: \qquad -\frac{\varrho r_{xy}}{t} = -\frac{\varrho_r R_{XY}}{T}\,. \tag{3.8}$$

Unlike the previous derivation, this decomposition results in two equations. We will write these in terms that do not make sense now but are more directly useful for the next stage of the derivation:

$$\frac{\mathrm{d}u}{\mathrm{d}U}\frac{\mathrm{d}Y}{\mathrm{d}y} = \left(\frac{\mu_r}{\mu}\right)\left(\frac{t}{T}\right), \tag{3.9}$$

$$r_{xy} = \left(\frac{\varrho_r}{\varrho}\right)\left(\frac{t}{T}\right)R_{XY}\,. \tag{3.10}$$

3.2.2 The production rate equation

Now, we should consider the only production mechanism in this simple one-dimensional shear flow. The only production term of the turbulent kinetic energy equation is

$$p_{xy} = -\varrho r_{xy} \frac{\mathrm{d}u}{\mathrm{d}y} \,. \tag{3.11}$$

If we apply the chain rule to this equation and then apply the previous results from the stress balance equation, we can write the variable-property production rate in terms of the constant-property production rate:

$$p_{xy} = \left(\frac{\mu_r}{\mu}\right)\left(\frac{t}{T}\right)^2 \left[-\varrho_r R_{XY} \frac{\mathrm{d}U}{\mathrm{d}Y}\right] = \left(\frac{\mu_r}{\mu}\right)\left(\frac{t}{T}\right)^2 P_{XY} \,. \tag{3.12}$$

The production rates between the two regimes are not the same. My working definition of Morkovin's hypothesis posits that the production mechanisms are the same, but it allows for the precise production rates to vary between the two regimes. We see that idea play out here. What this means is that the production rates must be transformed to recover the proper incompressible behavior. The transformed production rate as a function of the untransformed production rate is

$$P_{XY} = \left(\frac{\mu}{\mu_r}\right)\left(\frac{T}{t}\right)^2 p_{xy} \,. \tag{3.13}$$

This equation states that two variables affect how the production rates change between the two regimes: the mean viscosity and the transformed shear stress.

Classical turbulence theory posits that viscosity is unimportant, only serving to dissipate energy in the small scales. Viscosity's presence here seemingly breaks that idea, though a more nuanced view supports the old ideas. The production terms are the product of a Reynolds stress and a velocity gradient. Without considering mean momentum conservation, the mean viscosity would not appear in this equation. This observation means that the viscosity appears here due to the velocity gradient and not the Reynolds stress term (we can see that in the two equations from the previous section). Moreover, this theory does not actually state that viscosity itself matters in affecting the turbulence structure. It merely states that mean viscosity variation matters, the amount that the mean viscosity deviates from the reference state, since that changes the momentum transfer.

The production rate transformation is a direct function of the shear stress transformation T/t. In the TL transformation, the transformed shear stress equals the variable shear stress, but this property is just an assumption. In that case, the production rate scaling is

$$P_{XY} = \left(\frac{\mu}{\mu_r}\right) p_{xy}. \tag{3.14}$$

This production rate transformation allows us to examine the validity of this assumption. In the next section, we will observe that the shear stresses do not need to be transformed, at least fairly close to the wall, for either boundary layers or channels. The viscous scaling matches the peak in the production profile in the buffer layer sufficiently.

3.3 Results

In this section, I will examine the transformed and untransformed production rates for various boundary layers in the database. Each figure will plot the untransformed production rate, the reference production rate, the re-scaled production plotted in untransformed coordinates (according to the viscous scaling in 3.14), and the TL-transformed production rates (which obey the stress balance and assume no shear stress transformation).

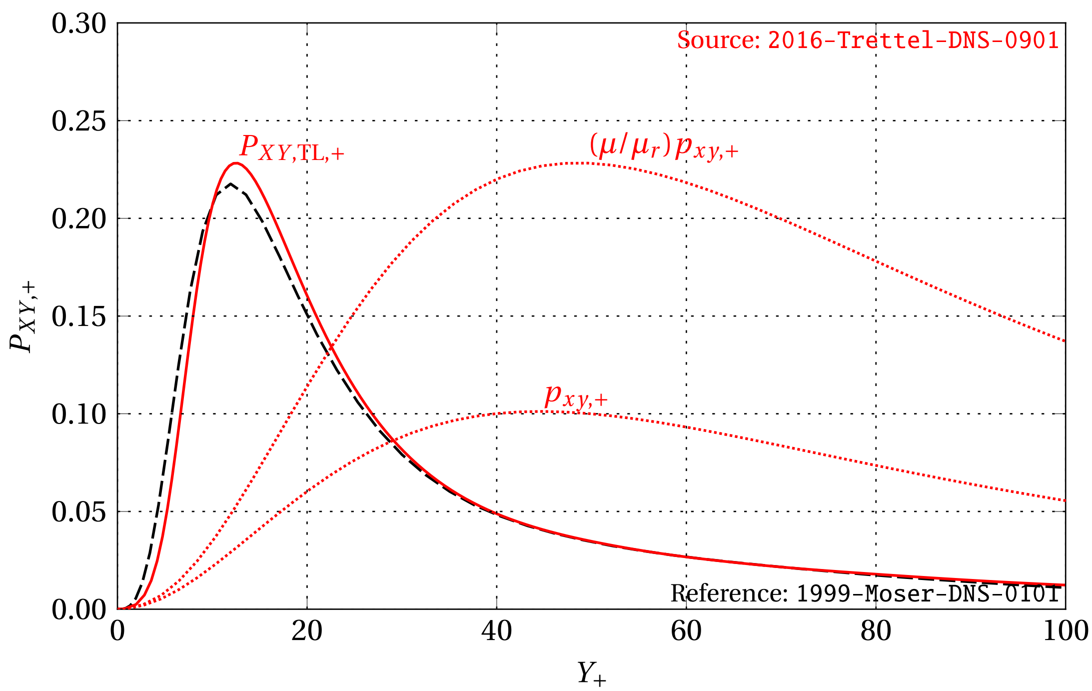

Figure 3.1: Transformed, re-scaled, and untransformed production rates the channel case of `2016-Trettel-DNS-0901` compared to the incompressible reference case of `1999-Moser-DNS-0101`. Solid red line, TL-transformed production rates; first dotted red line, untransformed production rates; second dotted red line, untransformed production rates re-scaled using viscosity ratio; dashed black line, incompressible reference.

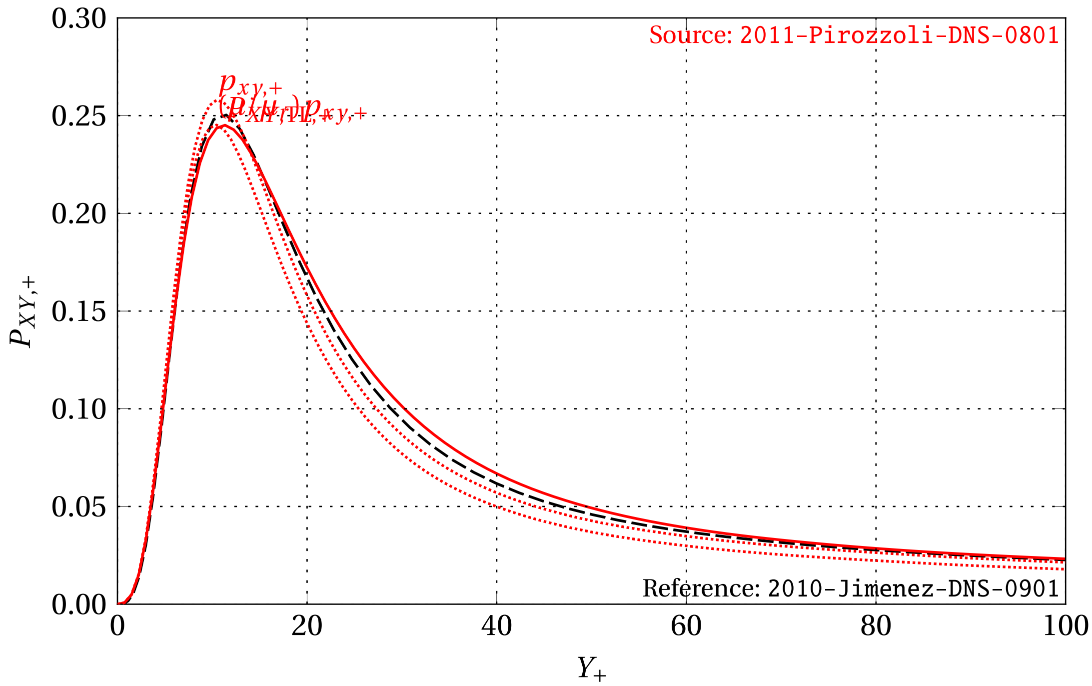

Figure 3.2: Transformed, re-scaled, and untransformed production rates the boundary layer case of `2011-Pirozzoli-DNS-0801` compared to the incompressible reference case of `2010-Jimenez-DNS-0901`. Solid red line, TL-transformed production rates; first dotted red line, untransformed production rates; second dotted red line, untransformed production rates re-scaled using viscosity ratio; dashed black line, incompressible reference.

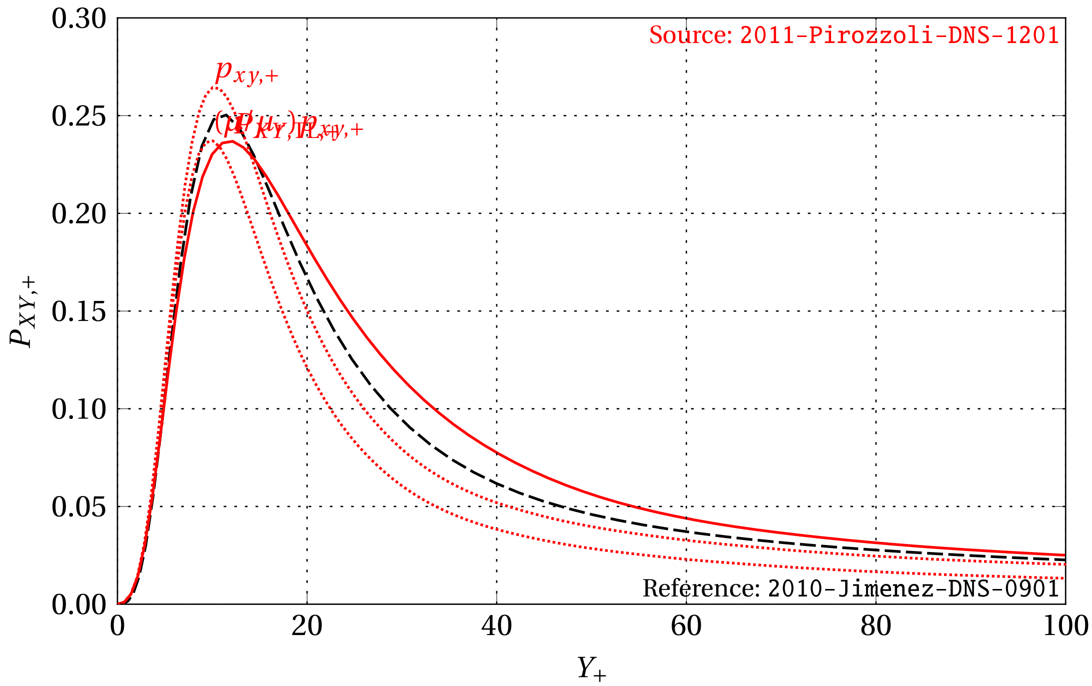

Figure 3.3: Transformed, re-scaled, and untransformed production rates the boundary layer case of `2011-Pirozzoli-DNS-1201` compared to the incompressible reference case of `2010-Jimenez-DNS-0901`. Solid red line, TL-transformed production rates; first dotted red line, untransformed production rates; second dotted red line, untransformed production rates re-scaled using viscosity ratio; dashed black line, incompressible reference.

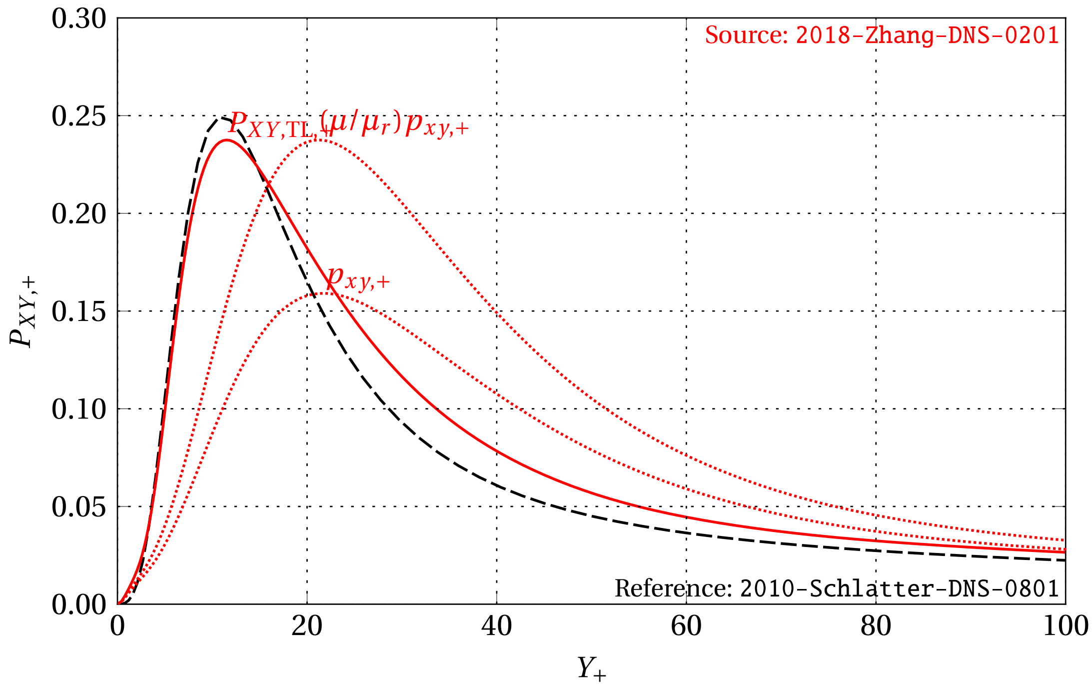

Figure 3.4: Transformed, re-scaled, and untransformed production rates the boundary layer case of `2018-Zhang-DNS-0201` compared to the incompressible reference case of `2010-Schlatter-DNS-0801`. Solid red line, TL-transformed production rates; first dotted red line, untransformed production rates; second dotted red line, untransformed production rates re-scaled using viscosity ratio; dashed black line, incompressible reference.

The clearest and best results are given for channels. Consider figure 3.1. In this figure, the peak of the untransformed production rate is no longer in the buffer layer. Plotting this using the semi-local scaling correctly adjusts the peak's location to the buffer layer. We can also see that the viscous production scaling recovers the correct magnitude of the peak at this Reynolds number, as plotted in the re-scaled curve. The TL transformation does both of these, and in general the TL-transformed production rates fit the incompressible reference production rates well, with some disagreement in the viscous sublayer, but nearly perfect agreement farther from the wall.

Note that for the assumption that the shear stress is not transformed works well here for all parts of the flow. We could interpret any error in this plot to being from that assumption, but because the error is small, that assumption holds up.

For boundary layers, the results are more mixed. In general, we see that the TL transformation correctly matches the magnitude and location of the production rate's peak in the buffer layer, but the agreement falls apart farther from the wall. Figure 3.2 plots the results for a Mach 2 adiabatic wall boundary layer, and figure 3.3 plots the results for a Mach 4 adiabatic wall boundary layer. Near the wall the lines are indistinguishable, providing some evidence that the heat flux at the wall does appear to play a role, and that the viscous scaling does not fully capture this effect. As already stated, in both cases the magnitude and location of the peak agrees well with the incompressible data, but the agreement falls apart at higher Mach numbers and farther from the wall.

The same trends occur for cold wall boundary layers. Figure 3.4 depicts the production rates in a cold wall boundary layer. The agreement in the viscous sublayer is slightly worse than in the adiabatic wall case — again pointing to some effect due to wall heat transfer — but the peak's magnitude and location match well. Farther away from the wall, the agreement is worse.

For the boundary layers, we can also see the validity in assuming that the shear stress is untransformed, but we cannot eliminate the possibility that farther from the wall, the shear stress does require a transformation.

What conclusions can we draw about Morkovin's hypothesis from these results? The idea of Morkovin's hypothesis as an analogy between the turbulence production mechanisms, but not the production rates, holds up, especially close to the wall and in channels. The results also demonstrate that the mean viscosity variation does in fact affect the production rates and alters them from their expected incompressible values. The disagreement of the production rates in boundary layers farther from the wall could be from ignoring all of the production mechanisms. Here, we only considered the most important one, but 3 others exist in boundary layers and require that we treat the flow fundamentally as a two-dimensional flow. Chapter 5 re-derives the TL transformation under a two-dimensional framework and therefore includes these additional production mechanisms in its derivation.

Chapter 4

Outer layer effects

The results of chapters 2 and 4 suggest that the TL transformation does not perform well in the outer layers of boundary layers. In this chapter, I will explore the properties that any transformation must satisfy to work in the outer layer. I will then evaluate how well the TL transformation obeys these properties.

4.1 Self-similarity

Boundary layers often obey a rough form of self-similarity. Each profile looks quite similar to any other profile, so often self-similarity greatly simplifies how we interpret boundary layers. We therefore should consider how self-similarity affects the analogies that we seek to develop. Consider momentum conservation in boundary layers. We can do a self-similarity analysis and reduce the momentum equation to an ordinary differential equation, but since we are not interested in solving the equations — only in learning about properties of the equations — we do not need to consider the advection terms in the left-hand side. Instead, we will only consider the pressure gradient and shear stress terms on the right-hand side, greatly simplifying the analysis. The right-hand side is

$$\mathrm{RHS} = -\frac{\mathrm{d}p}{\mathrm{d}x} + \frac{\partial t}{\partial y}. \tag{4.1}$$

We can assume a similarity coordinate of the form

$$\eta = y/\ell. \tag{4.2}$$

where $\ell = f(x)$ is the similarity length. Since we are not solving the equations, we do not need to specify the form of the similarity length other than that it is a function of the streamwise coordinate. We must also assume that the shear stress follows a self-similar form:

$$t = \tau_\mathrm{w} f(\eta). \tag{4.3}$$

where $\tau_\mathrm{w} = f(x)$. We can now write the right-hand side in terms of self-similar variables:

$$\mathrm{RHS} = -\frac{\mathrm{d}p}{\mathrm{d}x} + \left(\frac{\tau_\mathrm{w}}{\ell}\right)\frac{\mathrm{d}}{\mathrm{d}\eta}\left(\frac{t}{\tau_\mathrm{w}}\right). \tag{4.4}$$

This equation makes more sense when non-dimensionalized:

$$\left(\frac{\ell}{\tau_\mathrm{w}}\right)\mathrm{RHS} = -\underbrace{\left(\frac{\ell}{\tau_\mathrm{w}}\right)\frac{\mathrm{d}p}{\mathrm{d}x}}_{\text{Clauser parameter}} + \frac{\mathrm{d}}{\mathrm{d}\eta}\left(\frac{t}{\tau_\mathrm{w}}\right). \tag{4.5}$$

This form of the equation reveals the Clauser parameter (Clauser, 1954; Clauser, 1956), which controls for self-similarity in turbulent boundary layers. Conventional analyses assume that the similarity length is the displacement thickness, but the concept holds for any length scale that scales with the similarity length. When a series of profiles have the same Clauser parameter, plots of $(u - u_\mathrm{e})/u_\tau$ versus y/δ collapse onto the same curve since the flow is self-similar.

We should also consider the constant-property version of the right-hand side:

$$\left(\frac{L}{\tau_\mathrm{w}}\right)\mathrm{RHS} = -\underbrace{\left(\frac{L}{\tau_\mathrm{w}}\right)\frac{\mathrm{d}P}{\mathrm{d}X}}_{\text{Clauser parameter}} + \frac{\mathrm{d}}{\mathrm{d}\eta_*}\left(\frac{T}{\tau_\mathrm{w}}\right). \tag{4.6}$$

We can now match corresponding terms. We end up with two equations. The pressure gradient term states that the Clauser parameters must match between the two regimes:

$$\left(\frac{L}{\tau_\mathrm{w}}\right)\frac{\mathrm{d}P}{\mathrm{d}X} = \left(\frac{\ell}{\tau_\mathrm{w}}\right)\frac{\mathrm{d}p}{\mathrm{d}x}. \tag{4.7}$$

We could use this equation to transform the pressure gradient. However, the database does not have any cases with pressure gradient, so matching the Clauser parameters cannot be validated presently.

Matching the shear stress term reveals that the similarity coordinates and shear stresses are linked:

$$\frac{\mathrm{d}\eta_*}{\mathrm{d}\eta} = \frac{\mathrm{d}(Y/L)}{\mathrm{d}(y/\ell)} = \frac{\mathrm{d}(T/\tau_\mathrm{w})}{\mathrm{d}(t/\tau_\mathrm{w})} = \frac{\mathrm{d}T}{\mathrm{d}t}. \tag{4.8}$$

As discussed in chapter 3, observations of the production rates suggest that the shear stress is not transformed (that is, $T = t$). If we assume that the shear stresses are not transformed, then the similarity coordinates are not transformed either, according to this equation. We can see this demonstrated using Morkovin's scaling for the Reynolds stresses in figure 4.1, which chapter 3 shows corresponds to the assumption that the shear stresses are untransformed. Figure 4.1 plots the Morkovin-scaled Reynolds shear stress in both incompressible and compressible zero-pressure-gradient turbulent boundary layers. While there is some variation, in general the curves do overlap in large part, thus demonstrating that the outer layer coordinates appear to be roughly the same between the two cases.

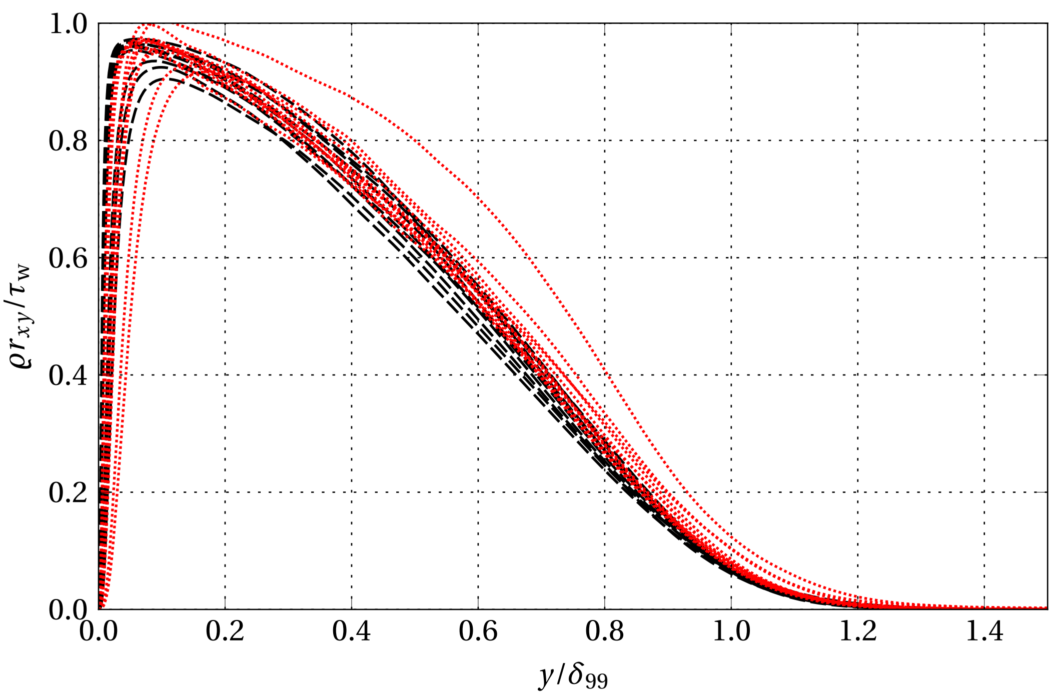

Figure 4.1: Morkovin's scaling presented in outer layer coordinates. Red dotted lines, compressible turbulent boundary layer data from Pirozzoli et al. (2011); black dashed lines, incompressible turbulent boundary layer data from Jiménez et al. (2010) and Sillero et al. (2013).

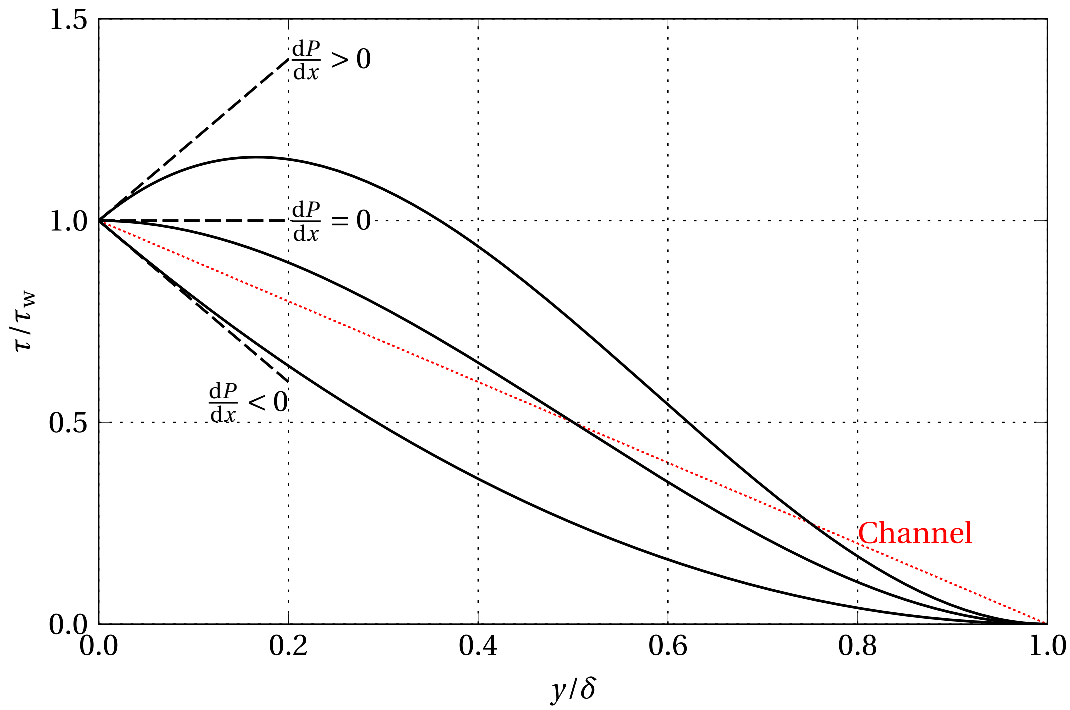

Figure 4.2: Schematic of the effects of pressure gradient on the shear stress distribution

Although not all boundary layers are strictly self-similar, many are and we generally can assume at least some kind of quasi-self-similarity. Therefore, we can also hypothesize that the outer layer coordinates are not transformed:[1]

$$\left(\frac{Y}{\Delta}\right) = \left(\frac{y}{\delta}\right). \tag{4.9}$$

This equation is the hypothesis I will explore for the rest of this chapter. I will call this the "outer layer coordinate matching" hypothesis. It is a more specific version of the principles given more generally in equation 4.8. Physically, we should expect that the transformation will not drastically change the large scales of the flow. The mean flow and turbulence

[1] I define the boundary layer thickness ambiguously here. This ambiguity is intentional. We should consider the boundary layer thickness to be a generic boundary layer thickness unless otherwise specified, like Δ_2 for the transformed momentum thickness.

structures that are the size of a boundary layer thickness should stay roughly that size (even if the ruler that is a boundary layer thickness changes). Moreover, we can reasonably assume that the outer layer coordinates and the shear stress distribution are linked. The shear stress distribution in boundary layers and channels is depicted in figure 4.2. The shear stress decreases to zero farther from the wall, at a distance on the order of a boundary layer thickness away. Therefore the shear stress distribution is function of the outer layer coordinate, since its characteristic variation is controlled by distances on the order of a boundary layer thickness. We can now perform a thought experiment. Suppose that a value of $y/\delta \approx 1$ maps to a point where $Y/\Delta \approx 0.5$. In the variable-property regime, the shear stress should be small and that momentum transfer should also be small. But in the constant-property regime, the shear stress would not be small and the momentum transfer therefore could be appreciable. In theory, this discrepancy means that a mismatch in the outer layer coordinate causes a mismatch in the shear stress, potentially leading to an error in how the transformation handles the momentum transfer. Matching the outer layer coordinates resolves this issue and provides some theoretical support for the hypothesis.

4.2 Channels

Channels are much simpler than boundary layers. One of the major simplifications is the shear stress profile in a channel. That shear stress profile, as depicted in figure 4.2, is linear and decreases to zero at the channel centerline. In the variable-property regime, the shear stress is

$$t = \tau_{\mathrm{w}} \left[1 - \left(\frac{y}{h} \right) \right] . \tag{4.10}$$

In the constant-property regime, the shear stress is

$$T = \tau_{\mathrm{w}} \left[1 - \left(\frac{Y}{H} \right) \right] . \tag{4.11}$$

The equivalent to the relationship between the outer layer coordinate and the shear stress (equation 4.8) for channels is

$$\frac{\mathrm{d}(Y/H)}{\mathrm{d}(y/h)} = \frac{\mathrm{d}T}{\mathrm{d}t} . \tag{4.12}$$

It is easy to see that channels always satisfy this equation (in theory, at least). To see this, we need to re-write the relationship between the outer layer coordinate and shear stress as

$$\frac{\mathrm{d}t}{\mathrm{d}(y/h)} = \frac{\mathrm{d}T}{\mathrm{d}(Y/H)} . \tag{4.13}$$

We can re-write this because the derivatives are exact. At this point all we need to do is plug in the known shear stress distributions to see that it is in fact always true (the equation becomes $-\tau_{\mathrm{w}} = -\tau_{\mathrm{w}}$). The TL theory assumes that the shear stresses are equal, and we can now see that for channels, this assumption fundamentally comes down to how the outer layer coordinates are transformed (or untransformed, that is). We can see this directly by setting the shear stresses equal to each other:

$$\tau_{\mathrm{w}} \left[1 - \left(\frac{y}{h} \right) \right] = \tau_{\mathrm{w}} \left[1 - \left(\frac{Y}{H} \right) \right] . \tag{4.14}$$

This equation demonstrates that the outer layer coordinates are equal (in theory):

$$\left(\frac{Y}{H} \right) = \left(\frac{y}{h} \right) . \tag{4.15}$$

Again, we should not be surprised about this, since we also just showed that channels always satisfy our assumed relationship between the outer layer coordinate and the shear stress.

This result merely re-enforces that in theory, the outer layer coordinates should match if we assume that the shear stresses do too.

In practice, however, is a different story. If we assume that the outer layer coordinates are the same, we can use this result to solve for the transformed wall-normal coordinate:

$$Y = \left(\frac{H}{h} \right) y \,. \tag{4.16}$$

The immediate consequence from this equation is that we expect the first derivative of the transformed wall-normal coordinate to be constant. More specifically, we expect that

$$\frac{\mathrm{d}Y}{\mathrm{d}y} = \left(\frac{H}{h} \right) = \mathrm{const} > 0 \,, \tag{4.17}$$

$$\frac{\mathrm{d}^2 Y}{\mathrm{d}y^2} = 0 \,. \tag{4.18}$$

In effect, the second derivative of the transformed wall-normal coordinate measures how well we expect the outer layer coordinates to match (assuming that the shear stress is untransformed). If the outer layer coordinates match, then the second derivative is zero. In other cases, the second derivative measures the local amount of mismatch between the transformed and untransformed outer layer coordinates.

How does the outer layer coordinate matching hypothesis work on the semi-local scale in channels? So far we have only considered the shear stress distribution in channels and made broad statements about the nature of the transformed wall-normal coordinate for an arbitrary transformation theory. If the semi-local scaling obeys the outer layer coordinate matching hypothesis, then we can expect equation 4.16 to equal the semi-local scaling:

$$Y = \left(\frac{H}{h} \right) y = \left(\frac{\varrho}{\varrho_r} \right)^{+1/2} \left(\frac{\mu}{\mu_r} \right)^{-1} y \,. \tag{4.19}$$

In this equation, H/h is a constant. This equation then specifies that

$$\left(\frac{H}{h}\right) = \left(\frac{\varrho}{\varrho_r}\right)^{+1/2} \left(\frac{\mu}{\mu_r}\right)^{-1}. \tag{4.20}$$

The left-hand side is a constant, so the right-hand side must be as well. As a consequence, the semi-local scaling only matches the outer layer coordinates when the viscosity scales with square root of the density:[2]

$$\left(\frac{\mu}{\mu_r}\right) \sim \left(\frac{\varrho}{\varrho_r}\right)^{+1/2}. \tag{4.21}$$

As long as the fluid properties satisfy this condition, H/h will be a constant, and the second derivative of the transformed coordinate will be zero, and the transformed outer layer coordinate equals the untransformed outer layer coordinate. We can see this again by calculating the second derivative of the semi-local scale:

$$\frac{\mathrm{d}^2 Y}{\mathrm{d}y^2} = \left[2 + y\frac{\mathrm{d}}{\mathrm{d}y}\right] \frac{\mathrm{d}}{\mathrm{d}y} \left[\left(\frac{\varrho}{\varrho_r}\right)^{+1/2} \left(\frac{\mu}{\mu_r}\right)^{-1}\right]. \tag{4.22}$$

This equation demonstrates that the second derivative is zero in regions where there is little heat transfer (no gradients in mean density and viscosity).

I should note that the idea that the outer layer coordinates must match has been somewhat explored before in subsection 2.5.2, though that subsection presents the idea indirectly and only applies it to the semi-local scaling in channel flows exclusively. That subsection lacked the general principle that we are discussing currently. The work of Patel, Peeters, et al. (2015) and Patel et al. (2016) considered profiles of a point-wise semi-local Reynolds number based

[2] I should note that this relationship is somewhat similar to the Chapman-Rubesin parameter with different exponents (Chapman et al., 1949). That parameter is sometimes exploited as a simplifying relationship in some boundary layer analyses.

on the semi-local scaling:

$$\mathrm{Re}_{\tau,\mathrm{local}} = \left(\frac{\varrho}{\varrho_r}\right)^{+1/2} \left(\frac{\mu}{\mu_r}\right)^{-1} \mathrm{Re}_\tau \,. \tag{2.35}$$

This equation is basically a non-dimensionalized form of equation 4.19. Essentially, Patel, Peeters, et al. (2015) and Patel et al. (2016) considered this function as measuring the range of Reynolds numbers that the flow occupies and that it controls for similarity in some sense. My interpretation is different and more general: the physical meaning of this quantity distinctly involves the relationship between the untransformed and transformed outer layer coordinates, and it connects back to the nature of the shear stress transformation. The relationship to the Reynolds number is only a particular framing around a more general concept.

Moreover, Patel, Peeters, et al. (2015) and Patel et al. (2016) limited their discussion to how this quantity controls for similarity and quasi-similarity, and how to write the TL theory in terms of this quantity. Their work never considered a more in-depth explanation of where this quantity comes from or how the variable relates to how well the outer layer coordinates match. In fact, the idea encapsulated in their point-wise semi-local Reynolds number is much broader and more general than their work suggests, provided that we take a step back and consider it under a new framework and notation, namely considering the second derivation of the transformed coordinate.

4.3 Boundary layers

Unlike channels, boundary layers do not have a shear stress distribution known beforehand. As depicted in figure 4.2, the primary variable that affects the shear stress distribution is the pressure gradient. The equivalent formula to the relationship between the outer layer coordinate and the shear stress (equation 4.8) for boundary layers is

$$\frac{\mathrm{d}(Y/\Delta)}{\mathrm{d}(y/\delta)} = \frac{\mathrm{d}T}{\mathrm{d}t}\,. \tag{4.23}$$

Unlike channels, though, we have no means to prove that boundary layers satisfy this more general relationship. Instead, we must assume that boundary layer satisfy the more specific outer layer coordinate matching hypothesis:

$$\left(\frac{Y}{\Delta}\right) = \left(\frac{y}{\delta}\right). \tag{4.24}$$

The difference here between channels and boundary layers is that δ is a function of x and Δ is a function of X. In channels these are constants. The transformed wall-normal coordinate is

$$Y = \left(\frac{\Delta}{\delta}\right) y\,. \tag{4.25}$$

Similar to the case of channels, the first and second derivatives of the transformed wall-normal coordinate are

$$\frac{\partial Y}{\partial y} = \left(\frac{\Delta}{\delta}\right) = f(x) > 0\,, \tag{4.26}$$

$$\frac{\partial^2 Y}{\partial y^2} = 0\,. \tag{4.27}$$

Here, I have assumed that the transformed streamwise coordinate X is a function of the untransformed streamwise coordinate x only. Chapter 5 demonstrates this result but I assume it for the time being.

As with channels, we expect the second partial derivative of the transformed coordinate to be zero, so any deviation from zero measures the degree that the outer layer coordinates differ.

The partial derivative of the transformed wall-normal coordinate in the streamwise direction also comes into play in any boundary layer transformation. This quantity is

$$\frac{\partial Y}{\partial x} = y \frac{\mathrm{d}}{\mathrm{d}x}\left(\frac{\Delta}{\delta}\right) = \left(\frac{y}{\delta}\right) \underbrace{\left[\frac{\mathrm{d}X}{\mathrm{d}x}\frac{\mathrm{d}\Delta}{\mathrm{d}X} - \left(\frac{\Delta}{\delta}\right)\frac{\mathrm{d}\delta}{\mathrm{d}x}\right]}_{f(x)\text{ only}} = \left(\frac{y}{\delta}\right) \underbrace{\left[\frac{\mathrm{d}\Delta}{\mathrm{d}\delta} - \left(\frac{\Delta}{\delta}\right)\right]\frac{\mathrm{d}\delta}{\mathrm{d}x}}_{f(x)\text{ only}}. \tag{4.28}$$

The first term shows that for close to the wall, as $y/\delta \to 0$, we expect the transformed wall-normal coordinate Y to be a function of only y. However, farther from the wall, the rate of spatial development comes into play through how quickly the boundary layer thickness changes. This equation demonstrates that the rate of spatial development and the outer layer coordinate are directly linked. Chapter 5 discusses this equation in more detail in the context of a two-dimensional extension of the TL transformation.

If the semi-local scaling obeys the outer layer coordinate matching hypothesis, then we can expect equation 4.16 to equal the semi-local scaling:

$$Y = \left(\frac{\Delta}{\delta}\right) y = \left(\frac{\varrho}{\varrho_r}\right)^{+1/2} \left(\frac{\mu}{\mu_r}\right)^{-1} y. \tag{4.29}$$

However, this equation differs from its channel counterpart, because now we have spatial development to contend with. The local ratio of transformed-to-untransformed boundary layer thicknesses is

$$\left(\frac{\Delta}{\delta}\right) = \left(\frac{\varrho}{\varrho_r}\right)^{+1/2} \left(\frac{\mu}{\mu_r}\right)^{-1}. \tag{4.30}$$

As in the case for channels, the only way for the transformed outer layer coordinate to match the untransformed outer layer coordinate is when a special relationship exists between the mean viscosity and mean density:

$$\left(\frac{\mu}{\mu_r}\right) \sim \left(\frac{\varrho}{\varrho_r}\right)^{+1/2} f(x). \tag{4.31}$$

In practice, equation 4.21 satisfies this equation too.

4.4 Results

In practice, no real fluid will obey the relationship between the mean density and mean viscosity given in equation 4.21. This relationship is necessary to match the outer layer coordinates but does not match any expected relationship for gases (either from kinetic theory, statistical mechanics, or otherwise).

To that end, we should examine the second derivative of the semi-local scaling to see how large this quantity becomes. Figures 4.3a, 4.3b, and 4.3c depict the second derivative of the semi-local scaling in a channel, an adiabatic wall boundary layer, and a cold wall boundary layer, respectively.

In all cases, the absolute value of the dimensionless second derivative is small, never exceeding 0.25 in the viscous sublayer or 0.025 in the buffer layer. In all cases, the value of the second derivative approaches a constant value. In the channel case, the second derivative starts out at a highly negative value but rapidly approaches zero after $y_+ \approx 20$.

However, in both boundary layer cases, it approaches a small positive value. This observation is critical to understanding the potential source of the error in the TL transformation for boundary layers. In all cases, the second derivative's largest absolute value is in the viscous sublayer. These peaks are meaningless in the context of the outer layer coordinate, though, since the outer layer coordinate in the viscous sublayer is always zero. Therefore a non-zero second derivative there does not contribute to any error in the transformation. However, once the flow is in the buffer layer, the outer layer coordinate is now non-zero for small Reynolds numbers, and any non-zero value of the second derivative could contribute in those cases. As a consequence, the positive second derivative for boundary layers after $y_+ \approx 20$ means that

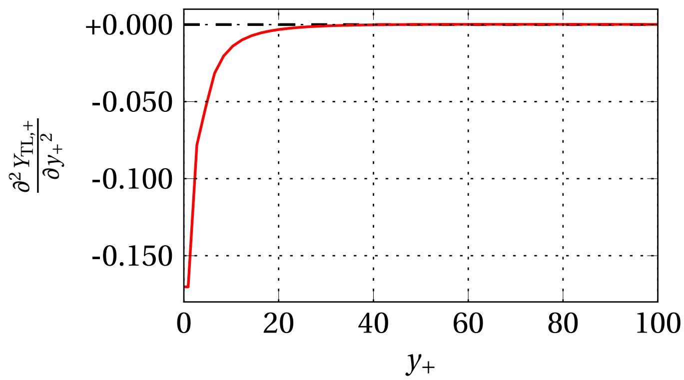

(a) Channel (`2016-Trettel-DNS-0901`)

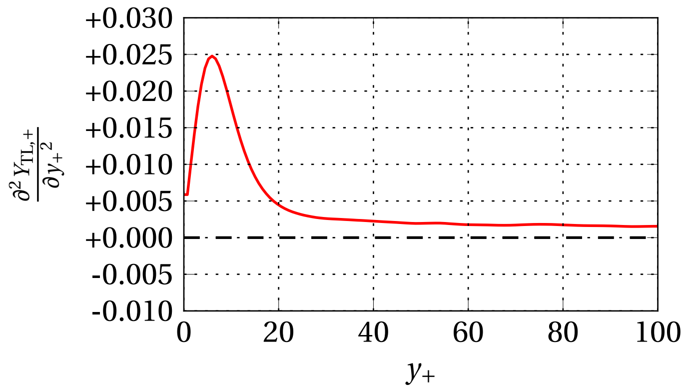

(b) Adiabatic wall boundary layer (`2011-Pirozzoli-DNS-0801`)

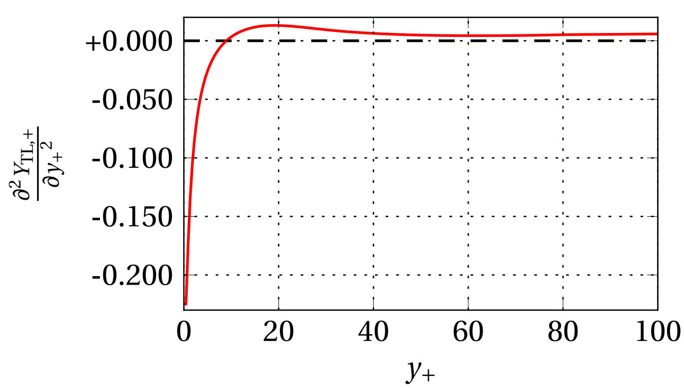

(c) Cold wall boundary layer (`2018-Zhang-DNS-0201`)

Figure 4.3: Second derivatives of the TL-transformed coordinate (semi-local scaling) in the near-wall region

transformed the outer layer coordinate does not equal the untransformed outer layer coordinate, and this mismatch should compound the farther from the wall we get.

Why does the second derivative go to zero in channels but not in boundary layers? This property emerges from the location of the temperature profile's peak and the nature of the heat transfer in channels and boundary layers. Channels have no spatial development and are fully-developed flows. The wall temperature is a constant, and viscous heating therefore only adds energy to the flow, heating up only the center of the channel. The peak temperature therefore is always at the channel's centerline. The turbulence also blunts any temperature gradients outside of the viscous sublayer, so the temperature profile is relatively flat for most of the flow. As a consequence, the temperature gradients rapidly approach zero farther from the wall, and we could therefore expect little to no property variation. The second derivative of the semi-local scaling would then go towards zero.

Figure 4.4a depicts the temperature profile in the near-wall region of a channel flow. Channels are cold wall flows, so the wall temperature is less than "edge" temperature (centerline temperature, in reality). The temperature profile is monotonically increasing, and most of the heat transfer occurs before reaching $y_+ \approx 50$. The mean temperature is quite close to the centerline temperature at $y \approx 100$ even.

Boundary layers have not had the time and space necessary for their wall heating and viscous heating to propagate throughout the whole flow. As a consequence, the temperature profile tends to decrease, and it takes a much longer distance for a boundary layer's temperature to reach the edge temperature (when compared to channels). The temperature peaks are also close to the wall rather than farther from it, sharping the temperature gradients in the buffer layer especially. Figure 4.4b depicts the temperature profile for an adiabatic wall boundary

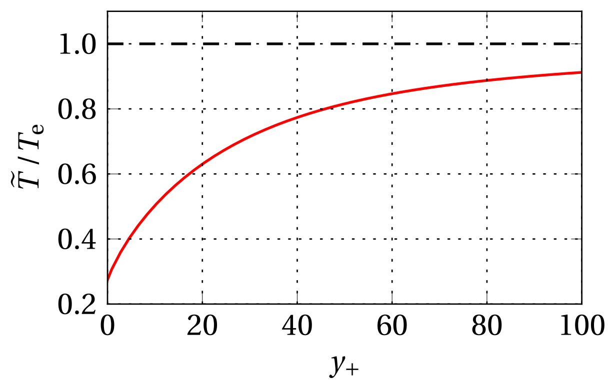

(a) Channel (`2016-Trettel-DNS-0901`)

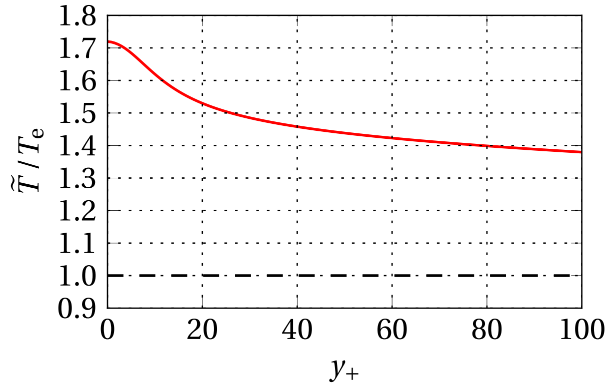

(b) Adiabatic wall boundary layer (`2011-Pirozzoli-DNS-0801`)

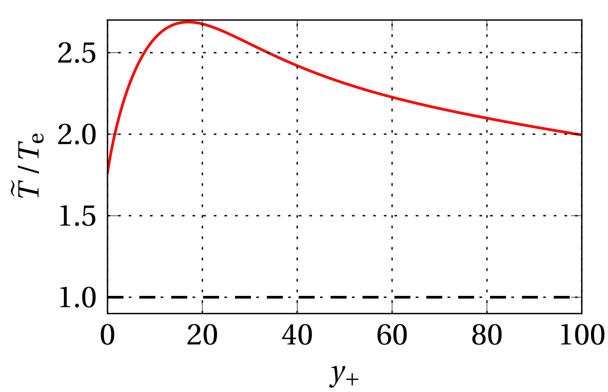

(c) Cold wall boundary layer (`2018-Zhang-DNS-0201`)

Figure 4.4: Mean temperature in the near-wall region

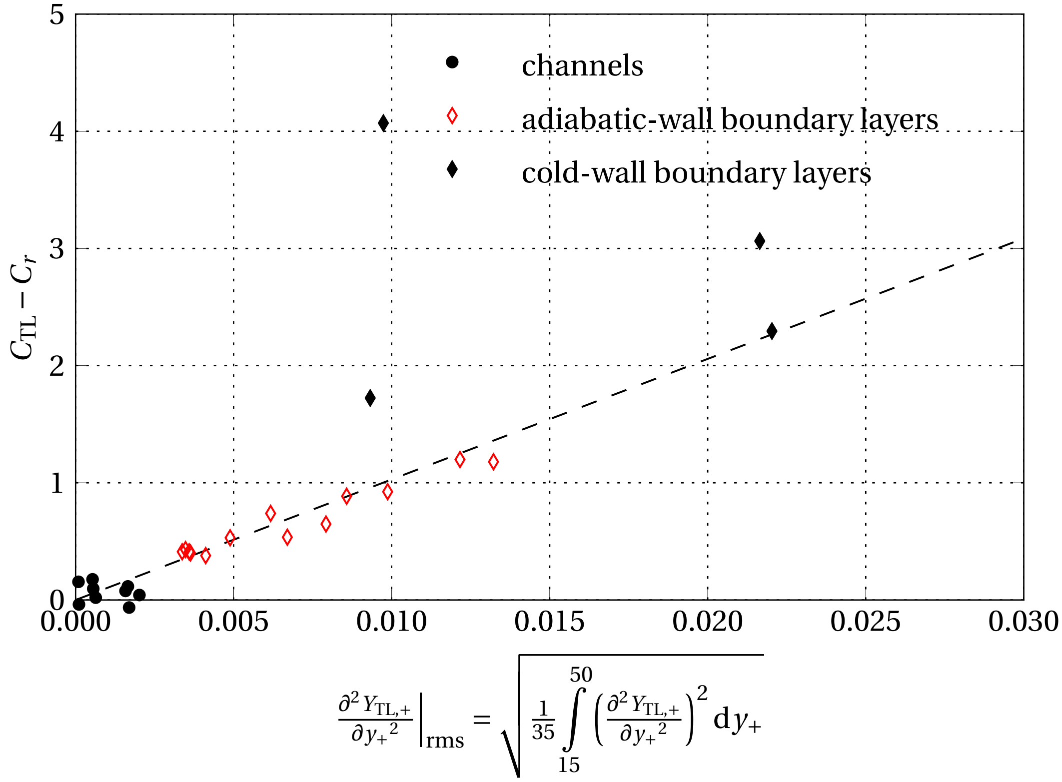

Figure 4.5: Error in the TL-transformed log-law intercept as a function of the RMS of the second derivative of the semi-local scaling in the buffer layer and lower part of the log-law. Dashed line, curve fit for adiabatic wall data.

layer, and 4.4c depicts the temperature profile for a cold wall boundary layer. In both cases, at $y_+ \approx 100$, the temperature is far from the edge temperature. Therefore the temperature gradient will continue to be large for the bulk of the flow. The gradients do not decrease to zero close to the wall. The second derivative of the semi-local scaling will not decrease to zero close to the wall due to all of these factors.

So far I have only considered the second derivative of the semi-local scaling for specific cases. We now can take a more global look at the second derivative and its effect on the error in the log-law intercept of the TL-transformed profile more directly.

Figure 4.5 plots the error in the TL-transformed log-law intercept against the RMS value of the second derivative of the semi-local scaling in the buffer layer and the start of the log-law region. I used this region as the measurement location for several reasons. First, the viscous sublayer is always at $Y/\Delta \approx 0$, so the value of the second derivative there will not contribute to any overall error in the transformation. Second, this region is where the error in the TL transformation first appears. Third, the second derivative approaches a constant in the buffer layer, so considering the log-law region would not necessarily change the answer but would take longer to calculate.

In this figure, the data for all adiabatic wall boundary layers for all Reynolds numbers and all Mach number now collapses onto the same line. The filled-in diamond farthest up on the line is a near adiabatic wall boundary layer, so we could also consider that point as lying on the line even though it is not strictly an adiabatic wall boundary layer. The error for channels is small, and we can see that the RMS value of the second derivative for the channels is also small. Note however that later theoretical analysis in subsection 5.10.4 demonstrates that the second derivative does not need to be zero provided that there is no spatial development (provided the flow is a channel). That is, matching the outer layer coordinates is sufficient but unnecessary in some circumstances, since the rate of spatial development mediates the requirement that the outer layer coordinates must match. I discuss this point in more detail later.

The collapse onto a single line greatly improves on the previous figures given in chapter 2, but it does not definitively prove that the transformed outer layer coordinate must match the untransformed outer layer coordinate. At the moment, this plot shows a strong correlation between the RMS second derivative and the error in the TL transformation. This plot is more of an uncontrolled observational study than a controlled study, since we do not directly control for whether or not the second derivative is identically zero. We merely observe its value in existing data. Observational studies suffice in many circumstances, but in this case we have a way to control for the proposed source of the error. We can run new simulations that control for the second derivative by setting the viscosity relationship to $\mu \sim \varrho^{+1/2}$ (equation 4.21). If the outer layer coordinate matching hypothesis is true, then the TL transformation would work well for those new cases. This is the most obvious way to control for this. Until researchers run such new simulations to establish the mechanism as the source of the error, we can only conclude with certainty that a strong correlation exists at present.

Chapter 5

A two-dimensional extension of the Trettel-Larsson transformation

5.1 Motivation

The TL transformation assumes that the flow is one-dimensional. For boundary layers, this assumption fails. Boundary layers fundamentally are two-dimensional flows, and any transformation should consider them as such. To that end, I will derive a two-dimensional extension of the TL transformation that also seeks to address the issues related to Morkovin's hypothesis discussed in chapter 3 and the issues related to the outer layer coordinate addressed in 4. The rest of this section details what changes that we must include to recognize the two-dimensionality of the flow.

5.1.1 Mass conservation

The TL transformation does not consider mass conservation. How could the transformation work without including one of the most basic conservation laws? Mass conservation matters even more in two dimensions, so we cannot exclude it from a two-dimensional extension of the TL transformation.

Classically, boundary layer analyses use the stream function to satisfy the two-dimensional mass conservation equation. However, it is difficult to use the stream function without also requiring that the coordinate is the Howarth-Dorodnitsin transformation (Howarth, 1948; Dorodnitsin, 1942):

$$Y_{\mathrm{HD}} = \int_0^y \left(\frac{\varrho}{\varrho_r}\right) \mathrm{d}y. \tag{5.1}$$

Stewartson (1964, pp. 29–30) discusses this coordinate at length. This coordinate achieves several tasks, the most direct being that it adjusts the location of the streamlines such that mass remains conserved between them. The issue with this coordinate, for our purposes, is that we cannot use the semi-local scaling or another similar coordinate while also using this coordinate. The use of the stream function makes the coordinate overdetermined if we need to satisfy both the log-law and some kind of momentum conservation condition. We would have too many equations to satisfy and too few degrees of freedom to satisfy them. This is not to say that we cannot use the stream function. Coles (1962) and Coles (1964) are older transformation theories that use the stream function, but as a consequence they do not and cannot use a log-law condition like the Van Driest transformation does.

Fortunately, there are other methods to satisfy mass conservation without using the stream function. The most direct is to use the continuity equation with both velocities:

$$\frac{\partial u}{\partial x} + \frac{\partial v}{\partial y} = 0. \tag{5.2}$$

As discussed in chapter 3, non-hypersonic turbulent boundary layers do not have large values of the mean dilatation rate. Therefore we may use the incompressible continuity equation to satisfy mass conservation. I will discuss how to implement mass conservation this way later in this chapter.

5.1.2 Momentum conservation

As discussed in chapter 3, we can consider a more general stress balance for momentum conservation. This stress balance equation allows for the shear stress to be transformed if desired. The resulting stress balance is

$$1 = \left(\frac{\mu}{t}\right)\frac{\partial u}{\partial y} - \frac{\varrho r_{xy}}{t}. \tag{5.3}$$

5.1.3 The log-law

The log-law condition does not change except for the inclusion of partial derivatives:

$$\frac{1}{\kappa} = y\left(\frac{\varrho}{\tau_{\mathrm{w}}}\right)^{+1/2}\frac{\partial u}{\partial y}. \tag{5.4}$$

5.1.4 Energy conservation

The TL transformation does not consider energy conservation. Energy conservation matters for compressible flow, but usually does not come up in incompressible flow unless heat transfer occurs. However, the extended transformation will not include energy conservation due to our desire for the transformation to be agnostic to the mechanism of density and viscosity variation.

There are many different ways that the local density could vary in a fluid. For compressible gases, the most obvious ways involve changing the temperature or pressure. But this is not the only way that the local density could vary. Consider the density of a binary mixture of two constant density fluids (Sandoval, 1995, p. 11):

$$\frac{1}{\varrho} = \frac{C_1}{\varrho_1} + \frac{1 - C_1}{\varrho_2}. \tag{5.5}$$

Here, ϱ_1 is the density of fluid 1 in isolation, ϱ_2 is the density of fluid 2 in isolation, and C_1 is the local mass fraction of fluid 1. This kind of equation of state is used frequently in simulations of buoyancy-driven turbulence.

The point here is the transformation should work no matter what causes the density and viscosity to vary. I want the transformation to work just as well in ideal gas, real gas, or binary fluid circumstances, so the transformation should ignore what causes the density and viscosity variation and just treat the mean density and viscosity as known variables. That is how I treated it in chapter 2 and how I will continue to treat it here.

This is not to say that past work has always ignored energy conservation. In fact, it is useful to include energy conservation when you do need a specific form of the more general transformation. For example, Van Driest (1951) does not contain the integral form of the Van Driest transformation, but it does have a less general form, the trigonometric Van Driest transformation, which is the Van Driest transformation assuming an ideal gas and a Crocco-Busemann relation (to satisfy energy conservation). This transformation still is theoretically valid but its application is limited to ideal gases with near unity Prandtl numbers. We seek to surpass such limitations, so we ignore any equations of state or energy conservation in general.[1]

5.2 Coordinate and velocity transformations, and their inverses

We expect the coordinate and velocity transformations that we create to be one-to-one. Each coordinate will map to a single transformed coordinate and vice versa. In one-dimensional problems, discussed in chapter 2, the inversion process is simple. The exact derivatives signify that the inverse of the coordinate transformation inverts the relationship between the variables, letting you find the transformed coordinate from the untransformed coordinate and vice versa. In two dimensions, the relationship between the 2 regimes is not an exact inverse but we can nonetheless generalize the inversion procedure using linear algebra.

We can again use the chain rule to calculate the differentials of the transformed coordi-

[1] There is also another more subtle reason to ignore energy conservation. We want to transform the velocities according to the law-of-the-wall. That is, according to a scaling based on the amount of momentum transfer at the wall (the wall shear stress). When there is no momentum transfer at the wall — for a separating boundary layer — there is no law-of-the-wall. But this is only one law-of-the-wall. There are multiple: one for momentum transfer, one for energy transfer, and even one for the mass transfer. In each case, the law-of-the-wall is defined by the nonzero total amount of transfer of a conserved quantity. For energy transfer, the wall heat flux defines the thermal law-of-the-wall (the law-of-the-wall for temperature profiles). Patel et al. (2017) covers an extension of the TL transformation to the thermal law-of-the-wall in channels, for example. However, adiabatic walls have zero wall heat flux, so it is impossible to define a thermal law-of-the-wall for the adiabatic wall case. For that reason we cannot transform the temperature according to the thermal law-of-the-wall, since it does not exist for adiabatic walls.

nates as functions of the untransformed coordinates:

$$\mathrm{d}X = \frac{\partial X}{\partial x}\mathrm{d}x + \frac{\partial X}{\partial y}\mathrm{d}y, \tag{5.6}$$

$$\mathrm{d}Y = \frac{\partial Y}{\partial x}\mathrm{d}x + \frac{\partial Y}{\partial y}\mathrm{d}y. \tag{5.7}$$

We can also use the chain rule to find the inverse relationship to calculate the differentials of the untransformed coordinates as functions of the transformed coordinates:

$$\mathrm{d}x = \frac{\partial x}{\partial X}\mathrm{d}X + \frac{\partial x}{\partial Y}\mathrm{d}Y, \tag{5.8}$$

$$\mathrm{d}y = \frac{\partial y}{\partial X}\mathrm{d}X + \frac{\partial y}{\partial Y}\mathrm{d}Y. \tag{5.9}$$

We can write these sets of equations as matrices:

$$\begin{bmatrix} \mathrm{d}X \\ \mathrm{d}Y \end{bmatrix} = \begin{bmatrix} \frac{\partial X}{\partial x} & \frac{\partial X}{\partial y} \\ \frac{\partial Y}{\partial x} & \frac{\partial Y}{\partial y} \end{bmatrix} \begin{bmatrix} \mathrm{d}x \\ \mathrm{d}y \end{bmatrix}, \tag{5.10}$$

$$\begin{bmatrix} \mathrm{d}x \\ \mathrm{d}y \end{bmatrix} = \begin{bmatrix} \frac{\partial x}{\partial X} & \frac{\partial x}{\partial Y} \\ \frac{\partial y}{\partial X} & \frac{\partial y}{\partial Y} \end{bmatrix} \begin{bmatrix} \mathrm{d}X \\ \mathrm{d}Y \end{bmatrix}. \tag{5.11}$$

From these equations, we can see that the coordinate transformation derivatives are in fact related by the inverse of the opposing matrix:

$$\begin{bmatrix} \frac{\partial x}{\partial X} & \frac{\partial x}{\partial Y} \\ \frac{\partial y}{\partial X} & \frac{\partial y}{\partial Y} \end{bmatrix} = \begin{bmatrix} \frac{\partial X}{\partial x} & \frac{\partial X}{\partial y} \\ \frac{\partial Y}{\partial x} & \frac{\partial Y}{\partial y} \end{bmatrix}^{-1}. \tag{5.12}$$

As a consequence, we can solve for the untransformed coordinate derivatives in terms of the transformed coordinate derivatives:

$$\frac{\partial x}{\partial X} = +\frac{1}{J_{XY}}\frac{\partial Y}{\partial y}, \tag{5.13}$$

$$\frac{\partial x}{\partial Y} = -\frac{1}{J_{XY}}\frac{\partial X}{\partial y}, \tag{5.14}$$

$$\frac{\partial y}{\partial X} = -\frac{1}{J_{XY}}\frac{\partial Y}{\partial x}, \tag{5.15}$$

$$\frac{\partial y}{\partial Y} = +\frac{1}{J_{XY}}\frac{\partial X}{\partial x}, \tag{5.16}$$

The coordinate transformation Jacobian determinant plays are a role in these equations. This Jacobian is

$$J_{XY} = \frac{\partial X}{\partial x}\frac{\partial Y}{\partial y} - \frac{\partial X}{\partial y}\frac{\partial Y}{\partial x} \tag{5.17}$$

These derivatives will allow us to state our chain rule purely in terms of variables in one regime.

A similar procedure works for the velocity transformations. This procedure generates the following inverse relations between the velocity transformation derivatives:

$$\frac{\partial u}{\partial U} = +\frac{1}{J_{UV}}\frac{\partial V}{\partial v}, \tag{5.18}$$

$$\frac{\partial u}{\partial V} = -\frac{1}{J_{UV}}\frac{\partial U}{\partial v}, \tag{5.19}$$

$$\frac{\partial v}{\partial U} = -\frac{1}{J_{UV}}\frac{\partial V}{\partial u}, \tag{5.20}$$

$$\frac{\partial v}{\partial V} = +\frac{1}{J_{UV}}\frac{\partial U}{\partial u}, \tag{5.21}$$

The velocity transformation Jacobian determinant is

$$J_{UV} = \frac{\partial U}{\partial u}\frac{\partial V}{\partial v} - \frac{\partial U}{\partial v}\frac{\partial V}{\partial u} \tag{5.22}$$

5.3 The chain rule for two-dimensional flows

The chain rule for a one-dimensional shear flow is simple. It involves only one gradient term. However, the chain rule in two dimensions involves four gradient terms and is much more complex. We can write out this chain rule to express all four of the untransformed velocity gradients as a function of all four of the transformed velocity gradients:

$$\frac{\partial u}{\partial x} = +\frac{\partial X}{\partial x}\frac{\partial u}{\partial U}\frac{\partial U}{\partial X} + \frac{\partial Y}{\partial x}\frac{\partial u}{\partial U}\frac{\partial U}{\partial Y} + \frac{\partial X}{\partial x}\frac{\partial u}{\partial V}\frac{\partial V}{\partial X} + \frac{\partial Y}{\partial x}\frac{\partial u}{\partial V}\frac{\partial V}{\partial Y}, \tag{5.23}$$

$$\frac{\partial u}{\partial y} = +\frac{\partial X}{\partial y}\frac{\partial u}{\partial U}\frac{\partial U}{\partial X} + \frac{\partial Y}{\partial y}\frac{\partial u}{\partial U}\frac{\partial U}{\partial Y} + \frac{\partial X}{\partial y}\frac{\partial u}{\partial V}\frac{\partial V}{\partial X} + \frac{\partial Y}{\partial y}\frac{\partial u}{\partial V}\frac{\partial V}{\partial Y}, \tag{5.24}$$

$$\frac{\partial v}{\partial x} = +\frac{\partial X}{\partial x}\frac{\partial v}{\partial U}\frac{\partial U}{\partial X} + \frac{\partial Y}{\partial x}\frac{\partial v}{\partial U}\frac{\partial U}{\partial Y} + \frac{\partial X}{\partial x}\frac{\partial v}{\partial V}\frac{\partial V}{\partial X} + \frac{\partial Y}{\partial x}\frac{\partial v}{\partial V}\frac{\partial V}{\partial Y}, \tag{5.25}$$

$$\frac{\partial v}{\partial y} = +\frac{\partial X}{\partial y}\frac{\partial v}{\partial U}\frac{\partial U}{\partial X} + \frac{\partial Y}{\partial y}\frac{\partial v}{\partial U}\frac{\partial U}{\partial Y} + \frac{\partial X}{\partial y}\frac{\partial v}{\partial V}\frac{\partial V}{\partial X} + \frac{\partial Y}{\partial y}\frac{\partial v}{\partial V}\frac{\partial V}{\partial Y}. \tag{5.26}$$

This equation is not in the most useful form, though, since it involves terms like $\frac{\partial u}{\partial U}$. It would be much more useful to express the chain rule in terms of the transformed variables only. To achieve that, we will insert the inverse velocity transformation relations to make the right-hand side in terms of derivatives of variables in the transformed regime:

$$\frac{\partial u}{\partial x} = \frac{1}{J_{UV}}\left[+\frac{\partial X}{\partial x}\frac{\partial V}{\partial v}\frac{\partial U}{\partial X} + \frac{\partial Y}{\partial x}\frac{\partial V}{\partial v}\frac{\partial U}{\partial Y} - \frac{\partial X}{\partial x}\frac{\partial U}{\partial v}\frac{\partial V}{\partial X} - \frac{\partial Y}{\partial x}\frac{\partial U}{\partial v}\frac{\partial V}{\partial Y}\right], \tag{5.27}$$

$$\frac{\partial u}{\partial y} = \frac{1}{J_{UV}}\left[+\frac{\partial X}{\partial y}\frac{\partial V}{\partial v}\frac{\partial U}{\partial X} + \frac{\partial Y}{\partial y}\frac{\partial V}{\partial v}\frac{\partial U}{\partial Y} - \frac{\partial X}{\partial y}\frac{\partial U}{\partial v}\frac{\partial V}{\partial X} - \frac{\partial Y}{\partial y}\frac{\partial U}{\partial v}\frac{\partial V}{\partial Y}\right], \tag{5.28}$$

$$\frac{\partial v}{\partial x} = \frac{1}{J_{UV}}\left[-\frac{\partial X}{\partial x}\frac{\partial V}{\partial u}\frac{\partial U}{\partial X} - \frac{\partial Y}{\partial x}\frac{\partial V}{\partial u}\frac{\partial U}{\partial Y} + \frac{\partial X}{\partial x}\frac{\partial U}{\partial u}\frac{\partial V}{\partial X} + \frac{\partial Y}{\partial x}\frac{\partial U}{\partial u}\frac{\partial V}{\partial Y}\right], \tag{5.29}$$

$$\frac{\partial v}{\partial y} = \frac{1}{J_{UV}}\left[-\frac{\partial X}{\partial y}\frac{\partial V}{\partial u}\frac{\partial U}{\partial X} - \frac{\partial Y}{\partial y}\frac{\partial V}{\partial u}\frac{\partial U}{\partial Y} + \frac{\partial X}{\partial y}\frac{\partial U}{\partial u}\frac{\partial V}{\partial X} + \frac{\partial Y}{\partial y}\frac{\partial U}{\partial u}\frac{\partial V}{\partial Y}\right]. \tag{5.30}$$

This equation serves as the basis for the chain rule that we will use later. First, however, we must simplify it further by making the chain rule obey mass conservation.

5.4 Mass conservation for flows with negligible dilatation rates

As stated in the motivation section, we will assume that the flow has a negligible dilatation rate. The incompressible continuity equation then would satisfy mass conservation. The variable-property equation already is written in terms of a constant:

$$\frac{\partial u}{\partial x} + \frac{\partial v}{\partial y} = 0 \tag{5.2}$$

The constant-property counterpart to this equation is

$$\frac{\partial U}{\partial X} + \frac{\partial V}{\partial Y} = 0\,. \tag{5.31}$$

The next step is to apply the chain rule to the variable-property equation to write it in terms of constant-property variables:

$$\begin{aligned} 0 = \frac{\partial u}{\partial x} + \frac{\partial v}{\partial y} = \frac{1}{J_{UV}}\Big[\quad & + \frac{\partial U}{\partial X}\left(+ \frac{\partial X}{\partial x}\frac{\partial V}{\partial v} - \frac{\partial X}{\partial y}\frac{\partial V}{\partial u}\right) \\ & + \frac{\partial U}{\partial Y}\left(+ \frac{\partial Y}{\partial x}\frac{\partial V}{\partial v} - \frac{\partial Y}{\partial y}\frac{\partial V}{\partial u}\right) \\ & + \frac{\partial V}{\partial X}\left(- \frac{\partial X}{\partial x}\frac{\partial U}{\partial v} + \frac{\partial X}{\partial y}\frac{\partial U}{\partial u}\right) \\ & + \frac{\partial V}{\partial Y}\left(- \frac{\partial Y}{\partial x}\frac{\partial U}{\partial v} + \frac{\partial Y}{\partial y}\frac{\partial U}{\partial u}\right)\Big]\,. \end{aligned} \tag{5.32}$$

Finally, we now match each component of the equation. For this equation to match the constant-property version, every coefficient for each velocity gradient component must be equal. As a consequence, the following conditions apply:

$$\frac{\partial U}{\partial X}: \qquad + \frac{\partial X}{\partial x}\frac{\partial V}{\partial v} - \frac{\partial X}{\partial y}\frac{\partial V}{\partial u} = J_{UV}\,, \tag{5.33}$$

$$\frac{\partial U}{\partial Y}: \qquad + \frac{\partial Y}{\partial x}\frac{\partial V}{\partial v} - \frac{\partial Y}{\partial y}\frac{\partial V}{\partial u} = 0\,, \tag{5.34}$$

$$\frac{\partial V}{\partial X}: \qquad - \frac{\partial X}{\partial x}\frac{\partial U}{\partial v} + \frac{\partial X}{\partial y}\frac{\partial U}{\partial u} = 0\,, \tag{5.35}$$

$$\frac{\partial V}{\partial Y}: \qquad - \frac{\partial Y}{\partial x}\frac{\partial U}{\partial v} + \frac{\partial Y}{\partial y}\frac{\partial U}{\partial u} = J_{UV}\,. \tag{5.36}$$

We can use linear algebra to solve this system of equations. Mass conservation then becomes a series of relationships between the coordinate transformations and the velocity transformations:

$$\frac{\partial U}{\partial u} = \frac{\partial X}{\partial x}\,, \tag{5.37}$$

$$\frac{\partial U}{\partial v} = \frac{\partial X}{\partial y}\,, \tag{5.38}$$

$$\frac{\partial V}{\partial u} = \frac{\partial Y}{\partial x}\,, \tag{5.39}$$

$$\frac{\partial V}{\partial v} = \frac{\partial Y}{\partial y}\,. \tag{5.40}$$

A consequence of these relations is that the Jacobian determinants are the same:

$$J_{UV} = J_{XY} = J\,. \tag{5.41}$$

5.5 The chain rule for mass-conserving thin-shear layers

Now that we have the velocity-coordinate relations, we can apply mass conservation to the chain rule itself. This process develops a mass-conserving chain rule written purely in terms of the coordinate transformations. We can then use the coordinate transformations to later solve for the velocity transformations. We can start by inserting the velocity-coordinate relations into the previous chain rule for the velocity gradients:

$$\frac{\partial u}{\partial x} = \frac{1}{J}\left[+\frac{\partial X}{\partial x}\frac{\partial Y}{\partial y}\frac{\partial U}{\partial X} + \frac{\partial Y}{\partial x}\frac{\partial Y}{\partial y}\frac{\partial U}{\partial Y} - \frac{\partial X}{\partial x}\frac{\partial X}{\partial y}\frac{\partial V}{\partial X} - \frac{\partial Y}{\partial x}\frac{\partial X}{\partial y}\frac{\partial V}{\partial Y}\right], \tag{5.42}$$

$$\frac{\partial u}{\partial y} = \frac{1}{J}\left[+\frac{\partial X}{\partial y}\frac{\partial Y}{\partial y}\frac{\partial U}{\partial X} + \frac{\partial Y}{\partial y}\frac{\partial Y}{\partial y}\frac{\partial U}{\partial Y} - \frac{\partial X}{\partial y}\frac{\partial X}{\partial y}\frac{\partial V}{\partial X} - \frac{\partial Y}{\partial y}\frac{\partial X}{\partial y}\frac{\partial V}{\partial Y}\right], \tag{5.43}$$

$$\frac{\partial v}{\partial x} = \frac{1}{J}\left[-\frac{\partial X}{\partial x}\frac{\partial Y}{\partial x}\frac{\partial U}{\partial X} - \frac{\partial Y}{\partial x}\frac{\partial Y}{\partial x}\frac{\partial U}{\partial Y} + \frac{\partial X}{\partial x}\frac{\partial X}{\partial x}\frac{\partial V}{\partial X} + \frac{\partial Y}{\partial x}\frac{\partial X}{\partial x}\frac{\partial V}{\partial Y}\right], \tag{5.44}$$

$$\frac{\partial v}{\partial y} = \frac{1}{J}\left[-\frac{\partial X}{\partial y}\frac{\partial Y}{\partial x}\frac{\partial U}{\partial X} - \frac{\partial Y}{\partial y}\frac{\partial Y}{\partial x}\frac{\partial U}{\partial Y} + \frac{\partial X}{\partial y}\frac{\partial X}{\partial x}\frac{\partial V}{\partial X} + \frac{\partial Y}{\partial y}\frac{\partial X}{\partial x}\frac{\partial V}{\partial Y}\right]. \tag{5.45}$$

The next step is apply the continuity equation itself to combine the fourth term of each equation with the first term. That is, we set

$$\frac{\partial V}{\partial Y} = -\frac{\partial U}{\partial X} \tag{5.46}$$

and simplify the equations accordingly. Boundary layer theory also notes that the third velocity gradient is negligible compared to the others:

$$\frac{\partial V}{\partial X} \approx 0\,. \tag{5.47}$$

These conditions greatly simplify the chain rule into something much more manageable:

$$\frac{\partial u}{\partial x} = \frac{1}{J}\Big[\left(+\frac{\partial X}{\partial x}\frac{\partial Y}{\partial y} + \frac{\partial X}{\partial y}\frac{\partial Y}{\partial x}\right)\frac{\partial U}{\partial X} + \frac{\partial Y}{\partial x}\frac{\partial Y}{\partial y}\frac{\partial U}{\partial Y}\Big], \tag{5.48}$$

$$\frac{\partial u}{\partial y} = \frac{1}{J}\Big[+2\frac{\partial X}{\partial y}\frac{\partial Y}{\partial y}\frac{\partial U}{\partial X} + \left(\frac{\partial Y}{\partial y}\right)^2\frac{\partial U}{\partial Y}\Big], \tag{5.49}$$

This version of the chain rule we will use in the stress balance condition, but the stress balance condition reveals an additional simplification. We will use that version of the chain rule for the rest of the derivation.

5.6 Stress balance condition

We have now set up the problem and are ready to consider more physical conditions. We will start with the stress balance, which approximates inner layer momentum conservation in a simple form. As in chapter 3, we will consider a re-written form of the stress balance that allows for a shear stress transformation.

The first step is to write the stress balance in terms of a constant, as I first did for equation 3.4:

$$1 = \left(\frac{\mu}{t}\right)\frac{\partial u}{\partial y} - \frac{\varrho r_{xy}}{t}\,, \tag{5.3}$$

The constant-property counterpart to this equation is

$$1 = \left(\frac{\mu_r}{T}\right)\frac{\partial U}{\partial Y} - \frac{\varrho_r R_{XY}}{T}\,. \tag{5.50}$$

The next step is to apply the chain rule to the variable-property equation to write it in terms of constant-property variables:

$$1 = \left(\frac{\mu}{t}\right)\frac{1}{J}\left[+2\frac{\partial X}{\partial y}\frac{\partial Y}{\partial y}\frac{\partial U}{\partial X} + \left(\frac{\partial Y}{\partial y}\right)^2\frac{\partial U}{\partial Y}\right] - \frac{\varrho r_{xy}}{t}\,. \tag{5.51}$$

Finally, we can set each corresponding component of this equation equal to its corresponding component in the constant-property equation:

$$\frac{\partial U}{\partial X}: \qquad \left(\frac{\mu}{t}\right)\frac{1}{J}2\frac{\partial X}{\partial y}\frac{\partial Y}{\partial y} = 0\,, \tag{5.52}$$

$$\frac{\partial U}{\partial Y}: \qquad \left(\frac{\mu}{t}\right)\frac{1}{J}\left(\frac{\partial Y}{\partial y}\right)^2 = \left(\frac{\mu_r}{T}\right), \tag{5.53}$$

$$R_{XY}: \qquad -\frac{\varrho r_{xy}}{t} = -\frac{\varrho_r R_{XY}}{T}\,. \tag{5.54}$$

This results in three equations:

$$\frac{\partial X}{\partial y} = 0\,, \tag{5.55}$$

$$\frac{\mathrm{d}X}{\mathrm{d}x} = \left(\frac{\mu}{\mu_r}\right)\left(\frac{T}{t}\right)\frac{\partial Y}{\partial y}\,, \tag{5.56}$$

$$R_{XY} = \left(\frac{\varrho}{\varrho_r}\right)\left(\frac{T}{t}\right)r_{xy}\,. \tag{5.57}$$

Here, it is important to take a step back and to think about these three equations and what they mean. The third equation was already discussed in chapter 3; it demonstrates that the assuming Morkovin's scaling is true is that same as assuming that the shear stresses are untransformed. The more interesting point arises with the combination of the first and second equations. The first equation states that the transformed streamwise coordinate is not a function of the untransformed wall-normal coordinate. Geometrically this means that a vertical profile at a single value of x transforms to another vertical profile at a single value of X. The second then states that the streamwise coordinate transformation (which is also the streamwise velocity transformation) is a function of the mean viscosity ratio, the shear stress ratio, and part of the wall-normal coordinate transformation. The left-hand side term is a function only of the streamwise coordinate, which the right-hand side should also be a function of the wall-normal coordinate. This contradicts the first equation. As a result, we have another difference between what should work in theory versus what should work in practice. In theory, $\frac{\partial X}{\partial y} = 0$, but in practice $\frac{\partial X}{\partial y} \neq 0$. This point will be discussed more in a later section on the streamwise coordinate.

If we assume that $\frac{\partial X}{\partial y} = 0$, we can further simplify the chain rule:

$$\frac{\partial u}{\partial x} = \frac{1}{J}\Big[\qquad + \frac{\mathrm{d}X}{\mathrm{d}x}\frac{\partial Y}{\partial y}\frac{\partial U}{\partial X} \qquad + \frac{\partial Y}{\partial x}\frac{\partial Y}{\partial y}\frac{\partial U}{\partial Y}\Big], \tag{5.58}$$

$$\frac{\partial u}{\partial y} = \frac{1}{J}\Big[\qquad + \left(\frac{\partial Y}{\partial y}\right)^2\frac{\partial U}{\partial Y}\Big], \tag{5.59}$$

The Jacobian determinant now is

$$J = \frac{\mathrm{d}X}{\mathrm{d}x}\frac{\partial Y}{\partial y}. \tag{5.60}$$

5.7 Log-law condition

As in chapter 2, we will consider the “diagnostic function” version of the log-law:

$$\frac{1}{\kappa} = y\left(\frac{\varrho}{\tau_\mathrm{w}}\right)^{1/2}\frac{\partial u}{\partial y}, \tag{5.4}$$

The constant-property counterpart of this equation is

$$\frac{1}{\kappa} = Y\left(\frac{\varrho_r}{\tau_\mathrm{w}}\right)^{1/2}\frac{\partial U}{\partial Y}. \tag{5.61}$$

Due to the simplifications in the chain rule in the previous section, there is only a single term to consider, so the comparison process is simple. We can start by applying the chain rule to the variable-property equation:

$$\frac{1}{\kappa} = y\left(\frac{\varrho}{\tau_{\mathrm{w}}}\right)^{1/2}\frac{1}{J}\left(\frac{\partial Y}{\partial y}\right)^{2}\frac{\partial U}{\partial Y}. \tag{5.62}$$

The final step is to match corresponding components. Again, there is only one term we need to match:

$$\frac{\partial U}{\partial Y}: \qquad y\left(\frac{\varrho}{\tau_{\mathrm{w}}}\right)^{1/2}\frac{1}{J}\left(\frac{\partial Y}{\partial y}\right)^{2} = Y\left(\frac{\varrho_r}{\tau_{\mathrm{w}}}\right)^{1/2}. \tag{5.63}$$

The log-law can therefore be satisfied through the following condition:

$$\frac{\mathrm{d}X}{\mathrm{d}x} = \left(\frac{y}{Y}\right)\left(\frac{\varrho}{\varrho_r}\right)^{1/2}\frac{\partial Y}{\partial y}. \tag{5.64}$$

This equation is almost identical to the equation given in chapter 2. The only difference is the partial derivative in the right-hand side.

I should also note that this equation also does not appear to satisfy $\frac{\partial X}{\partial y} = 0$ in practice. Again, I will discuss this contradiction more in the later section on the streamwise coordinate.

5.8 The transformed wall-normal coordinate

5.8.1 The semi-local scaling and the shear stress transformation

As in chapter 2, we now have 2 equations. However, we have more than two unknowns. Still, we can continue by setting the stress balance condition equal to the log-law condition as done before:

$$\frac{\mathrm{d}X}{\mathrm{d}x} = \left(\frac{\mu}{\mu_r}\right)\left(\frac{T}{t}\right)\frac{\partial Y}{\partial y} = \left(\frac{y}{Y}\right)\left(\frac{\varrho}{\varrho_r}\right)^{1/2}\frac{\partial Y}{\partial y}. \tag{5.65}$$

From this equation, we can see that

$$\left(\frac{\mu}{\mu_r}\right)\left(\frac{T}{t}\right) = \left(\frac{y}{Y}\right)\left(\frac{\varrho}{\varrho_r}\right)^{1/2}. \tag{5.66}$$

This equation appears odd at first, but we can re-arrange it to reveal a more useful equation:

$$\left(\frac{T}{t}\right) = \left(\frac{\varrho}{\varrho_r}\right)^{+1/2}\left(\frac{\mu}{\mu_r}\right)^{-1}\left(\frac{y}{Y}\right) = \left(\frac{Y_{\mathrm{SL}}}{Y}\right). \tag{5.67}$$

We can write this equation in several useful ways:[2]

$$\left(\frac{Y}{Y_{\mathrm{SL}}}\right) = \left(\frac{T}{t}\right)^{-1}, \tag{5.68}$$

$$Y\,T = Y_{\mathrm{SL}}\,t\,. \tag{5.69}$$

Note that these equations attribute any difference between the transformed wall-normal coordinate to a change in the shear stress transformation. However, provided that the shear stresses are equal, as observations in previous chapters show, the transformed coordinate must be the semi-local scaling for the log-law to conserve mass and momentum in the inner layer. As in chapter 2, no other coordinate is possible.

5.8.2 Outer layer effects

We should stop and re-consider the results in the chapter 4 on outer layer effects. The second derivative of the transformed wall-normal coordinate Y must be zero for the untransformed

[2] Assuming that the shear stresses are close to each other, we can linearize this equation to

$$\left(\frac{Y}{Y_{\mathrm{SL}}}\right) \approx 2 - \left(\frac{T}{t}\right).$$

This form could simplify any theory that allows for a shear stress transformation.

outer layer coordinate to match the transformed outer layer coordinate. If the wall-normal coordinate is the semi-local scaling, then the only way to satisfy this constraint is to set $\mu \sim \varrho^{+1/2}$ (equation 4.21). However, equation 5.67 has the transformed shear stress as an unknown. We can always choose a shear stress transformation that sets the coordinate's second derivative to zero, for example. Consider setting the transformed coordinate equal to the untransformed coordinate:

$$Y = y\,. \tag{5.70}$$

By definition, the second derivative of this transformed coordinate is zero.[3] Therefore the outer layer coordinate is never transformed. The transformed shear stress distribution then becomes "semi-local" in nature:

$$T = \left(\frac{\varrho}{\varrho_r}\right)^{+1/2} \left(\frac{\mu}{\mu_r}\right)^{-1} t\,. \tag{5.71}$$

But this shear stress transformation does not agree with observations. We should not expect this idea to work. In fact, the velocity transformation for this transformed coordinate and shear stress transformation is the Van Driest transformation:

$$\frac{\mathrm{d}X}{\mathrm{d}x} = \left(\frac{\mu}{\mu_r}\right)\left(\frac{T}{t}\right)\frac{\partial Y}{\partial y} = \cancel{\left(\frac{\mu}{\mu_r}\right)}\left(\frac{\varrho}{\varrho_r}\right)^{+1/2} \cancel{\left(\frac{\mu}{\mu_r}\right)^{-1}} = \left(\frac{\varrho}{\varrho_r}\right)^{+1/2}. \tag{5.72}$$

As a consequence, choosing a shear stress distribution to force the transformed outer layer coordinate to equal the untransformed outer layer coordinate solves one problem, but creates another, since the Van Driest transformation does not work for cold walls. There is no simple way to modify the TL transformation theory to match the outer layer coordinates.

[3] The first derivative must equal 1, assuming that we non-dimensionalize using wall reference variables.

5.8.3 The assumption of no shear stress transformation

The simplest way forward is to assume that the shear stresses are not transformed:

$$T = t\,. \tag{5.73}$$

The derivation given in chapter 2 required this assumption immediately for the stress balances to match. This derivation is more general but nonetheless cannot avoid this assumption. The transformed wall-normal coordinate then is the semi-local scaling:

$$Y = Y_{\mathrm{SL}} = \left(\frac{\varrho}{\varrho_r}\right)^{+1/2} \left(\frac{\mu}{\mu_r}\right)^{-1} y\,. \tag{2.29}$$

For the rest of this chapter, I will not necessarily assume that the shear stresses are untransformed, but at the end I will present all of the answers assuming that.

5.9 The production rates, matching the whole equation

At this point, we have largely considered all of the major components of the TL transformation theory as presented in chapter 2. The TL transformation does not directly specify the Reynolds stress scalings or transformations for the normal Reynolds stresses, only the Reynolds shear stress since the stress balance contains it. To that end, we can transform the production rates themselves to add additional physics to the transformation. This process will directly involve the Reynolds normal stresses, so we would have the means to derive some kind of transformation involving them. The most direct way to do this would be to transform all of the production rate terms in the TKE equation as a single equation. As stated in section 2.2, the choice of corresponding components requires some interpretation. For the production rates, we have two options:

1. transforming all of the production rate terms as a single unit, or

2. transforming each production rate term individually.

Note that the choice is not completely arbitrary. The second option — transforming each term individually — matches the working definition of Morkovin's hypothesis given in chapter 3 in the sense that we transform each turbulence production mechanism individually. However, this option is quite limiting, since we eliminate the possibility that the gradient terms from the chain rule will mix together. Nonetheless, the first option runs into a physical contradiction that reveals why the second option, and its working definition of Morkovin's hypothesis, proves more useful.

The production rate terms of the TKE equation are

$$p = -\bar{\varrho}\,\widetilde{u_i u_j}\,\frac{\partial \widetilde{u}_i}{\partial x_j} = -\varrho\left[r_{xx}\frac{\partial u}{\partial x} + r_{xy}\frac{\partial u}{\partial y} + r_{xy}\frac{\partial v}{\partial x} + r_{yy}\frac{\partial v}{\partial y}\right]. \tag{5.74}$$

As previously stated, in channel flows only one term remains (the second). In boundary layers, there are four terms. Nonetheless, boundary layer theory and mass conservation can simplify the production rate equation into something more useful. Again, boundary layer theory demonstrates that the streamwise gradient of the wall-normal velocity is negligible:

$$\frac{\partial v}{\partial x} \approx 0. \tag{5.75}$$

Mass conservation also allows us to eliminate another term:

$$\frac{\partial v}{\partial y} = -\frac{\partial u}{\partial x}. \tag{5.76}$$

The variable-property production rate equation now becomes

$$p = -\varrho\left[\left(r_{xx} - r_{yy}\right)\frac{\partial u}{\partial x} + r_{xy}\frac{\partial u}{\partial y}\right]. \tag{5.77}$$

Our first step is to re-write this equation as a constant:

$$-1 = \left(\frac{\varrho}{p}\right)\left[\left(r_{xx} - r_{yy}\right)\frac{\partial u}{\partial x} + r_{xy}\frac{\partial u}{\partial y}\right] \tag{5.78}$$

The constant-property counterpart to this equation is

$$-1 = \left(\frac{\varrho_r}{P}\right)\left[\left(R_{XX} - R_{YY}\right)\frac{\partial U}{\partial X} + R_{XY}\frac{\partial U}{\partial Y}\right]. \tag{5.79}$$

Next, we apply the chain to the variable-property equation:

$$-1 = \left(\frac{\varrho}{p}\right)\frac{1}{J}\Bigg[+ \frac{\partial U}{\partial X}\left[+\frac{\mathrm{d}X}{\mathrm{d}x}\frac{\partial Y}{\partial y}\left(r_{xx} - r_{yy}\right)\right] \tag{5.80}$$

$$+ \frac{\partial U}{\partial Y}\left[+\frac{\partial Y}{\partial x}\frac{\partial Y}{\partial y}\left(r_{xx} - r_{yy}\right) + \left(\frac{\partial Y}{\partial y}\right)^2 r_{xy}\right]\Bigg]. \tag{5.81}$$

Finally, we set each corresponding component of this equation to its constant-property counterpart. Here, the component are the gradient terms.

$$\frac{\partial U}{\partial X}: \qquad \left(\frac{\varrho}{p}\right)\frac{1}{J}\frac{\mathrm{d}X}{\mathrm{d}x}\frac{\partial Y}{\partial y}\left(r_{xx} - r_{yy}\right) = \left(\frac{\varrho_r}{P}\right)\left(R_{XX} - R_{YY}\right), \tag{5.82}$$

$$\frac{\partial U}{\partial Y}: \qquad \left(\frac{\varrho}{p}\right)\frac{1}{J}\left[\frac{\partial Y}{\partial x}\frac{\partial Y}{\partial y}\left(r_{xx} - r_{yy}\right) + \left(\frac{\partial Y}{\partial y}\right)^2 r_{xy}\right] = \left(\frac{\varrho_r}{P}\right)R_{XY}. \tag{5.83}$$

This results in the following two equations:

$$\left(\frac{\varrho}{\varrho_r}\right)\left(\frac{P}{p}\right)\left(r_{xx} - r_{yy}\right) = \left(R_{XX} - R_{YY}\right), \tag{5.84}$$

$$\left(\frac{\varrho}{\varrho_r}\right)\left(\frac{P}{p}\right)\left[\left(r_{xx} - r_{yy}\right)\frac{\partial Y}{\partial x} + r_{xy}\frac{\partial Y}{\partial y}\right] = R_{XY}\frac{\mathrm{d}X}{\mathrm{d}x}. \tag{5.85}$$

These equations create 2 problems, one of them fatal:

1. The equations cannot solve for R_{XX} or R_{YY}, only $(R_{XX} - R_{YY})$. As a result, we cannot derive any useful transformation for the Reynolds normal stresses.

2. No single production scaling P/p exists that works for both equations and satisfies known empirical scalings for the Reynolds normal stresses (Morkovin's scaling).

The second is the fatal problem. To see this, we must consider the case of a channel flow (no spatial development in the transformed wall-normal coordinate). We can use Morkovin's scalings for the answers for the transformed Reynolds stresses:

$$R = \left(\frac{\varrho}{\varrho_r}\right) r\,. \tag{5.86}$$

At this point, we just need to solve for the production rate transformation that each equation then provides. The first equation is simple to solve:

$$\cancel{\left(\frac{\varrho}{\varrho_r}\right)}\left(\frac{P}{p}\right)\cancel{\left(r_{xx}-r_{yy}\right)} = \cancel{\left(\frac{\varrho}{\varrho_r}\right)\left(r_{xx}-r_{yy}\right)}\,. \tag{5.87}$$

The production scaling required for the first equation then is

$$\frac{P}{p} = 1\,. \tag{5.88}$$

Now we can consider the second equation. We can use the stress balance condition for $\frac{\mathrm{d}X}{\mathrm{d}x}$ in the right-hand side:

$$\cancel{\left(\frac{\varrho}{\varrho_r}\right)}\left(\frac{P}{p}\right)\cancel{r_{xy}}\frac{\mathrm{d}Y}{\mathrm{d}y} = \cancel{\left(\frac{\varrho}{\varrho_r}\right)r_{xy}}\frac{\mathrm{d}X}{\mathrm{d}x}\,. \tag{5.89}$$

Using the stress balance condition, this equation becomes

$$\left(\frac{P}{p}\right)\frac{\mathrm{d}Y}{\mathrm{d}y} = \frac{\mathrm{d}X}{\mathrm{d}x} = \left(\frac{\mu}{\mu_r}\right)\frac{\mathrm{d}Y}{\mathrm{d}y}\,. \tag{5.90}$$

The production scaling then is the scaling considered in chapter 3:

$$\left(\frac{P}{p}\right) = \left(\frac{\mu}{\mu_r}\right). \tag{5.91}$$

These production scales are inconsistent. This inconsistency means that considering the production terms as a whole cannot make a transformation that works, since either the Reynolds normal stresses will disagree with the empirically known scaling, or the Reynolds shear stress will, even in the case of channels. Therefore, transforming the production equation as a whole equation is incorrect since it only allows for a single production rate scaling. Instead, we must transform each term of the equation individually (a term-by-term transformation).

5.10 The production rates, matching term-by-term

Now we can try to match each production rate term individually. This method harkens back to my working definition of Morkovin's hypothesis. We will treat each production mechanism as analogous, but the production rates themselves can differ. Unlike before, this method allows for each production mechanism to have its own production rate scaling. This property proves key to making the transformation work.

We can start by decomposing the production rate equation in individual terms:

$$p = p_{xx} + p_{xy} + p_{yy}\,, \tag{5.92}$$

$$P = P_{XX} + P_{XY} + P_{YY}\,. \tag{5.93}$$

At this point, we just need to transform each term individually, but in a form that allows for the production rates to be different in each regime.

5.10.1 The first production rate term

The first production rate term is p_{xx}:

$$p_{xx} = -\varrho r_{xx} \frac{\partial u}{\partial x}\,. \tag{5.94}$$

First, we need to write the equation in terms of a constant:

$$-1 = \left(\frac{\varrho r_{xx}}{p_{xx}}\right) \frac{\partial u}{\partial x}\,. \tag{5.95}$$

The constant-property counterpart to this equation is

$$-1 = \left(\frac{\varrho_r R_{XX}}{P_{XX}} \right) \frac{\partial U}{\partial X} \,. \tag{5.96}$$

Next, we need to apply the chain rule to the variable-property equation:

$$-1 = \left(\frac{\varrho r_{xx}}{p_{xx}} \right) \frac{1}{J} \left[+ \frac{\mathrm{d}X}{\mathrm{d}x} \frac{\partial Y}{\partial y} \frac{\partial U}{\partial X} + \frac{\partial Y}{\partial x} \frac{\partial Y}{\partial y} \frac{\partial U}{\partial Y} \right] . \tag{5.97}$$

Finally, we set each corresponding component equal to its counterpart. Again, those components are the gradient terms:

$$\frac{\partial U}{\partial X}: \qquad \left(\frac{\varrho r_{xx}}{p_{xx}} \right) \frac{1}{J} \frac{\mathrm{d}X}{\mathrm{d}x} \frac{\partial Y}{\partial y} = \left(\frac{\varrho_r R_{XX}}{P_{XX}} \right) , \tag{5.98}$$

$$\frac{\partial U}{\partial Y}: \qquad \left(\frac{\varrho r_{xx}}{p_{xx}} \right) \frac{1}{J} \frac{\partial Y}{\partial x} \frac{\partial Y}{\partial y} = 0 \,. \tag{5.99}$$

We end up with two equations. The first equation simplifies to

$$R_{XX} = \left(\frac{\varrho}{\varrho_r} \right) \left(\frac{P_{XX}}{p_{xx}} \right) r_{xx} \,. \tag{5.100}$$

Conventionally, Morkovin's scaling is the Reynolds stress scaling for this term, but as shown in chapter 2, this scaling does not work well for this particular Reynolds stress. We can attribute the error to an error in the production rate scaling, but we do not have any particular scaling to use or physics to apply. As a result, I will assume the validity of Morkovin's scaling in this section:

$$R_{XX} = \left(\frac{\varrho}{\varrho_r} \right) r_{xx} \,. \tag{5.101}$$

If we assume that the Reynolds stresses follow Morkovin's scaling, the production rate scaling for P_{XX} is

$$\left(\frac{P_{XX}}{p_{xx}} \right) = 1 \,. \tag{5.102}$$

This production rate scaling agrees with the idea stated in the previous section. Physically, it states that this production rate will not be transformed.

The second equation from the decomposition must equal zero. Given that all of the other terms must have a finite value, the only term that should be zero is

$$\frac{\partial Y}{\partial x} = 0\,. \tag{5.103}$$

We will discuss this term in detail later in this chapter.

5.10.2 The second production rate term

The second production rate term is p_{xy}:

$$p_{xy} = -\varrho r_{xy} \frac{\partial u}{\partial y}\,. \tag{5.104}$$

First, we need to write the equation in terms of a constant:

$$-1 = \left(\frac{\varrho r_{xy}}{p_{xy}}\right) \frac{\partial u}{\partial y}\,. \tag{5.105}$$

The constant-property counterpart to this equation is

$$-1 = \left(\frac{\varrho_r R_{XY}}{P_{XY}}\right) \frac{\partial U}{\partial Y}\,. \tag{5.106}$$

Next, we need to apply the chain rule to the variable-property equation:

$$-1 = \left(\frac{\varrho r_{xy}}{p_{xy}}\right) \frac{1}{J} \left(\frac{\partial Y}{\partial y}\right)^2 \frac{\partial U}{\partial Y}\,. \tag{5.107}$$

There is only one term to compare. The resulting equation is

$$\left(\frac{\varrho}{\varrho_r}\right) \left(\frac{P_{XY}}{p_{xy}}\right) r_{xy} \frac{\partial Y}{\partial y} = R_{XY} \frac{\mathrm{d}X}{\mathrm{d}x}\,. \tag{5.108}$$

This equation is the same equation as in the chapter 3. If we apply the streamwise coordinate transformation and the Reynolds shear stress from the stress balance equation, we can see that the production rate scaling required is

$$\left(\frac{P_{XY}}{p_{xy}}\right) = \left(\frac{\mu}{\mu_r}\right)\left(\frac{T}{t}\right)^2 . \tag{3.13}$$

Again, this is the same result as in the chapter 3. If we expect Morkovin's scaling to work, then $T = t$ and

$$\left(\frac{P_{XY}}{p_{xy}}\right) = \left(\frac{\mu}{\mu_r}\right) . \tag{3.14}$$

As demonstrated in chapter 3, this production rate scaling matches the P_{XY} production rate well for channels but generally only matches the peak and trend of the production rate in boundary layers.

5.10.3 The third production rate

The third production rate term is p_{yy}:

$$p_{yy} = -\varrho r_{yy}\frac{\partial v}{\partial y} = +\varrho r_{yy}\frac{\partial u}{\partial x} . \tag{5.109}$$

First, we need to write the equation in terms of a constant:

$$+1 = \left(\frac{\varrho r_{yy}}{p_{yy}}\right)\frac{\partial u}{\partial x} . \tag{5.110}$$

The constant-property counterpart to this equation is

$$+1 = \left(\frac{\varrho_r R_{YY}}{P_{YY}}\right)\frac{\partial U}{\partial X} . \tag{5.111}$$

Next, we need to apply the chain rule to the variable-property equation:

$$+1 = \left(\frac{\varrho r_{yy}}{p_{yy}}\right)\frac{1}{J}\left[+\frac{\mathrm{d}X}{\mathrm{d}x}\frac{\partial Y}{\partial y}\frac{\partial U}{\partial X} + \frac{\partial Y}{\partial x}\frac{\partial Y}{\partial y}\frac{\partial U}{\partial Y}\right] . \tag{5.112}$$

And finally, we compare each corresponding component:

$$\frac{\partial U}{\partial X}: \qquad \left(\frac{\varrho r_{yy}}{p_{yy}}\right)\frac{1}{J}\frac{\mathrm{d}X}{\mathrm{d}x}\frac{\partial Y}{\partial y} = \left(\frac{\varrho_r R_{YY}}{P_{YY}}\right), \tag{5.113}$$

$$\frac{\partial U}{\partial Y}: \qquad \left(\frac{\varrho r_{yy}}{p_{yy}}\right)\frac{1}{J}\frac{\partial Y}{\partial x}\frac{\partial Y}{\partial y} = 0. \tag{5.114}$$

These equations are just like the previous equations for p_{xx}. The resulting production rate scaling to satisfy Morkovin's scaling is

$$\left(\frac{P_{YY}}{p_{yy}}\right) = 1. \tag{5.115}$$

As in the case of the first production rate, this production rate remains untransformed.

5.10.4 The condition that $\frac{\partial Y}{\partial x} = 0$

The analysis for the first and third production rates required that the transformed wall-normal coordinate cannot be a function of the streamwise coordinate:

$$\frac{\partial Y}{\partial x} = 0. \tag{5.103}$$

This equation at first glance appears insignificant but it contains many significant results that explain why the TL transformation works well for channels and why it works poorly for boundary layers. We can consider this variable from two points-of-view. The first is from the point-of-view of the outer layer coordinate:

$$\frac{\partial Y}{\partial x} = \left(\frac{y}{\delta}\right)\left[\frac{\mathrm{d}\Delta}{\mathrm{d}\delta} - \left(\frac{\Delta}{\delta}\right)\right]\frac{\mathrm{d}\delta}{\mathrm{d}x}. \tag{4.28}$$

The second is from the point-of-view of the semi-local scaling:

$$\frac{\partial Y}{\partial x} = y\frac{\partial}{\partial x}\left[\left(\frac{\varrho}{\varrho_r}\right)^{+1/2}\left(\frac{\mu}{\mu_r}\right)^{-1}\right]. \tag{5.116}$$

There are four conditions that make this equation equal zero:

1. in the inner layer (where $y/\delta \to 0$), or

2. in an incompressible flow (where $\Delta = \delta$), or

3. in a channel flow (where derivatives in the streamwise direction like $\frac{\mathrm{d}\delta}{\mathrm{d}x}$ are zero), or

4. for flows where $\mu \sim \varrho^{+1/2}$ (see equation 4.21, the viscosity relationship required for the transformed outer layer coordinate to equal the untransformed outer layer coordinate).

The second and third cases are trivial, but the first and fourth require more discussion. Ultimately, both the first and fourth conditions prove why the TL transformation does not work for most boundary layers.

The inner layer of a boundary layer flow, where $y/\delta \to 0$, is a simpler and more universal region of the flow. From the point-of-view of the outer layer, provided that $y/\delta \to 0$, the value of $\frac{\partial Y}{\partial x}$ will approach zero. For low Reynolds numbers, the size of the inner layer (strictly speaking here as where $y/\delta \to 0$) is quite small, but for high Reynolds numbers, the size of the inner layer could be substantial in terms of wall units. For example, for a boundary layer at a friction Reynolds number of $\mathrm{Re}_\tau = 10^3$, $y_+ = 10^2$ where $y/\delta = 0.1$ (one order of magnitude less than the boundary layer thickness). At this Reynolds number, the value of $\frac{\partial Y}{\partial x}$ should be nearly zero at $Y_{\mathrm{SL},+} \approx 50$. This property then would allow in theory for the transformation to work. For even higher Reynolds numbers, the size of the inner layer would grow even more and provide more opportunity for the condition that $\frac{\partial Y}{\partial x} = 0$. This line of reasoning could explain why the TL transformation appears to work better for higher Reynolds number boundary layers than lower Reynolds number boundary layers. Consider again the Mach 2 adiabatic wall boundary layer results plotted in figure 2.9 (the TL-transformed log-law intercept error plotted as a function of Mach number). Once controlled for the Mach number and the wall heat transfer rate, the highest Reynolds number case has the smallest error and the lowest Reynolds number case has the highest — just as we expect now — though in none of the cases does the error disappear. We can hypothesize that the error could disappear provided that the Reynolds number is high enough, but the question of what value of the Reynolds number suffices remains open. All that we can say for now is that the Reynolds number must be quite high ($\mathrm{Re}_\tau \to \infty$).[4]

However, the point-of-view of the outer layer coordinate is not the only point-of-view here, and strictly speaking we cannot assume that the transformed coordinate (the semi-local scale) will obey the outer layer coordinate matching hypothesis. Nonetheless, we can even see that $\frac{\partial Y}{\partial x} = 0$ is approximately true from the point-of-view of the semi-local scaling applied to boundary layers over isothermal walls. Isothermal walls do not have any streamwise variation in the mean density and mean viscosity at the wall, so they would have little to no streamwise variation near the wall as well. Provided that the Reynolds number is high enough that the size of the inner layer is large in wall units, the value of $\frac{\partial Y}{\partial x}$ could be close to zero.

The fourth case where $\frac{\partial Y}{\partial x} = 0$ is when the mean viscosity varies with the square root of the mean density. This condition is in the only condition that allows for the entire boundary layer to be transformed. As discussed in chapter 4, this kind of viscosity relationship is the only relationship that lets the transformed outer layer coordinate match the untransformed outer layer coordinate when the coordinate is the semi-local scaling. What this means in practice is

[4] This point somewhat invalidates the idea of using the point-wise semi-local friction Reynolds number of Patel, Peeters, et al. (2015) and Patel et al. (2016) in boundary layers. If the data must be at a very high Reynolds number for the TL transformation to even potentially work, the concept of a Reynolds number transformation breaks down. All that we can say is that as the friction Reynolds number tends to infinity ($\mathrm{Re}_\tau \to \infty$) the point-wise local friction Reynolds number tends to infinity too ($\mathrm{Re}_{\tau,\mathrm{local}} \to \infty$).

that when the second derivative of the transformed coordinate is zero — when the outer layer coordinate matching hypothesis is true — $\frac{\partial Y}{\partial x}$ equals zero identically. The two conditions are actually directly connected. This observation supports the idea that the mismatch in the outer layer coordinates is the source of the error in the TL transformation, because we now see that it is directly related to how well the transformation will match the production rate terms.

Note also that the fourth condition is sufficient but unnecessary in channels. I eluded to this point earlier in section 4.4. As long as there is no spatial development, the equation for $\frac{\partial Y}{\partial x} = 0$ does not require that $\mu \sim \varrho^{+1/2}$. Only boundary layers require that the outer layer coordinates match (what the fourth condition specifies), since channels already satisfy the condition. This observation explains why the error in the TL transformation does not depend on the second derivative of the coordinate for the case of channels (see figure 4.5). Channels always satisfy the condition that $\frac{\partial Y}{\partial x} = 0$, so there is no need for the second derivative of their transformed coordinates to be zero too (though observations show that it is zero for $Y_{\mathrm{SL},+} > 20$).

5.11 The transformed streamwise coordinate

If we assume that the shear stress is untransformed ($T = t$), then the streamwise coordinate and velocity transformations become

$$\frac{\mathrm{d}X}{\mathrm{d}x} = \frac{\mathrm{d}U}{\mathrm{d}u} = \left(\frac{\mu}{\mu_r}\right)\frac{\mathrm{d}Y}{\mathrm{d}y} = \left(\frac{y}{Y}\right)\left(\frac{\varrho}{\varrho_r}\right)^{1/2}\frac{\mathrm{d}Y}{\mathrm{d}y} = \left(\frac{\varrho}{\varrho_r}\right)^{+1/2}\left[1 + \frac{1}{2}\frac{1}{\varrho}\frac{\partial \varrho}{\partial y}y - \frac{1}{\mu}\frac{\partial \mu}{\partial y}y\right]. \tag{2.37}$$

This equation is identical to the equation given in chapter 2, but our interpretation differs. All of the coordinate derivatives are now exact derivatives (in theory, at least), since $\frac{\partial X}{\partial y} = 0$ and $\frac{\partial Y}{\partial x} = 0$. The partial derivatives remain for the mean fluid properties, however. We also know that mass conservation states that the streamwise velocity transformation equals the streamwise coordinate transformation, which I will now discuss in detail.

First, we need to discuss the geometric interpretation of $\frac{\mathrm{d}X}{\mathrm{d}x}$. There are 3 cases that matter here:

1. $\frac{\mathrm{d}X}{\mathrm{d}x} = 1$. This case corresponds to the streamwise distances being the same in both regimes.

2. $\frac{\mathrm{d}X}{\mathrm{d}x} > 1$. This case corresponds to the transformed streamwise distance being longer than the untransformed streamwise distance. In that case, objects in a compressible flow appear shorter in length than they should in an equivalent incompressible flow since $\mathrm{d}x < \mathrm{d}X$.

3. $\frac{\mathrm{d}X}{\mathrm{d}x} < 1$. This case corresponds to the transformed streamwise distance being shorter than the untransformed streamwise distance. In that case, objects in a compressible flow appear longer in length than they should in an equivalent incompressible flow since $\mathrm{d}x > \mathrm{d}X$.

Second, we need to discuss why the differentials are exact here. To satisfy the stress balance and log-law condition, the wall-normal derivative of the transformed streamwise coordinate must equal zero:

$$\frac{\partial X}{\partial y} = 0\,. \tag{5.55}$$

This equation makes the differential exact. Equation 5.55 has a simple geometric interpretation. It specifies that an untransformed vertical profile at a single value of x transforms to another transformed vertical profile at a single value of X. A line perpendicular to the wall transforms to a line perpendicular to the wall, in other words.

Using this equation, we can see that the streamwise coordinate and velocity transformations must be flat by taking the derivative with respect to the wall-normal coordinate here:

$$\frac{\partial^2 X}{\partial x \partial y} = \frac{\partial}{\partial y}\left(\frac{\mathrm{d}X}{\mathrm{d}x}\right) = \frac{\partial}{\partial y}\left(\frac{\mathrm{d}U}{\mathrm{d}u}\right) = 0\,. \tag{5.117}$$

This mixed partial derivative term can be thought of like the second derivative of the wall-normal coordinate — a measurement of how well the transformation obeys its underlying equations. In theory, the value of this equation should be zero, but in practice it is not.

Figures 5.1a, 5.1b, and 5.1c plot the values of the streamwise coordinate and velocity transformations $\frac{\mathrm{d}X}{\mathrm{d}x} = \frac{\mathrm{d}U}{\mathrm{d}u}$. As stated before, the values plotted are not flat. The streamwise coordinate transformation varies as a function of the wall-normal coordinate. It varies substantially before the log-layer, and in the case of a cold wall boundary layer, continues to vary substantially farther from the wall. Fortunately, for channels and adiabatic wall boundary layers, the streamwise coordinate transformation reaches a plateau after the buffer layer. At this point, the error in the streamwise coordinate is zero, but elsewhere it would be difficult to state with certainty that a vertical line transforms into another vertical line.

How well does this theory about the streamwise coordinate agree with the data? There are some difficulties in validating this theory due to the lack of quantitative information about the spatial development of any flow. Most data collected involves profiles in the wall-normal direction and not the streamwise direction, so it is difficult to validate the theory here precisely. Nonetheless, we can examine the length of the streamwise streaks — long regions of streamwise velocity fluctuations in the buffer layer — to see if this theory agrees qualitatively with the data. We still run into some issues here: the definition of a streamwise streak is somewhat

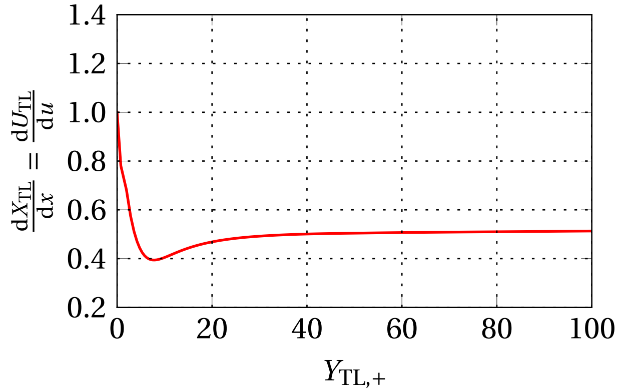

(a) Channel (`2016-Trettel-DNS-0901`)

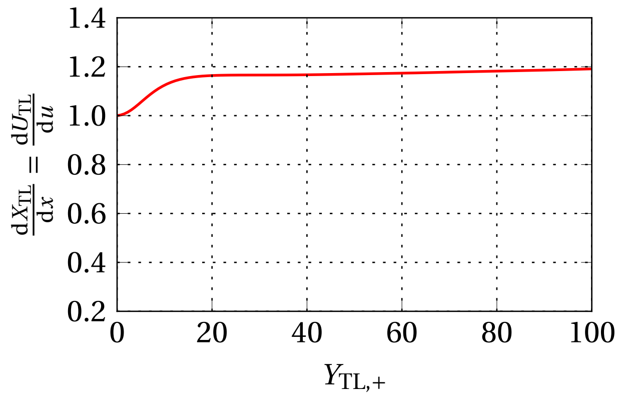

(b) Adiabatic wall boundary layer (`2011-Pirozzoli-DNS-0801`)

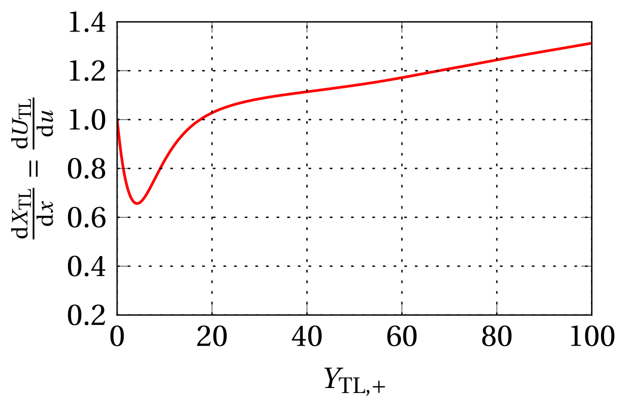

(c) Cold wall boundary layer (`2018-Zhang-DNS-0201`)

Figure 5.1: TL-transformed streamwise coordinate transformation and velocity transformation in the near wall region

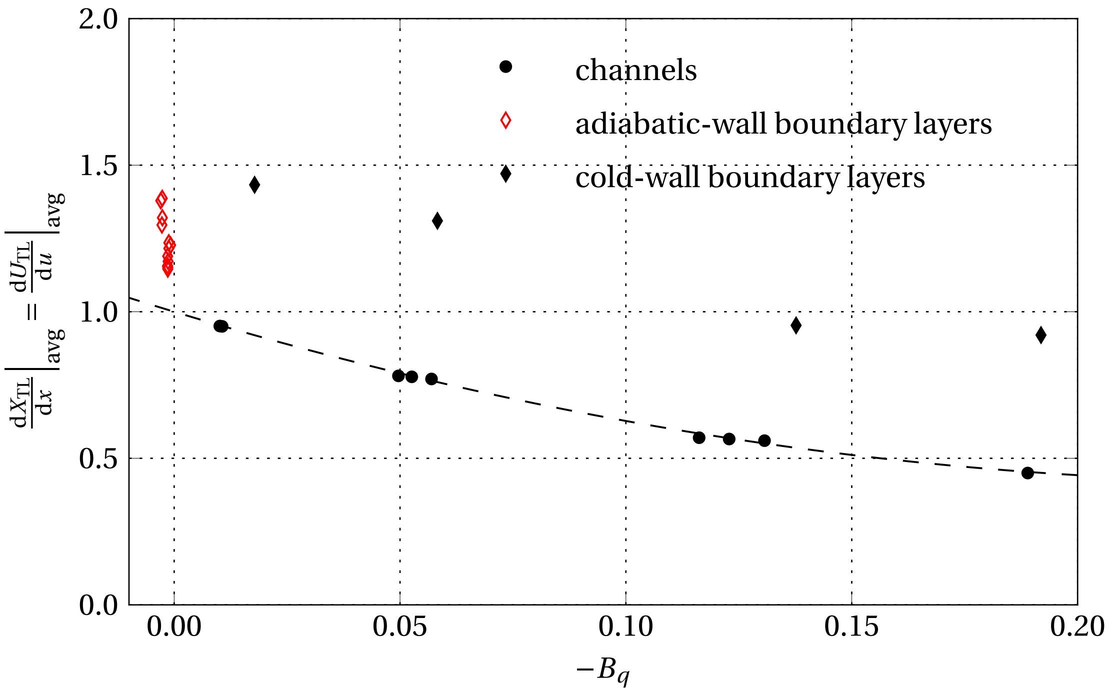

Figure 5.2: Average of the TL-transformed streamwise coordinate and velocity transformation in the buffer layer ($5 \leq Y_{\mathrm{TL},+} \leq 30$)

vague, so usually no precise lengths or even distributions of lengths of the streaks are measured. Despite these difficulties, the qualitative observations available agree with the theory.

Figure 5.2 plots the average value of $\frac{\mathrm{d}X}{\mathrm{d}x}$ in the buffer layer as a function of the dimensionless wall heat flux. The trend line follows the data for channels, which are always cold wall. Previous observations (Coleman et al., 1995; Duan et al., 2010) note that the streaks are longer in channels and cold wall boundary layers. This observation agrees with the theory. The channel data and trend line show that the streaks appear longer due to the value of $\frac{\mathrm{d}X}{\mathrm{d}x}$ being less than 1. In other words, the streaks appear longer because we are not measuring their length using the correct ruler. The streamwise coordinate itself has changed, so the streaks only appear longer when using the untransformed wall units as the Van Driest transformation used. Provided we use the correct streamwise coordinates, the streaks themselves may not have changed their length at all. However, I do not have the data to support such a precise statement. Future work should examine the streamwise coordinate more closely.

5.12 Summary of the complete transformation

This section summarizes all parts of the TL transformation. It turns out that the one-dimensional TL transformation theory presented in chapter 2 is the same basic answer that this chapter obtains, but the previous derivation does not reveal the limitations of the theory or the transformations for any additional quantities.

5.12.1 The coordinate and velocity transformations

The streamwise coordinate and velocity transformations:

$$\frac{\mathrm{d}X_{\mathrm{TL}}}{\mathrm{d}x} = \frac{\mathrm{d}U_{\mathrm{TL}}}{\mathrm{d}u} = \left(\frac{\varrho}{\varrho_r}\right)^{+1/2} \left[1 + \frac{1}{2}\frac{1}{\varrho}\frac{\partial \varrho}{\partial y} y - \frac{1}{\mu}\frac{\partial \mu}{\partial y} y\right]. \tag{2.37}$$

The wall-normal coordinate and velocity transformations:

$$\frac{\mathrm{d}Y_{\mathrm{TL}}}{\mathrm{d}y} = \frac{\mathrm{d}V_{\mathrm{TL}}}{\mathrm{d}v} = \left(\frac{\varrho}{\varrho_r}\right)^{+1/2} \left(\frac{\mu}{\mu_r}\right)^{-1} \left[1 + \frac{1}{2}\frac{1}{\varrho}\frac{\partial \varrho}{\partial y} y - \frac{1}{\mu}\frac{\partial \mu}{\partial y} y\right]. \tag{2.36}$$

The transformed wall-normal coordinate (the semi-local scaling):

$$Y_{\mathrm{TL}} = Y_{\mathrm{SL}} = \left(\frac{\varrho}{\varrho_r}\right)^{+1/2} \left(\frac{\mu}{\mu_r}\right)^{-1} y. \tag{2.29}$$

The dimensionless transformed wall-normal coordinate:

$$Y_{\mathrm{TL},+} = Y_{\mathrm{SL},+} = \frac{\varrho\left(\tau_{\mathrm{w}}/\varrho\right)^{1/2} y}{\mu} = \frac{\left(\tau_{\mathrm{w}}\varrho\right)^{1/2} y}{\mu}. \tag{2.30}$$

The dimensionless transformed streamwise velocity:

$$U_{\mathrm{TL},+} = \int_0^{u_+} \left(\frac{\varrho}{\varrho_r}\right)^{+1/2} \left[1 + \frac{1}{2}\frac{1}{\varrho}\frac{\partial \varrho}{\partial y} y - \frac{1}{\mu}\frac{\partial \mu}{\partial y} y\right] \mathrm{d}u_+ = \int_0^{u} \left[1 + \frac{1}{2}\frac{1}{\varrho}\frac{\partial \varrho}{\partial y} y - \frac{1}{\mu}\frac{\partial \mu}{\partial y} y\right] \frac{\mathrm{d}u}{\sqrt{\tau_\mathrm{w}/\varrho}} . \tag{2.38}$$

5.12.2 The Reynolds stress and shear stress transformations

The Reynolds stress scaling (Morkovin's scaling):

$$R_{\mathrm{TL},+} = \left(\frac{\varrho}{\varrho_r}\right) r_+ = \frac{r}{\tau_\mathrm{w}/\varrho} = \frac{\varrho r}{\tau_\mathrm{w}} . \tag{2.21}$$

The shear stress transformation:

$$T_{\mathrm{TL}} = t . \tag{5.73}$$

5.12.3 The production rate transformations

The primary production rate scaling:

$$P_{XY,\mathrm{TL}} = \left(\frac{\mu}{\mu_r}\right) p_{xy} . \tag{3.14}$$

The other production rate scalings:

$$P_{XX,\mathrm{TL}} = p_{xx} , \tag{5.102}$$

$$P_{YY,\mathrm{TL}} = p_{yy} . \tag{5.115}$$

5.12.4 The limiting conditions

The outer layer coordinate matching condition:

$$\frac{\partial^2 Y_{\mathrm{TL}}}{\partial y^2} = 0 . \tag{4.27}$$

The stress balance and log-law matching condition:

$$\frac{\partial X_{\mathrm{TL}}}{\partial y} = 0\,. \tag{5.55}$$

The production rate matching condition:

$$\frac{\partial Y_{\mathrm{TL}}}{\partial x} = 0\,. \tag{5.103}$$

Chapter 6

Conclusions

6.1 Conclusions

The requirements that $\frac{\partial Y}{\partial x} = 0$ and $\frac{\partial^2 Y}{\partial y^2} = 0$ prove the difficulty inherent in developing an analogy between compressible turbulent boundary layers and incompressible turbulent boundary layers. These two requirements suggest that such an analogy is impossible in most circumstances. It shows that the previous results for channels are only one of a few edge cases where the transformation theory can work. Channels are the primary edge case, but compressible channels are not real-world flows in many respects. Therefore, the issue of developing a useful analogy between compressible turbulent boundary layers and incompressible turbulent boundary layers is still an open question.

As stated in chapter 1, analogies have limitations and we should not expect them to work in all situations. Nonetheless, the two-dimensional extension to the TL transformation theory does provide many more components than the previous one-dimensional theory, including a new streamwise coordinate and new scalings for the production rates.

The failure of the TL transformation for boundary layers raises a good question: why does Morkovin's hypothesis work better in channels than in boundary layers? Are the turbulence production mechanisms equivalent when there is more than one present? The fit for the Reynolds stresses using Morkovin's scaling is far better for channels than for boundary layers, especially farther from the wall. The same goes for the production rates. A simple answer to the question is that channels only have one turbulence production mechanism and boundary layers have four, so it is much easier to match one mechanism than all four. In short, the more complex the physics are, the more limitations emerge.

Another answer comes from the physics of the situation. Morkovin's hypothesis may not be wrong, but the interpretation of it as an analogy falls apart in some circumstances. None of the results here demonstrate that compressibility plays a role in the turbulence structure (with the exception of the streamwise Reynolds normal stress). This idea lays at the heart of Morkovin's hypothesis. However, the results do show that the turbulence structure itself is not completely analogous to its incompressible counterpart (regardless of the effects of compressibility). While I have not identified the precise difference between the turbulence in compressible and incompressible turbulent boundary layers, the evidence here suggests that a difference exists. There may be no compressibility effects, but that does not mean that the turbulence itself is precisely the same, even if it is similar.

We must also consider that the TL transformation may lack some important physics that it should include. The Van Driest transformation lacked momentum conservation, for example, and its error in the viscous sublayer disappears when momentum is conserved properly. However, the two-dimensional formulation now contains mass and momentum conservation, so it is more difficult for it to ignore certain physical laws. Nonetheless, it may just implement them incorrectly. For example, my working definition of Morkovin's hypothesis requires us to interpret each production mechanism individually, and this choice ultimately creates the requirement that $\frac{\partial Y}{\partial x} = 0$. A different interpretation of Morkovin's hypothesis could eliminate that requirement all together, though my attempt eliminate that requirement (see subsection 5.9) runs into contradictions. These contradictions do not emerge when using my working definition of Morkovin's hypothesis, providing some support for it. Ultimately, the analogy may just fall apart and turbulence in boundary layers may fundamentally differ between the two regimes.

Still, the failure of the TL transformation for boundary layers does not necessarily mean that compressible turbulent boundary layers are beyond scientific understanding. All transformations are analogies and analogies have limitations. Regardless of whether an exact and useful analogy between compressible turbulent boundary layers and incompressible turbulent boundary layers exists, we still can approach the problem of compressible turbulent boundary layers on its own terms rather than forcing it into more familiar territory. New phenomena often call for new concepts, and the new concepts may actually explain compressible turbulent boundary layers better than assuming they are always equivalent to older concepts. And that may be what lies ahead.

6.2 Future work

1. Future work should include new boundary layer simulations that use the viscosity relationship $\mu \sim \varrho^{+1/2}$. If the outer layer coordinate matching hypothesis is true, then we should expect the transformation to work here. These simulations would then verify

or falsify the outer layer coordinate matching hypothesis by directly controlling for the value of the transformed coordinate's second derivative.

2. Future work should include measurements of the entire two-dimensional flow field for a boundary layer. The measurements must include the mean viscosity, the mean wall-normal velocity and all quantities related to the spatial development of the flow, including both Reynolds- and Favre-averaged quantities. Future transformation theories need better data to be validated, and velocity profiles alone no longer suffice.

3. Future work should address why the streamwise Reynolds normal stress does not match when scaled with Morkovin's scaling. The TL theory does not provide an answer for this question, but we can use it to note that perhaps this Reynolds stress needs a different production rate scaling.

4. Future work should include measurements of the distribution and length of the streamwise streaks in the buffer layer for both incompressible and compressible flow scenarios in both channels and boundary layers. The point of these measurements is to provide a basis to quantitatively validate the streamwise coordinate. Channels are the cheapest and best option to validate the theory, but validation in boundary layers also matters too, especially for flows where $\mu \sim \varrho^{+1/2}$.

5. Future work should investigate the effects of the transformed streamwise and wall-normal coordinates on the spectra and two-point correlations. The question is how the transformation affects the wavenumber and whether the we should also transform the wavenumber too.

6. Future work should investigate whether the shear stress needs to be transformed. The TL theory does not consider a shear stress transformation due to the success of Morkovin's scaling in matching the peak of the Reynolds shear stress, but this observation only makes the lack of a shear stress transformation an assumption underlying the theory. It would be beneficial to have an explanation as to why the shear stress does not need to be transformed at the least.

Bibliography

Alvarez, M. (2017). "Mach Number Effects on Rough-Wall Turbulent Boundary Layers". PhD thesis. University of California, Los Angeles. URL: https://escholarship.org/uc/item/65z4b9tr.

Bradshaw, Peter (1967). "The insensitivity of turbulent flow to changes in Reynolds number and Mach number". English. In: NPL Aero Note 1057. URL: https://ntrl.ntis.gov/NTRL/dashboard/searchResults/titleDetail/N6824729.xhtml. NPL Aero Note 1057, N68-24729.

— (1974). "The effect of mean compression or dilatation on the turbulence structure of supersonic boundary layers". English. In: Journal of Fluid Mechanics 63 (03), pp. 449–464. ISSN: 1469-7645. DOI: 10.1017/S0022112074001728.

— (1994). "Turbulence: the chief outstanding difficulty of our subject". English. In: Experiments in Fluids 16.3-4, pp. 203–216. ISSN: 0723-4864. DOI: 10.1007/BF00206540.

Bradshaw, Peter and D. H. Ferriss (1971). "Calculation of boundary-layer development using the turbulent energy equation: compressible flow on adiabatic walls". English. In: Journal of Fluid Mechanics 46 (01), pp. 83–110. ISSN: 1469-7645. DOI: 10.1017/S0022112071000417.

Brun, Christophe, Margareta Petrovan Boiarciuc, Marie Haberkorn, and Pierre Comte (2008). "Large eddy simulation of compressible channel flow". English. In: Theoretical and Computational Fluid Dynamics 22.3-4, pp. 189–212. ISSN: 0935-4964. DOI: 10.1007/s00162-007-0073-y.

Busemann, Adolf (1931). "Gasdynamik". German. In: Handbuch der experimentalphysik 4.1, pp. 341–460. English translation available as R.T.P. translations 2207 to 2212.

— (1935). "Gasströmung mit laminarer Grenzschicht entlang einer Platte". German. In: Zeitschrift für Angewandte Mathematik und Mechanik 15.1-2, pp. 23–25. ISSN: 1521-4001. DOI: 10.1002/zamm.19350150106. English translated abstract available in Desk Catalog of German and Japanese Air-Technical Documents, volume 1, section 962, abstract 3564.

Carvin, C., J. F. Debieve, and A. J. Smits (1988). "The Near-Wall Temperature Profile of Turbulent Boundary Layers". In: AIAA 26th Aerospace Sciences Meeting. AIAA-88-0136. DOI: 10.2514/6.1988-136.

Cebeci, Tuncer and Peter Bradshaw (1984). Physical and Computational Aspects of Convective Heat Transfer. English. Springer New York. ISBN: 978-0-387-96821-6. DOI: 10.1007/978-1-4612-3918-5.

Cebeci, Tuncer and A.M.O. Smith (1974). Analysis of Turbulent Boundary Layers. Academic Press. ISBN: 978-0124313040.

Chapman, Dean R. and Morris W. Rubesin (1949). "Temperature and Velocity Profiles in the Compressible Laminar Boundary Layer with Arbitrary Distribution of Surface Temperature". English. In: Journal of the Aeronautical Sciences 16.9, pp. 547–565. ISSN: 1936-9956. DOI: 10.2514/8.11853.

Clauser, Francis H. (1954). “Turbulent Boundary Layers in Adverse Pressure Gradients”. English. In: Journal of the aeronautical sciences 21 (2), pp. 91–108. ISSN: 0095-9812.

— (1956). “The Turbulent Boundary Layer”. In: ed. by Hugh L. Dryden and Theodore von Kármán. Vol. 4. Advances in Applied Mechanics. Elsevier, pp. 1–51. DOI: 10.1016/S0065-2156(08)70370-3.

Coleman, G. N., J. Kim, and R. D. Moser (1995). “A numerical study of turbulent supersonic isothermal-wall channel flow”. In: Journal of Fluid Mechanics 305, pp. 159–183. ISSN: 1469-7645. DOI: 10.1017/S0022112095004587.

Coles, Donald E. (1962). The Turbulent Boundary Layer in a Compressible Fluid. English. Tech. rep. URL: https://www.rand.org/pubs/reports/R403.html. R-403-PR.

— (1964). “The Turbulent Boundary Layer in a Compressible Fluid”. In: Physics of Fluids 7.9, pp. 1403–1423. ISSN: 0031-9171. DOI: 10.1063/1.1711395.

Cope, W. F. and D. R. Hartree (1948). “The Laminar Boundary Layer in Compressible Flow”. In: Philosophical Transactions of the Royal Society of London. Series A, Mathematical and Physical Sciences 241.827, pp. 1–69. ISSN: 0080-4614.

Crocco, Luigi (1932a). “Sulla trasmissione del calore da una lamina piana a un fluido scorrente ad alta velocità”. Italian. In: L’Aerotecnica 12 (2), pp. 181–197. ISSN: 0001-9453. English translation available as Crocco (1932b).

— (1932b). Transmission of heat from a flat plate to a fluid flowing at a high velocity. English. Tech. rep. National Advisory Committee for Aeronautics. URL: https://ntrs.nasa.gov/search.jsp?R=19930094726. NACA-TM-690.

Danberg, James E. (1964). "Characteristics of the turbulent boundary layer with heat and mass transfer at $M = 6.7$". English. PhD thesis. Catholic University of America. URL: https://apps.dtic.mil/docs/citations/AD0452471.

Dorodnitsin, A. A. (1942). "Пограничный слой в сжимаемом газе (The boundary layer in a compressible gas)". Russian. In: Прикладная математика и механика (Prikladnaia Matematika i Mekhanika) 6, pp. 449–486. ISSN: 0032-8235. English translated abstract available in NACA Research Abstracts No. 20, page 5.

Duan, L., I. Beekman, and M.P. Martín (2010). "Direct numerical simulation of hypersonic turbulent boundary layers. Part 2. Effect of wall temperature". In: Journal of Fluid Mechanics 655, pp. 419–445. ISSN: 1469-7645. DOI: 10.1017/S0022112010000959.

Frankl, F. and V. Voishel (1937). "Трение в турбулентном пограничном слое около пластины в плоскопараллельном потоке сжимаемого газа при больших скоростях". Russian. In: Труды Центрального аэро-гидродинамического института им. проф. Н. Е.Жуковского. Труды ЦАГИ № 321. English translation available as Frankl and Voishel (1943).

— (1943). "Turbulent friction in the boundary layer of a flat plate in a two-dimensional compressible flow at high speeds". English. Trans. by S. Reiss. In: NACA technical memorandum 1053. ISSN: 0096-7602. URL: https://ntrs.nasa.gov/search.jsp?R=20050029417. NACA-TM-1053.

Haberkorn, Marie (2004). "Simulations des grandes échelles en canal plan turbulent : Effets de compressibilité et propagation acoustique". French. PhD thesis. Université Louis Pasteur. URL: https://www.theses.fr/2004STR13181.

Howarth, L. (1948). "Concerning the Effect of Compressibility on Laminar Boundary Layers and their Separation". In: Proceedings of the Royal Society of London. Series A. Mathematical and Physical Sciences 194.1036, pp. 16–42. DOI: 10.1098/rspa.1948.0064.

Huang, P. G., G. N. Coleman, and P. Bradshaw (1995). "Compressible turbulent channel flows: DNS results and modelling". In: Journal of Fluid Mechanics 305, pp. 185–218. ISSN: 1469-7645. DOI: 10.1017/S0022112095004599.

Ievlev, V. M. (1975). Турбулентное движение высокотемпературных сплошных сред (Turbulent motion of high-temperature continuous media). Russian. Nauka.

Jiménez, Javier, Sergio Hoyas, Mark P. Simens, and Yoshinori Mizuno (2010). "Turbulent boundary layers and channels at moderate Reynolds numbers". In: Journal of Fluid Mechanics 657, pp. 335–360. ISSN: 1469-7645. DOI: 10.1017/S0022112010001370.

Kármán, Theodore von (1930). "Mechanische Ähnlichkeit und Turbulenz". German. In: Nachrichten von der Gesellschaft der Wissenschaften zu Göttingen, Mathematisch-Physikalische Klasse, pp. 58–76. URL: http://gdz.sub.uni-goettingen.de/dms/load/img/?PPN=PPN252457811_1930&DMDID=DMDLOG_0014. English translation available as Kármán (1931).

— (1931). Mechanical Similitude and Turbulence. English. Tech. rep. 611. National Advisory Committee for Aeronautics. URL: https://ntrs.nasa.gov/search.jsp?R=19930094805. NACA-TM-611.

Kistler, Alan L. (1959). "Fluctuation Measurements in a Supersonic Turbulent Boundary Layer". English. In: Physics of Fluids 2.3, pp. 290–296. DOI: 10.1063/1.1705925.

Kutateladze, S. S. and A. I. Leont'ev (1964). Turbulent Boundary Layers in Compressible Gases. Trans. by D. B. Spalding. Academic Press.

Lagha, M., J. Kim, J. D. Eldredge, and X. Zhong (2011). "A numerical study of compressible turbulent boundary layers". In: Physics of Fluids (1994-present) 23.1. DOI: 10.1063/1.3541841.

Larsson, Johan, Ivan Bermejo-Moreno, and Sanjiva K. Lele (2013). "Reynolds- and Mach-number effects in canonical shock–turbulence interaction". English. In: Journal of Fluid Mechanics 717, pp. 293–321. ISSN: 1469-7645. DOI: 10.1017/jfm.2012.573.

Lobb, R. Kenneth, Eva M. Winkler, and Jerome Persh (1955a). "Experimental Investigation of Turbulent Boundary Layers in Hypersonic Flow". English. In: Journal of the aeronautical sciences 22 (1), pp. 1–9. ISSN: 1936-9956. DOI: 10.2514/8.3262.

— (1955b). "NOL hypersonic tunnel no. 4 results VII: experimental investigation of turbulent boundary layers in hypersonic flow". English. In: NAVORD report 3880. URL: http://www.dtic.mil/docs/citations/AD0068499. NAVORD Report 3880, Aeroballistic Research Report 262, AD-68499.

Maeder, Thierry (2000). "Numerical investigation of supersonic turbulent boundary layers". PhD thesis. Swiss Federal Institute of Technology Zürich. URL: http://e-collection.library.ethz.ch/view/eth:23611.

Mieghem, Jacques van (1973). Atmospheric Energetics. Claredon Press. ISBN: 9780198516057.

Modesti, Davide and Sergio Pirozzoli (2016). "Reynolds and Mach number effects in compressible turbulent channel flow". In: International Journal of Heat and Fluid Flow 59, pp. 33–49. ISSN: 0142-727X. DOI: http://dx.doi.org/10.1016/j.ijheatfluidflow.2016.01.007.

Modesti, Davide and Sergio Pirozzoli (2019). "Direct numerical simulation of supersonic pipe flow at moderate Reynolds number". English. In: International Journal of Heat and Fluid Flow 76, pp. 100–112. ISSN: 0142-727X. DOI: 10.1016/j.ijheatfluidflow.2019.02.001.

Morinishi, Y., S. Tamano, and K. Nakabayashi (2004). "Direct numerical simulation of compressible turbulent channel flow between adiabatic and isothermal walls". English. In: Journal of Fluid Mechanics 502, pp. 273–308. DOI: 10.1017/S0022112003007705.

Morkovin, Mark V. (1962). "Effects of compressibility on turbulent flows". In: Mécanique de la turbulence. Paris, Éditions du Centre National de la Recherche Scientifique, pp. 367–380.

— (1992). "Mach Number Effects on Free and Wall Turbulent Structures In Light of Instability Flow Interactions". English. In: Studies in Turbulence. Ed. by Thomas B. Gatski, Charles G. Speziale, and Sutanu Sarkar. Springer New York, pp. 269–284. ISBN: 978-1-4612-7672-2. DOI: 10.1007/978-1-4612-2792-2_20.

Moser, Robert D., John Kim, and Nagi N. Mansour (1999). "Direct numerical simulation of turbulent channel flow up to $Re_\tau = 590$". In: Physics of Fluids 11.4, pp. 943–945. ISSN: 1070-6631. DOI: 10.1063/1.869966.

Panton, Ronald (2005). Incompressible Flow. 3rd. Wiley. ISBN: 978-0-471-26122-3.

Patel, Ashish, Bendiks J. Boersma, and Rene Pecnik (2016). "The influence of near-wall density and viscosity gradients on turbulence in channel flows". In: Journal of Fluid Mechanics 809, pp. 793–820. DOI: 10.1017/jfm.2016.689.

— (2017). "Scalar statistics in variable property turbulent channel flows". In: Phys. Rev. Fluids 2 (8), p. 084604. DOI: 10.1103/PhysRevFluids.2.084604. URL: https://link.aps.org/doi/10.1103/PhysRevFluids.2.084604.

Patel, Ashish, Jurriaan W. R. Peeters, Bendiks J. Boersma, and Rene Pecnik (2015). “Semi-local scaling and turbulence modulation in variable property turbulent channel flows”. In: Physics of Fluids 27.9. DOI: 10.1063/1.4929813.

Pirozzoli, Sergio and Matteo Bernardini (2011). “Turbulence in supersonic boundary layers at moderate Reynolds number”. In: Journal of Fluid Mechanics 688, pp. 120–168. ISSN: 1469-7645. DOI: 10.1017/jfm.2011.368.

Prandtl, Ludwig (1925). “Bericht über Untersuchungen zur ausgebildeten Turbulenz”. German. In: Zeitschrift für Angewandte Mathematik und Mechanik 5 (2), pp. 136–139. ISSN: 1521-4001. English translation available as Prandtl (1949).

— (1932). “Zur turbulenten Strömung in Rohren und längs Platten”. German. In: Ergebnisse der Aerodynamischen Versuchsanstalt zu Göttingen 4, pp. 18–29. ISSN: 1863-1088.

— (1949). “Report on investigation of developed turbulence”. English. Trans. by J. Vanier. In: NACA technical memorandum 1231. ISSN: 0096-7602. URL: https://ntrs.nasa.gov/search.jsp?R=20050029454. NACA-TM-1231.

Rotta, Julius C. (1959). “Über den Einfluß der Machschen Zahl und des Wärmeübergangs auf das Wandgesetz turbulenter Strömung”. German. In: Zeitschrift für Flugwissenschaften 7, pp. 264–274. ISSN: 0044-2739. English translation available as Rotta (1988).

— (1963). “Bemerkung zum Einfluß der Dichteschwankungen in turbulenten Grenzschichten bei kompressibler Strömung”. German. In: Ingenieur-Archiv 32.3, pp. 187–190. ISSN: 0020-1154. DOI: 10.1007/BF00572240. English translation available as Rotta (1974).

— (1974). Remarks About The Influence of Density Fluctuations in Turbulent Boundary Layers For Compressible Flow. English. Tech. rep. 15989. National Aeronautics and Space Administration. URL: https://archive.org/details/nasa_techdoc_19750002281. NASA-TT-F-15989.

Rotta, Julius C. (1988). “The influence of Mach number and heat transfer on the turbulent flow wall law”. English. Trans. by SCITRAN. In: NASA technical translation 20230. ISSN: 0499-9355. NASA-TT-20230.

Sandoval, Donald L. (1995). “The Dynamics of Variable-Density Turbulence”. English. PhD thesis. University of Washington. URL: http://lanl-primo.hosted.exlibrisgroup.com/LANLCAT:alma_scope:01LANL_ALMA2190004460003761. LA-13037-T.

Schlatter, Philipp and Ramis Örlü (2010). “Assessment of direct numerical simulation data of turbulent boundary layers”. English. In: 659, pp. 116–126. DOI: 10.1017/S0022112010003113.

Sillero, Juan A., Javier Jiménez, and Robert D. Moser (2013). “One-point statistics for turbulent wall-bounded flows at Reynolds numbers up to $\delta^+ \approx 2000$”. In: Physics of Fluids 25.10. DOI: http://dx.doi.org/10.1063/1.4823831.

Smits, Alexander J. and Jean-Paul Dussauge (2006). Turbulent Shear Layers in Supersonic Flow. Springer. ISBN: 978-3540288763.

Stewartson, Keith (1964). The theory of the laminar boundary layer in compressible fluids. Oxford.

Trettel, Andrew (2015). “Velocity transformation for compressible wall turbulence with heat transfer”. MA thesis. University of Maryland, College Park. DOI: 10.13016/M2F33V.

Trettel, Andrew and Johan Larsson (2016). “Mean velocity scaling for compressible wall turbulence with heat transfer”. In: Physics of Fluids 28.2, 026102. DOI: 10.1063/1.4942022.

Van Driest, Edward R. (1951). “Turbulent boundary layer in compressible fluids”. In: Journal of the Aeronautical Sciences 18.3, pp. 1012–1028. ISSN: 0022-4650. DOI: 10.2514/2.7048.

Walz, Alfred (1969). Boundary layers of flow and temperature. English. Trans. by Hans Joerg Oser. M.I.T. Press.

White, Frank (2006). Viscous Fluid Flow. 3rd. McGraw-Hill. ISBN: 978-1-25-900212-0.

Williams, Owen, Tristen Hohman, Tyler Van Buren, Elie Bou-Zeid, and Alexander J. Smits (2017). “The effect of stable thermal stratification on turbulent boundary layer statistics”. English. In: Journal of Fluid Mechanics 812, pp. 1039–1075. DOI: 10.1017/jfm.2016.781.

Wilson, Robert E. (1950). “Turbulent Boundary-Layer Characteristics at Supersonic Speeds-Theory and Experiment”. English. In: Journal of the Aeronautical Sciences 17 (9), pp. 585–594. ISSN: 1936-9956. DOI: 10.2514/8.1727.

Zhang, Chao, Lian Duan, and Meelan M. Choudhari (2018). “Direct Numerical Simulation Database for Supersonic and Hypersonic Turbulent Boundary Layers”. English. In: AIAA Journal 56.11, pp. 4297–4311. ISSN: 0001-1452. DOI: 10.2514/1.J057296.